FUNCTION AND ACTIVATION OF SIGNAL TRANSDUCER AND ACTIVATOR OF TRANSCRIPTION 3 (STAT3) IN ADIPOSE TISSUE FORMATION AND METABOLISM

Erin R. Cernkovich

A dissertation submitted to the faculty of the University of North Carolina at Chapel Hill in partial fulfillment of the requirements for the degree of Doctor of Philosophy in the Department of Nutrition, School of Public Health.

Chapel Hill
2007

Approved by:

Advisor: Joyce B. Harp

Reader: Rosalind A. Coleman

Reader: Terry P. Combs

Reader: Tal M. Lewin

Reader: Nobuyuki Takahashi

© 2007
Erin R. Cernkovich
ALL RIGHTS RESERVED

ABSTRACT

Erin R. Cernkovich
Function and Activation of Signal Transducer and Activator of Transcription 3 (STAT3) in Adipose Tissue Formation and Metabolism
(Under the direction of Joyce B. Harp)

Obesity is a significant medical and public heath concern due to its prevalence, associated co-morbidities, and economic impact. Obesity ensues when adipocytes accommodate excess energy through enhanced triacylglycerol (TAG) storage, and when adipocytes increase in number via adipogenesis. Signal Transducer and Activator of Transcription 3 (STAT3), a mitogenic signaling protein, is activated during the proliferative phases of adipogenesis. We hypothesized therefore, that STAT3 plays a necessary role in adipogenesis. This dissertation describes two independent projects that examined the function and activation of STAT3 in adipose tissue formation and adipocyte metabolism.

Using an adipocyte cell line, we determined that STAT3 activation during adipogenesis occurred indirectly through the synthesis of an autocrine/paracrine factor. We identified the factor to be midkine, a pleiotrophic growth factor, and determined that the midkine-STAT3 signaling pathway plays a necessary role in adipogenesis. This study supported the hypothesis that STAT3 is necessary for adipogenesis and prompted a subsequent study aimed to determine the physiological role of STAT3 in adipogenesis in animals. In this study we used Cre-*loxP* DNA recombination to create mice with an adipocyte-specific disruption of the STAT3 gene (ASKO mice). aP2-Cre driven

disappearance of STAT3 expression occurred on day 6 of adipogenesis, a time point when preadipocytes have already undergone conversion to adipocytes. Thus, this knockout model examined the role of STAT3 in mature, but not differentiating adipocytes ASKO mice weighed more than their littermate controls and had increased adipose tissue mass associated with adipocyte hypertrophy, but not adipocyte hyperplasia, hyperphagia, or reduced energy expenditure. Leptin-induced lipolysis was impaired in ASKO adipocytes, which may partially explain the adipocyte hypertrophy. Despite reduced adiponectin and increased liver TAG, ASKO mice did not develop impaired glucose tolerance or other obesity-related metabolic perturbations.

Overall, this work improved our understanding of preadipocyte proliferation, differentiation, and metabolism by establishing a necessary role for STAT3 and the midkine/STAT3 signaling pathway in these processes. This work will help to direct efforts to identify potential adipose-tissue driven causes of obesity and to discover targets for the treatment of diseases such as obesity, hepatic steatosis, and insulin resistance.

To my 6th committee member, my mother, Judy Cernkovich

TABLE OF CONTENTS

Page

LIST OF TABLES x

LIST OF FIGURES xi

LIST OF ABBREVIATIONS xiii

CHAPTER

I. INTRODUCTION 1

A. BACKGROUND 1

B. SPECIFIC AIMS 3

II. LITERATURE REVIEW 4

A. ADIPOGENESIS 4

1. Inducers of Adipogenesis 4

2. Necessary Events in Adipogenesis 5

2.1 Growth Arrest at Confluence 5

2.2 Mitotic Clonal Expansion 5

2.3 Commitment to Terminal Differentiation 8

3. Adipogenic Transcription Factors 8

3.1 CCAAT/Enhancer-Binding Proteins (C/EBPs) 9

3.1.1 C/EBPβ and C/EBPδ 9

3.1.2 C/EBPα 10
3.2 Peroxisome Proliferator-Activated Receptors (PPARs) 11
3.2.1 PPARγ 11
B. SIGNAL TRANSDUCERS AND ACTIVATORS OF TRANSCRIPTION 13
1. Structural Features of STATs 13
2. Mechanisms of Activation 14
3. Functions of STATs 15
4. STATs Effects on Cell Proliferation 19
5. STATs in Adipogenesis 21
C. STAT ACTIVATING FACTORS 22
1. Leptin 22
1.1 Leptin Signaling 23
1.2 Metabolic Effects of Leptin in WAT 24
1.2.1 Leptin Induced Lipolysis 26
1.2.2 Leptin and Fatty Acid Oxidation/Lipogenesis 27
2. IL-6-Type Cytokines 28
2.1 IL-6-and CNTF Signaling 29
2.2 Metabolic Effects of IL-6 in WAT 29
2.3 Metabolic Effects of CNTF in WAT 30
3. Midkine 32
3.1 Midkine Signaling 32
3.2 Biological Effects of Midkine 32
III. MECHANISM OF STAT3 ACTIVATION DURING 3T3-L1 ADIPOGENESIS 34

Manuiscript #1: Midkine is an Autocrine Activator of STAT3 in 3T3-L1 Cells 35

A. ABSTRACT 35

B. INTRODUCTION 36

C. MATERIALS AND METHODS 38

D. RESULTS 42

E. DISCUSSION 54

IV. ROLE OF STAT3 IN ADIPOGENESIS AND ADIPOCYTE METABOLISM IN MICE 57

Manuscript #2: Adipocyte-Specific Disruption of Signal Transducer and Activator Transcription 3 (STAT3) Increases Body Weight and Adiposity 58

A. ABSTRACT 58

B. INTRODUCTION 59

C. MATERIALS AND METHODS 61

D. RESULTS 69

E. DISCUSSION 83

V. SYNTHESIS 88

A. OVERVIEW OF RESEARCH FINDINGS 88

1. Midkine is an Autocrine Activator of STAT3 in 3T3-L1 Cells 88

2. Adipocyte-Specific Disruption of Signal Transducer and Activator of Transcription 3 (STAT3) Increases Body Weight and Adiposity 88

B. DIRECTIONS FOR FUTURE RESEARCH 91

1. Adiponectin and fatty liver disease in ASKO mice 92

2. Evidence for a causal relationship between hepatic steatosis and insulin resistance in ASKO mice 93

3. Mechanism for the obese phenotype in ASKO mice 93

4. A new model of STAT3 deficiency 95
C. PUBLIC HEALTH SIGNIFICANCE 96
VI. DETAILED METHODS 98
A. ANIMAL MODELS 98
1. Assembly of the Targeting Vector 98
1.1 The OSfrt-*loxP* Plasmid 98
1.1.1 Positive-Negative Selection 99
1.1.2 Site-Specific Recombinase Systems: Cre-*loxP* and FlpE-FRT 100
1.2. Homologous Sequences 100
2. Production and Identification of Targeted ES Cell Clones 102
3. Removal of *Neo* by FlpE Recombinase 102
4. Production of Chimeras by Blastocyst Injection of Targeted ES Cells 103
5. Transmission of the Functional Allele through the Mouse Germline 103
6. Inactivation of the Functional Allele by Cre Recombinase 104
B. PRIMARY PREADIPOCYTES 104
1. Isolation and Culture of Stromal-Vascular Cells 104
REFERENCES 117

LIST OF TABLES

Page

Table 2.1 Role of STAT Proteins as Revealed by Gene Targeting in Mice……19

Table 2.2 Tissue-Specific Roles of STAT3 as Revealed by Conditional Gene Targeting in Mice…… 19

Table 4.1 Primers and Probes for Real-Time (TaqMan) RT-PCR……..68

Table 4.2 Normal Biochemical Parameters in ASKO Mice……....79

LIST OF FIGURES

Page

Figure 2.1 Necessary Events in 3T3-L1 Adipogenesis……..… 6

Figure 2.2 Conserved Domains of the STAT Family…….. 15

Figure 2.3 Mechanisms of STAT Activation…… 17

Figure 2.4 Metabolic Effects of Leptin in White Adipose Tissue…….26

Figure 3.1 Pattern of STAT3 Activation in 3T3-L1 Preadipocytes…….. 43

Figure 3.2 Effect of Conditioned Medium Stimulation on STAT3 Tyrosine Phosphorylation in 3T3-L1 Preadipocyte and Adipocytes…….. 43

Figure 3.3 Effect of Cycloheximide, Actinomycin D, and Heparin Affinity Column Pretreatment on Conditioned Medium-Induced Activation of STAT3…….. 45

Figure 3.4 Effect of Recombinant Midkine Stimulation on STAT3 Tyrosine Phosphorylation in 3T3-L1 Preadipocytes……..47

Figure 3.5 Midkine Expression in 3T3-L1 Preadipocytes…….……47

Figure 3.6 Effect of Midkine Neutralization on Midkine-Induced STAT3 Tyrosine Phosphorylation in 3T3-L1 Preadipocytes……...……..49

Figure 3.7 Effect of Recombinant Midkine Stimulation on the Proliferative Phases of Adipogenesis……51

Figure 3.8 Effect of Midkine Neutralization on Adipogenesis…….. 53

Figure 4.1 Generation of ASKO Mice…….. 70

Figure 4.2 Higher Body Weight and Increased Fat Mass in ASKO Mice…… 72

Figure 4.3 Increased Adiposity in ASKO Mice…… 74

Figure 4.4 Normal Gene Expression in WAT from ASKO Mice……. 75

Figure 4.5 Normal Food Intake and Energy Expenditure in ASKO Mice…….. 77

Figure 4.6 Normal Glucose Tolerance in ASKO Mice……. 79

Figure 4.7 Impaired Leptin Signaling in ASKO Mice…….. 81

Figure 4.8 Supplemental Data……... 87

Figure 6.1 Targeting Strategy…….. 106

Figure 6.2 The OSfrt-*loxP* Plasmid……. 107

Figure 6.3 Long Arm, Short Arm, Target Arm Amplification…… 108

Figure 6.4 The Assembled Targeting Vector…….. 109

Figure 6.5 Assessment of Homologous Recombination Using PCR…….. 110

Figure 6.6 Assessment of Homologous Recombination Using Southern Blot Analysis…….. 111

Figure 6.7 Screening for *Neo* Removal Using PCR…… 112

Figure 6.8 Blastocyst Microinjection…….. 113

Figure 6.9 Mating Strategy…….. 114

Figure 6.10 Assessment of STAT3 Recombination in Adipose Tissue…… 115

Figure 6.11 Lipid Accumulation in Primary Preadipocytes…….. 116

LIST OF ABBREVIATIONS

ACC	acetyl-CoA carboxylase
ACO	acyl-CoA oxidase
ACS	acyl-CoA synthase
ADD1	adipocyte determination and differentiation-dependent factor-1
ALK	anaplastic lymphoma kinase
AMPK	AMP-activated protein kinase
ASKO	adipocyte STAT3 knockout
BAT	brown adipose tissue
BMI	body mass index
BSA	bovine serum albumin
cAMP	cyclic AMP
C/EBP	CCAAT/enhancer binding protein
CDK	cyclin dependent kinase
CLC	cardiotrophin-like cytokine
CM	conditioned medium
CNTF	ciliary neurotrophic factor
CPT-1	carnitine palmitoyltransferase-1
CREB	cAMP response element binding protein
CSF-1	colony stimulating factor 1
CT-1	cardiotrophin-1
DIO	diet induced obese

DGAT	diacylglycerol acyltransferase
DMEM	Dulbecco's modified eagle's medium
EGF	epidermal growth factor
FABP	fatty acid binding protein
FAS	fatty acid synthase
FBS	fetal bovine serum
FFA	free fatty acid
GAPDH	glyceraldehyde-3-phosphate dehydrogenase
GPAT	glycerol-3-phosphate acyltransferase
HGF	hepatocyte growth factor
IGF-I	insulin-like growth factor-I
IL-6	interleukin-6
IRS-1	insulin receptor substrate-1
IRS-2	insulin receptor substrate-2
JAK	janus kinase
LIF	leukemia inhibitory factor
LPL	lipoprotein lipase
LRP	low-density-lipoprotein-receptor-related protein
MAPK	mitogen-activated protein kinase
MEF	mouse embryonic fibroblast
MIX	isobutylmethylxanthine
MDI	isobutylmethylxanthine, dexamethasone, insulin
NRTK	non-receptor tyrosine kinase

Ob-R	leptin receptor
OSM	oncostatin M
PBS	phosphate-buffered saline
PCR	polymerase chain reaction
PDGF	platelet derived growth factor
PEPCK	phosphoenolpyruvate carboxykinase
PI3K	phosphatidylinositol 3-kinase
PKC-ε	protein kinase C-ε
PPAR	peroxisome proliferator-activated receptor
PTPζ	receptor-type protein tyrosine phosphatase ζ
rhMK	recombinant human midkine
RT-PCR	reverse transcriptase PCR
SOCS3	suppressor of cytokine signaling-3
SREBP1	sterol regulatory element binding protein-1
STAT	signal transducer and activator of transcription
TAG	triacylglycerol
TK	thymidine kinase
WAT	white adipose tissue

CHAPTER I
INTRODUCTION

A. BACKGROUND

Obesity is a significant medical and public health concern due to its prevalence, associated co-morbidities, and economic impact (1). Obesity ensues when energy intake chronically exceeds energy expenditure (2). At the cellular level, white adipose tissue (WAT) expansion occurs in response to positive energy balance. WAT expands when adipocytes accommodate excess energy through enhanced triacylglycerol (TAG) storage. WAT also expands when adipocytes increase in number. It is postulated that adipocyte hyperplasia occurs when adipocytes reach a critical size threshold, during which signals are transmitted from adipocytes to preadipocytes to stimulate the formation of new adipocytes to store excess energy (3-5).

Many of the advances in our understanding of adipogenesis are based on studies in 3T3-L1 cells. 3T3-L1 preadipocytes are fibroblast-like cells committed to the adipocyte lineage. In culture, 3T3-L1 preadipocytes replicate until they form a confluent monolayer (6). At confluence, cell-cell contact triggers growth arrest. When induced with hormonal agents, often a cocktail of isobutylmethylxanthine, dexamethasone, and insulin (MDI), growth-arrested preadipocytes reenter the cell cycle and undergo 1-2 rounds of cell division known as mitotic clonal expansion (7). Following mitotic clonal expansion, preadipocytes exit the cell cycle, commit to terminal differentiation, and begin to express adipocyte specific

genes (8). **Although much is known about the mechanisms of preadipocyte differentiation, less is known about preadipocyte proliferation.**

The major transcriptional regulators of adipogenesis include proteins belonging to the CCAAT/enhancer binding protein (C/EBP) family and the peroxisome proliferator-activated receptor (PPAR) superfamily (9-11). A coordinated cascade involving the above mentioned factors typifies the differentiated phenotype. Specifically, C/EBPβ and C/EBPδ induce C/EBPα (12) and PPARγ (13) expression, which in turn promote the terminally differentiated state (14). Previous cell culture studies in our laboratory suggest that signal transducer and activator of transcription 3 (STAT3) is an important adipogenic transcription factor as well. STAT3 is abundantly expressed in preadipocytes and adipocytes (15), and highly activated and bound to DNA in proliferating preadipocytes and adipocytes (16). In addition, inhibition of endogenous STAT3 expression with antisense morpholino oligonucleotides significantly decreases preadipocyte proliferation (16). **The specific function of STAT3 in preadipocyte proliferation and differentiation, however, is not yet known.**

Cytokines and growth factors activate STAT3 by activating receptor and nonreceptor tyrosine kinases that phosphorylate STAT3 on a critical tyrosine residue (17). Upon activation, STAT3 dimerizes with other STATs and translocates to the nucleus where it binds to specific DNA regulatory sequences to stimulate the transcription of target genes. Previous cell culture studies in our laboratory report that STAT3 activation during adipogenesis is delayed. **The mechanism of delayed activation, however, is not yet known, but preliminary studies suggest that midkine, a heparin binding growth factor, is the**

autocrine activator of STAT3.

STAT3 is also activated in adipocytes by leptin, interleukin-6 (IL-6), and ciliary neurotrophic factor (CNTF). These cytokines have been shown to regulate body weight *via* anti-lipogenic and pro-lipolytic actions on adipocytes (18-32). Because STAT3 is a downstream target of leptin, IL-6 and CNTF signaling, it has been hypothesized that STAT3 mediates the effects of these cytokines. **The contribution of STAT3 to these aspects of body weight homeostasis, however, has yet to be determined.**

B. SPECIFIC AIMS

1. Identify the differentiation-induced STAT3 activating factor and determine its role in preadipocyte proliferation and differentiation.
2. Using Cre-*loxP* DNA recombination, generate mice with an adipose-specific disruption of the STAT3 gene (ASKO mice).
3. Determine the functional role of STAT3 in adipocyte formation and body weight homeostasis using ASKO mice and primary preadipocytes isolated from ASKO mice.

CHAPTER II
LITERATURE REVIEW

A. ADIPOGENESIS

Obesity is a significant medical and public health concern due to its prevalence, associated co-morbidities, and economic impact (1). Obesity ensues when energy intake chronically exceeds energy expenditure (2). At the cellular level, white adipose tissue (WAT) expansion occurs in response to positive energy balance. WAT expands when adipocytes accommodate excess energy through enhanced triacylglycerol (TAG) storage. WAT also expands when adipocytes increase in number. It is postulated that when adipocytes reach a critical size threshold, preadipocytes undergo adipogenesis (3-5).

Many of the advances in our understanding of adipogenesis are based on studies in embryonic derived 3T3-L1 cells. 3T3-L1 preadipocytes are a clonal subline of fibroblast-like cells committed to the adipocyte lineage (6, 33). When induced with hormonal agents, often a cocktail of isobutylmethylxanthine, dexamethasone, and insulin (MDI), this cell line can be differentiated into cells that biochemically and morphologically resemble mature adipocytes.

1. Inducers of Adipogenesis

The MDI protocol for the differentiation of 3T3-L1 preadipocytes was established in the late 1970s by Rubin *et al*.(34). Rubin *et al*. stimulated 2-day postconfluent preadipocytes

with isobutylmethylxanthine (MIX), dexamethasone, and insulin. MIX, a cAMP phosphodiesterase inhibitor, increases intracellular cAMP; dexamethasone, a synthetic glucocorticoid, activates the glucocorticoid receptor signaling pathway; and insulin, a mitogen, signals through the insulin-like growth factor-I (IGF-I) receptor. cAMP and dexamethasone promote adipogenesis by regulating the expression of adipogenic transcription factors, inhibitors of adipogenesis, and adipocyte-specific genes. The effects of insulin on differentiation have been shown to occur through activation of the IGF-I receptor and several distinct downstream signal transduction pathways, including the mitogen-activated protein kinase (MAPK) cascade (35).

2. Necessary Events in Adipogenesis

Adipogenesis *in vitro* follows a well-characterized temporal sequence **(Figure 2.1)**. 3T3-L1 preadipocytes replicate in culture until they form a confluent monolayer. At confluence, cell-cell contact triggers **growth arrest** in G_0/G_1 of the cell cycle. Upon stimulation with MDI, postconfluent growth-arrested preadipocytes reenter the cell cycle and undergo 1-2 rounds of cell division known as **mitotic clonal expansion.** Following mitotic clonal expansion, differentiating preadipocytes exit the cell cycle, arrest in G_0/G_1, **commit to terminal differentiation**, and begin to express adipocyte specific genes (8). Proteins belonging to the CCAAT/enhancer binding protein (C/EBP) family and peroxisome proliferator-activated receptor γ (PPARγ) regulate the above-mentioned events.

2.1 Growth Arrest at Confluence

The first stage in the differentiation of adipocytes is growth arrest. Growth arrest is

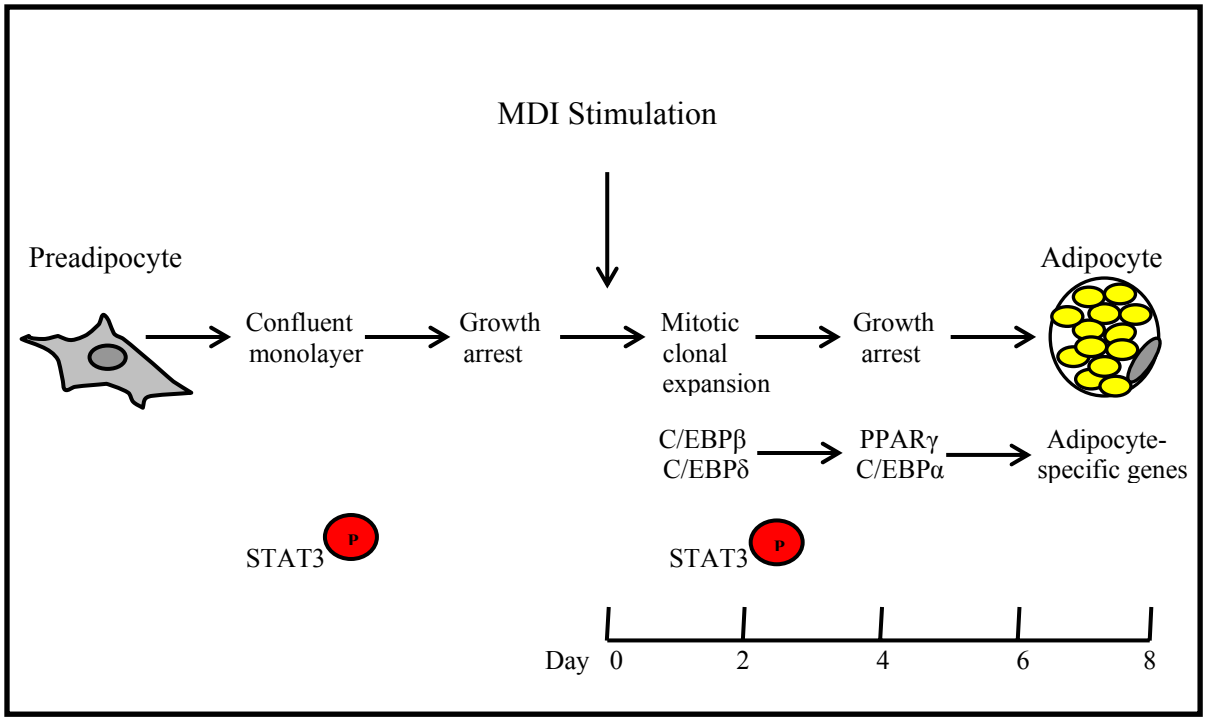


Figure 2.1 – Necessary events in 3T3-L1 adipogenesis.
Preadipocytes replicate until they form a confluent monolayer. At confluence, cell cell contact triggers growth arrest. When induced with hormonal agents, often a cocktail of isobutylmethylxanthine, dexamethasone, and insulin (MDI), growth arrested preadipocytes reenter the cell cycle and undergo 1-2 rounds of cell division known as mitotic clonal expansion.
Mitotic clonal expansion is characterized by an increase in the expression of the adipogenic transcription factors C/EBP β and δ and the tyrosine phosphorylation and activation of STAT3. Following mitotic clonal expansion, preadipocytes exit the cell cycle, commit to terminal differentiation and begin to express adipocyte specific genes.
PPARγ and C/EBPα expression coincides with the end of mitotic clonal expansion and induction of the second permanent period of growth arrest. PPARγ and C/EBPα induce expression of each other and act synergistically to promote differentiation and induce expression of adipocyte specific genes.

achieved following contact inhibition and is accompanied by changes in the pattern of gene expression; growth arrested preadipocytes express early, differentiation-specific markers. Pairault *et al.* have determined that growth arrest at confluence is necessary for preadipocyte differentiation (36).

2.2 Mitotic Clonal Expansion

Mitotic clonal expansion refers to the three-day period during which growth arrested preadipocytes synchronously enter the S phase of the cell cycle and undergo several rounds of cell division in response to MDI stimulation. Being a period of cellular proliferation, mitotic clonal expansion is characterized by the activation of cyclin dependent kinase 2 by cyclins E and A, the down regulation of the cyclin dependent kinase inhibitor p27, and the incorporation of [^{3}H] thymidine into DNA (37). Mitotic clonal expansion is also characterized by a transient increase in the expression of the transcription factors C/EBPβ (38) and C/EBPδ (38) as well as the tyrosine phosphorylation and activation of the transcription factor signal transducer and activator of transcription 3 (STAT3) (16).

Several groups have established that mitotic clonal expansion is required for progression through the differentiation program. Mitotic clonal expansion and differentiation are blocked by an inhibitor of DNA polymerase α (39). Consistent with these results, mitotic clonal expansion and differentiation are also blocked by blocking the down regulation of a cyclin dependent kinase inhibitor (40), and by blocking S phase entry with a cyclin dependent kinase inhibitor (37). The requirement of cell division for differentiation has been controversial, however. Some evidence suggests that primary preadipocytes can

differentiate in culture without undergoing clonal expansion (41).

2.3 Commitment to Terminal Differentiation

Following mitotic clonal expansion, preadipocytes exit the cell cycle, arrest in G_0/G_1, commit to terminal differentiation, and begin to express adipocyte-specific genes, including proteins required for lipogenesis and lipolysis (8). During this terminal phase, preadipocytes also alter the expression of cytoskeletal and extracellular matrix components and undergo dramatic morphological changes required for acquisition of the adipocyte phenotype, including conversion from a fibroblastic to a spherical shape with lipid-laden droplets.

This second period of growth arrest is permanent and coincides with a decline in C/EBPβ and C/EBPδ expression, and the onset of C/EBPα and PPARγ expression. Like growth arrest at confluence, growth arrest after mitotic clonal expansion is necessary for terminal differentiation (42).

3. Adipogenic Transcription Factors

The major transcriptional regulators of adipogenesis include proteins belonging to the C/EBP family and the PPAR superfamily (9-11). A coordinated cascade involving the above mentioned factors typifies the differentiated phenotype. Specifically, C/EBPβ and C/EBPδ induce C/EBPα and PPARγ expression, which in turn promote the terminally differentiated state. Adipocyte determination and differentiation-dependent factor-1 (ADD1/SREBP-1), cAMP response element binding protein (CREB), and signal transducers and activators of transcription (STATs) have also been implicated in the differentiation program.

3.1 CCAAT/Enhancer-Binding Proteins (C/EBPs)

The first transcription factors found to participate in adipogenesis were members of the C/EBP family. The C/EBP family has six members: -α, -β, -γ, -δ, -ε, and –ζ. C/EBPα, C/EBPβ, c/EBPδ, and C/EBPζ are expressed in adipose tissue and adipocyte cell lines (43).

3.1.1 C/EBPβ and C/EBPδ

Two to four hours after induction of differentiation, proliferating preadipocytes express C/EBPβ and C/EBPδ, with MIX inducing the expression of C/EBPβ and dexamethasone inducing C/EBPδ expression (38). Although C/EBPβ and C/EBPδ are expressed soon after induction of differentiation, they are unable to bind DNA, and thus cannot function as transcriptional activators (7). Tang *et al*. (7) report that acquisition of DNA-binding activity occurs 10-12 hours later as postconfluent growth-arrested preadipocytes reenter the cell cycle and begin mitotic clonal expansion. Upon acquiring DNA binding activity, C/EBPβ and C/EBPδ synergistically promote the expression of PPARγ (13) and C/EBPα (12). Gene expression is mediated by C/EBP regulatory elements present in the promoters of the PPARγ and C/EBPα genes (44, 45).

Gain and loss of function studies define a role for C/EBPβ and C/EBPδ in adipogenesis. Several groups confirm that C/EBPβ is necessary for mitotic clonal expansion and differentiation, while C/EBPδ plays a relatively minor role. Specifically, ectopic expression of C/EBPβ is sufficient to induce the differentiation of preadipocytes in the absence of hormonal inducers (12), while ectopic expression of C/EBPδ accelerates adipogenesis, but only in the presence of hormonal inducers. Additionally, mouse embryonic

fibroblasts (MEFs) lacking C/EBPδ show slight reductions in adipogenic potential (46), while MEFs from C/EBPβ knockout mice neither undergo mitotic clonal expansion nor differentiate into adipocytes (47).

In vivo results from mice lacking C/EBPβ and/or C/EBPδ are more ambiguous. These data suggest that C/EBPβ and C/EBPδ have a synergistic role in adipocyte differentiation. Specifically, mice lacking either C/EBPβ or C/EBPδ have normal WAT. Eighty-five percent of mice lacking both C/EBPβ and C/EBPδ, however, die during the prenatal period. The remaining 15% of these mice do not accumulate lipid droplets in their brown adipose tissue (BAT), and their epididymal fat pad weight is significantly reduced (46).

3.1.2 C/EBPα

C/EBPα is expressed late in the differentiation program. Its expression coincides with the end of mitotic clonal expansion and induction of the second, permanent period of growth arrest. C/EBPα expression remains elevated for the remainder of the differentiation program and throughout the life of the mature adipocyte. In view of its pattern of expression, an important role for C/EBPα in adipogenesis was suggested. This hypothesis was supported by the finding that, when ectopically expressed, C/EBPα stimulates the expression of gadd45 and p21, thus inducing growth arrest and terminating mitotic clonal expansion (48). It was further supported by studies showing that C/EBPα regulates the expression of adipocyte-specific genes including FABP2/aP2, GLUT-4, phosphoenolpyruvate carboxykinase (PEPCK), and insulin receptor (49-51).

Given its role in the acquisition of the growth arrested state and the terminally differentiated phenotype, it is not surprising that several laboratories have concluded that C/EBPα is critical for the adipogenic program. The involvement of C/EBPα in adipogenesis is strongly supported by *in vitro* and *in vivo* studies. In the absence of hormonal stimulants, constitutive expression of C/EBPα is sufficient for adipogenesis (52). Furthermore, diminution of endogenous C/EBPα expression by antisense oligonucleotides inhibits adipogenesis (53). Finally, MEFs lacking C/EBPα have reduced adipogenic potential (54), and mice with a homozygous deletion in C/EBPα have dramatically reduced fat accumulation in WAT (55).

3.2 Peroxisome Proliferator-Activated Receptors (PPARs)

Adipogenesis also requires the activity of PPARs, members of the nuclear receptor superfamily of ligand-activated transcription factors. The PPAR family has three members: -α, -γ, and -δ. Adipose tissue and adipocyte cell lines express high levels of PPARγ. PPARγ is expressed as two isoforms, PPARγ1 and PPARγ2. While many tissues express PPARγ1, PPARγ2 is expressed almost exclusively in white and brown adipose tissue (56).

3.2.1 PPARγ

PPARγ is expressed late in the differentiation program. Similar to C/EBPα, its expression coincides with the end of mitotic clonal expansion and induction of growth arrest. PPARγ expression also remains elevated for the remainder of the differentiation program and throughout the life of the mature adipocyte. This expression pattern suggested an important role for PPARγ in adipogenesis. This hypothesis was supported by the finding that PPARγ

stimulates the expression of the cyclin-dependent kinase inhibitors p18 and p21, thus inducing growth arrest and terminating mitotic clonal expansion (57). It was further supported by studies showing that PPARγ promotes differentiation by increasing the expression of adipocyte-specific genes that confer the adipocyte phenotype, including FABP2/aP2, lipoprotein lipase (LPL), acyl-CoA synthase (ACS), fatty acid synthase (FAS), and PEPCK (56, 58, 59)

Gain and loss of function studies further demonstrate the sufficiency of PPARγ for adipogenesis. Studies conducted in ES cells lacking PPARγ (60) and MEFs deficient in PPARγ show that PPARγ is necessary for *in vitro* differentiation. Additional studies confirm that PPARγ is sufficient for adipogenesis as well. Specifically, ectopic expression of PPARγ in non-adipogenic fibroblasts triggers the adipogenic program (61), and PPARγ ligands can substitute for adipogenic hormones during the differentiation of preadipocytes (62).

Loss of function experiments *in vivo* however proved difficult because mice with a homozygous deletion in PPARγ die in utero (63). To circumvent this difficulty, Rosen *et al.* (60) studied chimeric mice, made by mixing wild-type and PPARγ$^{-/-}$ embryonic stem (ES) cells. The adipose tissue from these mice developes normally. However, the tissue is derived predominately from wild-type cells, not PPARγ$^{-/-}$ cells. The relative contribution of each ES cell genotype provides evidence that PPARγ is required for the differentiation of adipose tissue *in vivo*. Studies performed in mice with an adipose specific deletion in PPARγ confirm this conclusion (64). These mice display progressive lipodystrophy and develop associated metabolic perturbations, including liver and WAT insulin resistance.

In the above mentioned mouse models, both PPARγ1 and PPARγ2 transcripts were inactivated. Because PPARγ2 is expressed almost exclusively in white and brown adipose tissue (56), it has been suggested that PPARγ2 may be more adipogenic than PPARγ1. Recently Zhang *et al*. (65) reported that a PPARγ2 deficiency impairs the development of adipose tissue. They conclude that, while both PPARγ1 and PPARγ2 can drive adipose tissue development, PPARγ2 plays the dominant role. Specifically, PPARγ2$^{-/-}$ mice exhibit an overall reduction in WAT. Furthermore, consistent with *in vivo* data, PPARγ2$^{-/-}$ MEFs show a dramatically reduced capacity for adipogenesis compared to wild-type MEFs.

Because C/EBPα and PPARγ act synergistically to promote adipocyte differentiation, important questions arose about the relative roles of PPARγ and C/EBPα in adipogenesis: do they operate independently in separate, parallel pathways of differentiation, or does a single pathway exist? Rosen *et al*. (66) demonstrated that C/EBPα and PPARγ participate in a single pathway with PPARγ being the primary regulator of adipogenesis. Specifically, MEFs from mice lacking C/EBPα fail to express PPARγ and are unable to differentiate into adipocytes (54). Similarly, MEFs from mice lacking PPARγ express greatly reduced levels of C/EBPα and are unable to differentiate into adipocytes (63). Adding PPARγ back to C/EBPα$^{-/-}$ fibroblasts, however restores their capacity to accumulate lipid and activate markers of adipogenesis (54). C/EBPα, however, can not rescue adipogenesis in PPAR$^{-/-}$ fibroblasts (66).

B. SIGNAL TRANSDUCERS AND ACTIVATORS OF TRANSCRIPTION (STATs)

STAT1, -2, -3, -4, -5A, -5B, and -6 comprise a group of cytosolic latent transcription

factors that participate in normal cellular events, including differentiation, proliferation, cell survival, and apoptosis, following activation by cytokines, peptides, and growth factors (17).

1. Structural Features of STATs

STATs share several conserved domains critical for STAT functions (67): a coiled-coil domain, a DNA binding domain, an SH2 domain, a linker domain, a critical tyrosine residue, and a transcriptional activation domain The coiled-coil domain contains four helical coils which provide protein-protein interaction sites. The SH2 domain is required for the recruitment of STATs to phosphorylated receptors and for the SH2-phosphotyrosine interactions between monomeric STATs (67). The linker domain precedes the SH2 domain and links it to the DNA binding domain. The conserved tyrosine residue exists near the carboxy-terminus of all STAT proteins. STATs are activated through phosphorylation of this tyrosine residue. The carboxy-terminus also contains the transcriptional activation domain. **Figure 2.2** shows these conserved domains of STAT proteins.

2. Mechanisms of Activation

STAT proteins are latent in the cytoplasm and become activated *via* tyrosine phosphorylation when extracellular proteins bind to their corresponding cell surface receptors **(Figure 2.3)**. That is, ligand binding triggers receptor dimerization. Dimerized receptors subsequently activate various receptor and non-receptor tyrosine kinases (NRTK) that phosphorylate and activate STAT proteins. Tyrosine phosphorylated STATs then homo- or heterodimerize through association between the SH2 domain of one STAT monomer and phosphotyrosine of another STAT monomer. Specifically, STATs 5A and 5B interact as

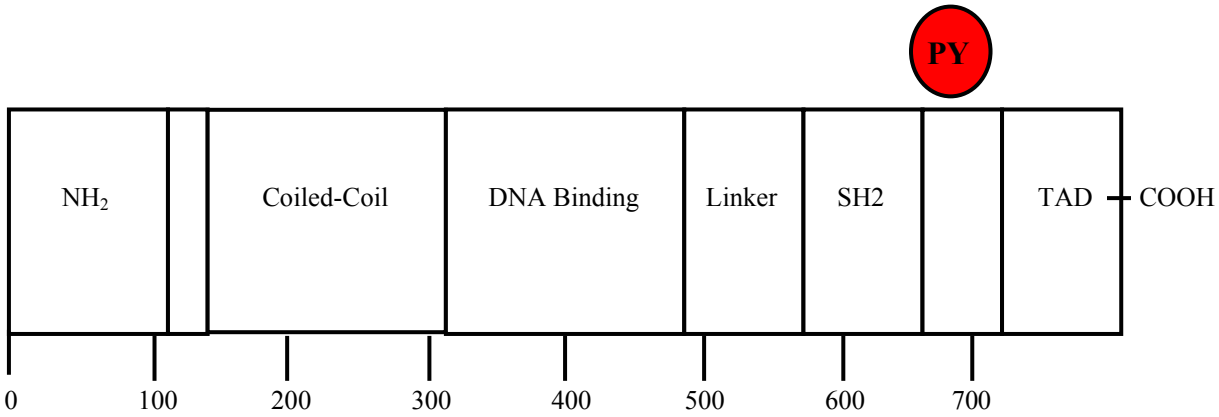


Figure 2.2 – Conserved domains of the STAT family.
The seven mammalian STAT proteins share six highly conserved domains, a coiled-coil domain, a DNA binding domain, a linker domain, an SH2 domain, a critical tyrosine residue, and a transcriptional activation domain.

heterodimers, while STATs 1, 3, 4, and 6 form homodimers (17). STAT1 also forms heterodimers with both STAT2 and STAT3 (17). Finally, activated STAT dimers translocate to the nucleus where they bind specific DNA regulatory sequences to stimulate the transcription of target genes.

Over 40 ligands have been shown to activate STAT proteins. Growth factors including epidermal growth factor (EGF), platelet derived growth factor (PDGF), colony stimulating factor-1 (CSF-1), and hepatocyte growth factor (HGF) (68-71), can activate STATs. Because growth factor receptors possess intrinsic tyrosine kinase activity, they can directly phosphorylate and activate STAT proteins following ligand binding. Activated growth factor receptors can also recruit NRTKs, including Src, Syk, and Abl, to phosphorylate and active STATs (68).

Cytokines can also activate STAT proteins (72). Cytokine receptors, however, do not have intrinsic kinase activity. Consequently, receptor associated cytoplasmic proteins from the Janus kinase (Jak) family, including Jak1, Jak2, Jak3, and Tyk4, provide the required tyrosine kinase activity (73). Upon ligand binding, these proteins bind to intracellular domains on the cytokine receptor and catalyze ligand-induced phosphorylation of themselves and of intracellular tyrosine residues on the cytokine receptor. These phosphorylated tyrosines provide docking sites for STATs. STAT proteins are recruited to the phosphorylated tyrosine, whereupon they are tyrosine phosphorylated by Jaks.

G-protein-coupled receptors, including receptors for angiotensin II (74) and serotonin

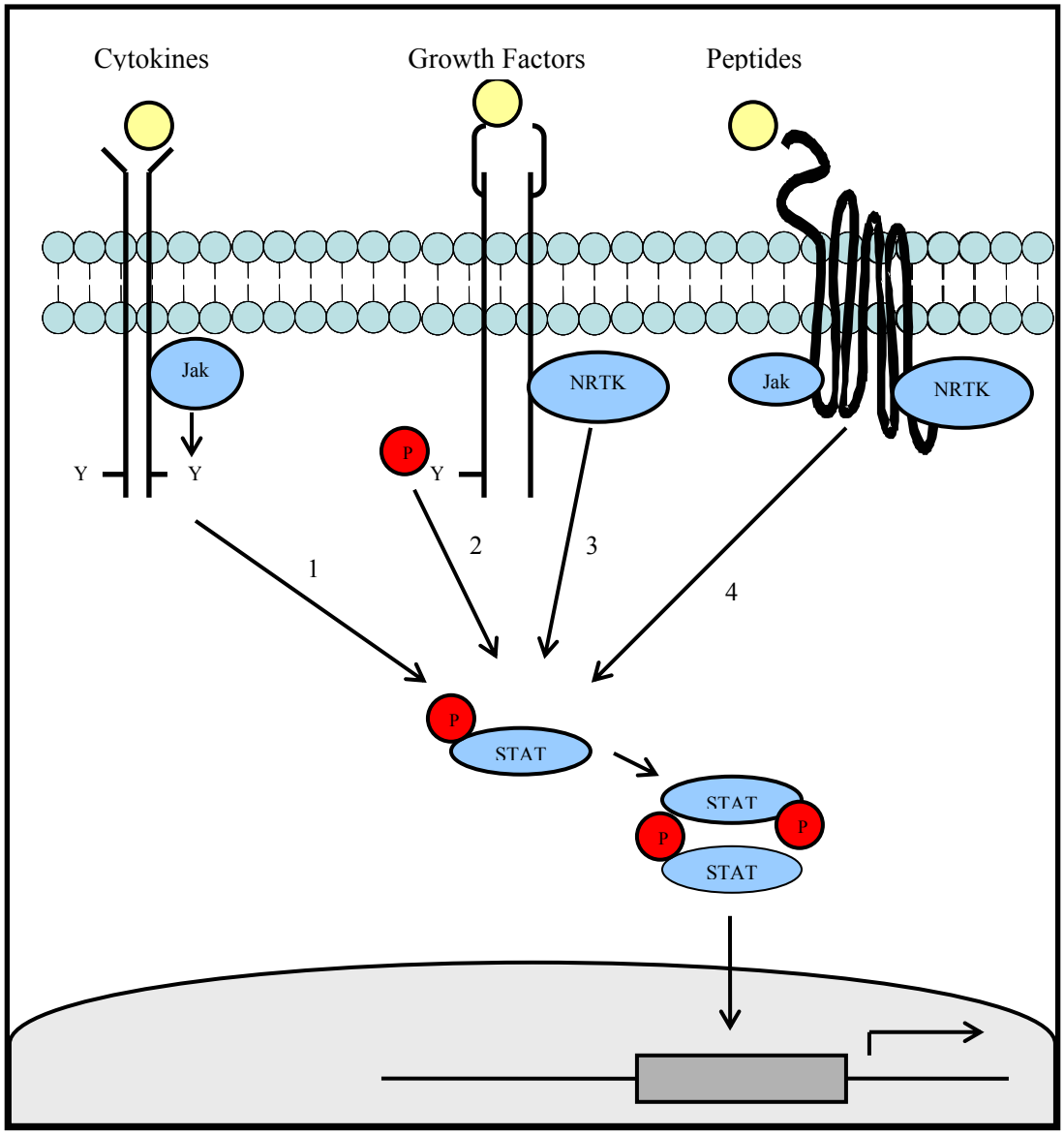


Figure 2.3 – Mechanisms of STAT activation
STATs become tyrosine phosphorylated by four different mechanisms: (1) Cytokine mediated activation by Jaks, (2) Growth factor mediated activation by receptor tyrosine kinases, (3) growth factor mediated activation by non-receptor tyrosine kinases (NRTK), and (4) G-protein mediated activation by Jaks and NRTK. Tyrosine phosphorylated STATs form homo- or heterodimers, and then translocate to the nucleus where they bind target sequences.

(75), have been shown to activate STATs as well (72). It has been proposed that STATs are activated by both Jaks and NRTKs associated with G-protein-coupled receptors (74, 76).

3. Functions of STATs

The physiological role of each STAT was examined through the study of knockout mice **(Table 2.1)**. Targeted disruption of STAT1 and STAT2 revealed that these STATs mediate the effects of interferons. Specifically, STAT1 deficient mice are unable to respond to type I and type II interferons and are subsequently susceptible to bacterial and viral pathogens (77, 78). Furthermore, STAT2 knockout mice are unresponsive to type I interferons and thus sensitive to infection as well (79). IL-12-mediated functions, including cellular proliferation and T helper 1 cell differentiation, are impaired in STAT4 knockout mice (80, 81). STAT6 knockout mice have defects in IL-4 mediated functions, including T-cell proliferation and T helper 2 cell development (82-84). STAT4 and STAT6, therefore, are essential for mediating the effects of IL-12 and IL-4 respectively. STAT5A knockout females have defects in breast tissue development (85). STAT5B knockout males grow slowly, weigh significantly less than control littermates, and exhibit female patterns of liver gene expression (86, 87). STAT5B, therefore, is required for physiological responses to growth hormone while STAT5A is required for physiological responses to prolactin (87).

STAT3 is indispensable during early embryogenesis. Consequently, targeted disruption of the STAT3 gene leads to early embryonic lethality; Takeda *et al*. (88) report that STAT3 deficient embryos show a rapid degeneration between embryonic days 6.5 and 7.5. The cause of lethality has yet to be determined. With the generation of the Cre-*loxP*

Target Gene	Phenotype of Null Mice	Reference
STAT1	Impaired responses to type I and type II interferons	(77, 78)
STAT2	Impaired responses to type I interferons	(79)
STAT3	Embryonic lethality	(88)
STAT4	Loss of IL-12 mediated functions	(80, 81)
STAT5A	Impaired breast development owing to loss of prolactin responsiveness	(85, 87)
STAT5B	Impaired growth owing to loss of growth hormone responsiveness	(86, 87)
STAT6	Loss of IL-4 mediated functions	(82-84)

Table 2.1 – Role of STAT proteins as revealed by gene targeting in mice

Target Tissue	Phenotype of Tissue-Specific STAT3 Null Mice	Reference
β cells/Hypothalamus	Obese, hyperphagic, hyperglycemic, hyperinsulinemic	(89)
Central Nervous System	Obese, hyperphagic, hyperleptinemic, diabetic, infertile	(90)
Liver	Obese, insulin resistant	(91)
Macrophages/Neutrophils	Enhanced inflammatory responses	(92)
Mammary glands	Impaired apoptosis	(93)
POMC Neurons	Mildly obese, hyperphagic	(94)
T lymphocytes	Impaired IL-6 induced proliferation	(95)

Table 2.2 - Tissue-specific roles of STAT3 as revealed by conditional gene targeting in mice

DNA recombination system (96), it has become possible to generate tissue-specific STAT3-deficient mice **(Table 2.2)**. Analysis of these mice reveals an essential role for STAT3 in body weight and energy homeostasis. Studies in mice with a neural-specific disruption in STAT3 demonstrate that STAT3 mediates most, if not all, hypothalamic leptin function (90). The phenotype of these mice resembles that of leptin deficient mice; mutant mice are hyperleptinemic, leptin resistant, obese, diabetic, and infertile. Mice with a β cell/hypothalamic defect in STAT3 (89) and mice with a liver-specific defect in STAT3 (91) display similar phenotypes. Through the study of these mice, Cui *et al*. (89) conclude that β-cell/hypothalamic STAT3 plays a critical role in the control of food intake, body weight, insulin sensitivity, and leptin sensitivity, while Inoue *et al*. conclude that liver STAT3 plays an essential role in normal glucose homeostasis by regulating the expression of gluconeogenic genes (91). Analyses of other tissue-specific STAT3 deficient mice elucidate essential roles for STAT3 in cytokine mediated biological functions and the promotion of cell proliferation through the prevention of apoptosis (92, 93, 95).

4. STATs Effects on Cell Proliferation

Recent discoveries underscore the importance of STAT proteins in cell proliferation. Fukuda *et al*. (97) established that STATs promote cell proliferation through the upregulation of genes encoding cell cycle regulators and apoptosis inhibitors. Specifically, they report that STAT3 plays a key role in the G_1 to S phase cell-cycle transition through the upregulation of the cyclin dependent kinase (CDK) activators cyclin D2, cyclin D3, cyclin A, and cdc25A, and the concomitant down regulation of the CDK inhibitors p21 and p27 (97). Their conclusions are supported by studies demonstrating that dominant negative forms of

STAT3 inhibit the induction cyclin D, cyclin A, and cdc25A, and consequently inhibit entry into S phase of the cell cycle (97). It is further supported by studies showing that cyclin D and the anti-apoptotic proteins Bcl-x_L and Mcl-1 are STAT3 target gene (98-100).

In addition to the fundamental role of STATs in normal cell proliferation, accumulating evidence is defining a role for aberrant STAT signaling in oncogenesis as well (101). Constitutively active STAT3 and STAT5 has been observed in a variety of human cancer cell lines and primary tumors, including blood malignancies (leukemia, lymphoma, multiple myeloma), and solid neoplasias (head and neck, brain, breast, lung, pancreas, prostate cancers) (101-105). Constitutively active STAT3 and STAT5 have also been shown to possess transforming properties and to be strongly associated with tumor development and progression (101). Several studies suggest that STAT3 and STAT5 participate in oncogenesis through the upregulation of genes encoding apoptosis inhibitors, and cell cycle regulators, including Bcl-xL and cyclin D respectively (98, 106).

5. STATs in Adipogenesis

STATs are abundantly expressed in cultured and native preadipocytes and adipocytes (15). The expression of STAT1, STAT5A, and STAT5B increases significantly after the induction of differentiation, STAT3 levels increase slightly, while STAT6 expression does not change. Expression of STATs 1, 5A, and 5B is regulated by PPARγ, suggesting a role for these STATs in the terminal phases of adipogenesis (107). Expression of STATs 3 and 6, however, is regulated upstream the C/EBP family of transcription factors, suggesting a role for these STATs in the early phases of adipogenesis (107).

Deng *et al*.(16) suggest a regulatory role for STAT3 during the proliferative phases of adipogenesis. They report that STAT3 is tyrosine phosphorylated and bound to DNA as 3T3-L1 cells proliferate and become confluent, as well as during mitotic clonal expansion when postconfluent growth-arrested preadipocytes undergo 1-2 rounds of cell division. STAT3 is not tyrosine phosphorylated, however, in growth arrested postconfluent preadipocytes or differentiating adipocytes. This pattern of activation is specific for STAT3 and does not occur for STAT1, STAT5A, STAT5B, or STAT6. To elucidate a potential role for STAT3 during the proliferative phases of adipogenesis, Deng *et al.* blocked STAT3 expression by antisense morpholino oligonucleotides. They repot that diminution of endogenous STAT3 expression significantly decreases preconfluent preadipocyte proliferation. The specific function of STAT3 in preadipocyte proliferation and differentiation, however, is not yet known.

C. STAT ACTIVATING FACTORS

STATs 2, 4, and 6 are activated by a small number of ligands. STATs 1 and 5, however, are activated by means of a number of ligands. STAT3 is also activated by several ligands including leptin, IL-6 family cytokines, and midkine.

1. Leptin

Leptin, the product of the *ob* gene, is a 16 kDa peptide hormone produced and secreted by adipocytes in proportion to adipose mass (108). Leptin regulates food intake, energy expenditure, and body weight *via* central and peripheral actions. The profound importance of leptin is demonstrated by mice with a homozygous mutation in the *ob* gene

(*ob/ob*) (109) or in its receptor (*db/db*) (110). These mice develop massive obesity, hyperglycemia, hyperinsulinemia, and display reduced fertility and a reduced basal metabolic rate.

1.1 Leptin Signaling

Leptin's effects are mediated *via* its interaction with the leptin receptor (Ob-R). Ob-R belongs to the class I cytokine receptor family and is produced in several alternatively spliced forms designated Ob-Ra, Ob-Rb, Ob-Rc, Ob-Rd, Ob-Re, and Ob-Rf (110). All five isoforms share a common extracellular domain and transmembrane domain. The intracellular domain is characteristic for each isoform (110). Ob-Ra, Ob-Rc, Ob-Rd, and Ob-Rf have a short intracellular domain and are thought to play a role in the clearance of leptin from circulation (111), and in the transport of leptin to the brain (112). Ob-Re lacks an intracellular domain and is believed to encode a soluble receptor (110). Ob-Rb has a long intracellular domain and mediates most of leptin signaling (113).

Effects of leptin are further mediated *via* Ob-R activation of the Jak/STAT pathway (114); activation of alternative pathways, including the MAPK pathway, the PI3K pathway, and the AMPK pathway have also been reported (115).

Upon leptin binding to the Ob-R, the Jak/STAT signaling cascade is initiated. Because the Ob-R does not have intrinsic kinase activity, the required tyrosine kinase activity is provided by receptor associated cytoplasmic proteins from the Jak family (116). Specifically, Jaks bind to intracellular domains on the Ob-R and catalyze ligand-induced

phosphorylation of themselves and of intracellular tyrosine residues on the Ob-R. These phosphorylated tyrosines provide docking sites for STATs. STAT proteins are recruited to these phosphorylated tyrosines, whereupon they are tyrosine phosphorylated by Jaks. The activated STATs dimerize, translocate to the nucleus, and stimulate gene transcription. Leptin receptor binding activation of STAT1, 3, 5, and 6, has been described (115).

Originally, it was thought that the hypothalamus was the only tissue expressing the long form of the leptin receptor. Recent evidence, however, confirmed that peripheral organs, including WAT, express the functional Ob-Rb as well (18, 117, 118). Recent studies performed *in vitro* and *in vivo* further demonstrate that adipocyte Ob-Rb can activate the Jak/STAT pathway. Specifically, incubation of 3T3-L1 adipocytes with recombinant leptin activates STAT3 (119). Furthermore, intraperitoneal leptin administration to wild-type and *ob/ob* mice causes prompt activation and nuclear translocation of STAT1 and 3 in WAT (119, 120). Kim *et al*. (119) confirm that this effect is mediated by the long form of the receptor; leptin injection in *db/db* mice does not result in STAT3 tyrosine phosphorylation. They further demonstrate that leptin directly activates STAT3 in WAT; intracerebroventricular administration of leptin does not result in adipocyte STAT3 tyrosine phosphorylation.

1.2 Metabolic Effects of Leptin in WAT

Leptin's metabolic effects are exerted at the level of the central nervous system, *via* Ob-Rb interaction in regions of the hypothalamus that control feeding behavior and hunger, body temperature and energy expenditure (121). The metabolic effects of leptin are not due

solely to actions *via* the central nervous system however. Several lines of evidence support direct peripheral effects of leptin as well. For example, the presence of the Ob-Rb on adipocytes, and the adipose reducing effects of leptin beyond that that can be accounted for by a reduction in food intake alone (122), suggest that leptin might have direct autocrine/paracrine effects on adipocytes (19). It is now clear from *in vivo* and *ex vivo* studies that leptin stimulates lipolysis in adipocytes **(Section 1.2.1)** (18-23). Recent *in vitro* and *in vivo* studies also confirm that leptin promotes adipocyte fatty acid oxidation and inhibits lipogenesis **(Section 1.2.2)** (23-25). Because STAT3 is a downstream target of leptin, STAT3 likely mediates the weight reducing effects of this cytokine on adipocytes. The contribution of STAT3 to these aspects of body weight homeostasis, however, has yet to be determined.

Given the fat depleting autocrine/paracrine actions of leptin, it is surprising that diet-induced obese (DIO) rodents undergo adipocyte hypertrophy despite hyperleptinemia within the fat-depleting range (123). These findings prompted Wang *et al.* (123) to determine if adipocyte leptin resistance contributes to the pathogenesis of obesity (123). In these studies, Wang *et al.* conclude that a leptinergic blockade, as demonstrated by a decrease in Ob-Rb expression, a decrease in STAT3 tyrosine phosphorylation, and an increase in suppressor of cytokine signaling-3 (SOCS3) expression, protects DIO rodents from leptin's fat depleting autocrine/paracrine actions. They also conclude that fat storage in adipocytes requires inactivation of leptin's autocrine/paracrine activities. Specifically, by restoring Ob-Rb expression, Ob-Rb activation of the Jak/STAT signaling pathway, and the downstream anti-lipogenic, and pro-lipolytic and -oxidative actions of leptin, transgenic mice that

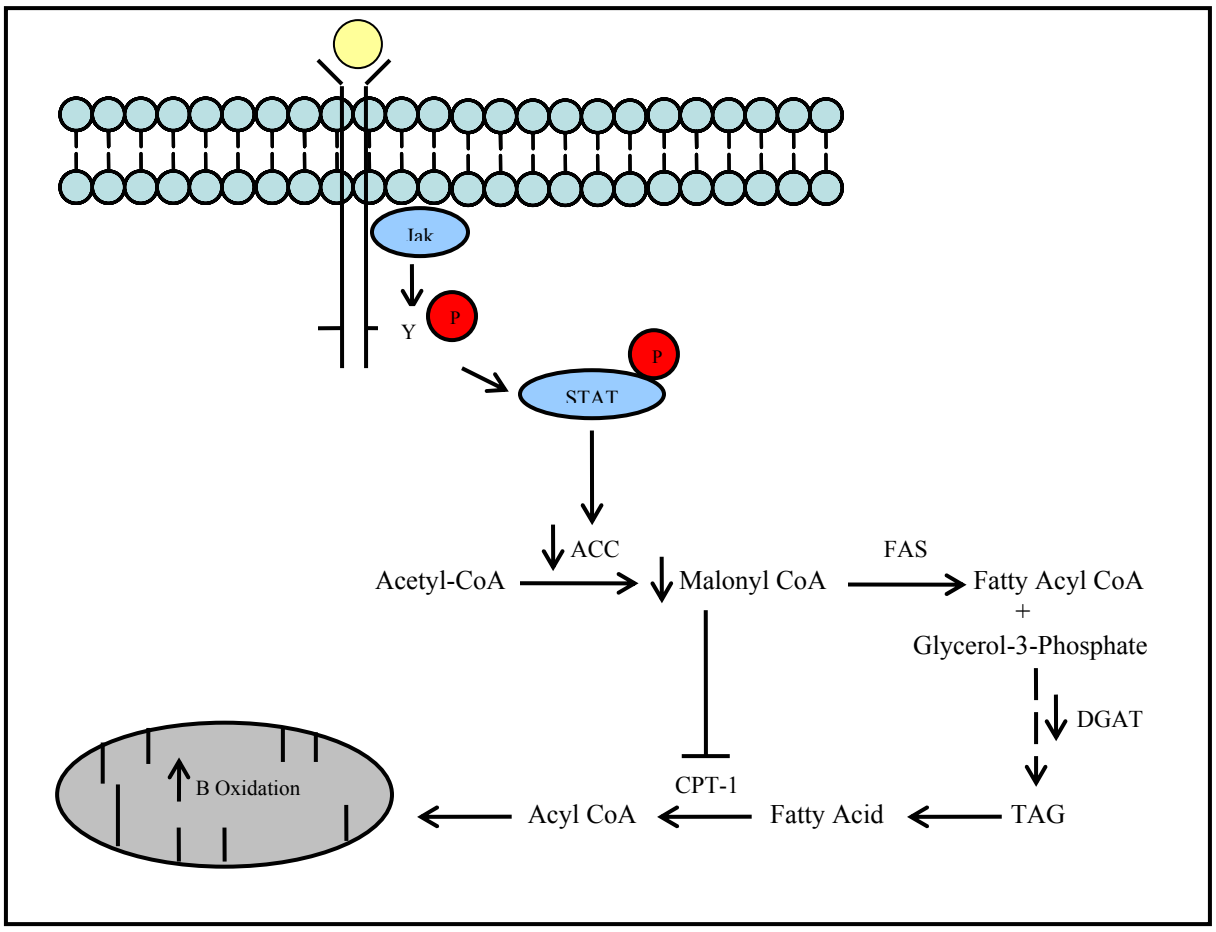


Figure 2.4 – Metabolic effects of leptin in white adipose tissue
Leptin, *via* Ob-Rb activation of the Jak/STAT pathway, causes a down regulation of genes encoding lipogenic enzymes including ACC, FAS, and DGAT. The down regulation of ACC results in a decrease in malonyl-CoA content and a subsequent increase in fatty acid oxidation by disinhibition of CPT1.

constitutively express Ob-Rb on adipocytes, remain slender on a high fat diet that causes obesity in wild-type controls. Wang *et al.* (123) confirm that the slender phenotype is a consequence of increased oxidation of fatty acids within adipocytes, coupled with a reduction in lipogenesis. Specifically, they report increased expression at the mRNA level of carnitine palmitoyltransferase-1 (CPT-1). Furthermore, consistent with a reduction in lipogenesis, they report decreased expression of lipogenic enzymes, including acetyl-CoA carboxylase-1 (ACC-1), diacylglycerol acyltransferase-1 (DGAT-1), diacylglycerol acyltransferase-2 (DGAT-2), and glycerol-3-phosphate acyltransferase-1 (GPAT-1).

1.2.1 Leptin Induced Lipolysis

Both *in vivo* and *ex vivo* studies confirm that leptin stimulates lipolysis in adipocytes. Specifically, leptin treatment *in vivo* dramatically reduces WAT triglyceride stores (19, 20). Additionally, in both *ob/ob* mice and lean mice, leptin increases glycerol release in a time- and dose-dependent manner (18, 21). Leptin-induced glycerol release, however, is unaccompanied by the parallel release of free fatty acids induced by other lipolytic hormones (23).

In contrast to *ob/ob* mice and lean mice, leptin's lipolytic effects are absent in fat pads from *db/db* mice and *fa/fa* rats. For example, in animal models lacking the functional Ob-Rb, injections of leptin have no significant effect on lipolytic activity (22). *Ex vivo* studies performed by Siegrist-Kaiser *et al*., (18), show similar results. Leptin stimulates basal lipolysis in white fat pads *ex vivo* in a time- and dose-dependent manner. This effect is absent in fat pads from *fa/fa* rats, thus confirming the requirement of a functional Ob-Rb.

1.2.2 Leptin and Fatty Acid Oxidation/Lipogenesis

In vitro and *in vivo* studies confirm that leptin stimulates fatty acid oxidation and inhibits lipogenesis in adipocytes. In 30A5 preadipocytes, leptin represses ACC gene expression and activity, and inhibits the subsequent processes of fatty acid synthesis and TAG synthesis (24). Zhou *et al*. (25) observed an increase in fatty acid oxidation and a reduction in lipogenesis in adenovirus-induced hyperleptinemic rats (25). Decreases in ACC expression and activity explained the observed changes in this mouse model; phosphorylation and inhibition of ACC reduced the capacity of adipocytes to form new fat and increased fatty acid oxidation by reducing malonyl CoA levels and thereby disinhibiting CPT-1. Orci *et al.* (23) further report that *in vivo* adenovirus induced hyperleptinemia decreases the expression of enzymes of fatty acid synthesis, including fatty acid synthase (FAS), and increases the expression of enzymes of fatty acid oxidation, including CPT-1 and acyl-CoA oxidase (ACO).

2. IL-6-Type Cytokines

The interleukin-6 (IL-6) family of cytokines is a family of structurally and functionally related proteins, including IL-6, IL-11, leukemia inhibitory factor (LIF), oncostatin M (OSM), ciliary neurotrophic factor (CNTF), cardiotrophin-1 (CT-1), and cardiotrophin-like cytokine (CLC). These cytokines activate target genes involved in proliferation, differentiation, and apoptosis (124). Two of the IL-6 family members, IL-6 and CNTF, have metabolic actions as well; both IL-6 and CNTF suppress appetite and induce weight loss. It was recently suggested that the anti-obesity effects of IL-6 and CNTF are due in part to direct autocrine/paracrine actions on adipocytes.

2.1 IL-6-and CNTF Signaling

IL-6 and CNTF exert their metabolic actions through binding, sequential assembly, and activation of a multi-subunit receptor complex composed of a ligand-specific α subunit and a signal transducing subunit. The binding of IL-6 and CNTF to their respective α receptor triggers the association and dimerization of the signal transducing subunit, leading to activation of the Jak/STAT pathway. Specifically, the binding of IL-6 to the IL-6Rα triggers the subsequent association and homodimerization of gp130 (125), while the binding of CNTF to the CNTFRα triggers the subsequent association and heterodimerization of the gp130 and LIFR (126).

2.2 Metabolic Effects of IL-6 in WAT

IL-6 is released from immune cells during inflammation whereupon it elicits pro-inflammatory effects including induction of the acute-phase response, and proliferation and differentiation of B- and T-lymphocytes (127). In the absence of inflammation, a large proportion of circulating IL-6 is derived from adipose tissue (128). Similarly to leptin, IL-6 levels in the serum correlate positively with BMI, suggesting an important role for this cytokine in body weight homeostasis. To investigate the role of IL-6 in the regulation of body weight, Wallenius *et al*. (129) created IL-6 knockout mice. These mice develop mature-onset obesity that is partially reversed by IL-6 replacement. The obesity related metabolic perturbations that accompany mature-onset obesity are also partially reversed by intraperitoneal injection of IL-6 (129). It was recently postulated by Wallenius *et al.* (130) that IL-6 functions as a lipostatic protein, similarly to leptin, to cause weight loss. This hypothesis is supported by the finding that the IL-6 receptor complex is distributed in regions

of the hypothalamus involved in the regulation of food intake and body weight (131, 132). It is further supported by studies showing that centrally administered IL-6 decreases body fat mass by increasing energy expenditure and decreasing food intake. The anti-obesity effects of IL-6 are not due solely to actions *via* the central nervous system however (133). Several lines of evidence also support direct peripheral effects of IL-6. Data presented by Path *et al*. (26) demonstrate autocrine/paracrine actions of IL-6 on adipocytes. IL-6 and the IL-6 receptor complex, including the ligand binding α subunit and the signal transducing gp130 subunit, are expressed in human adipocytes and 3T3-L1 cells (26). Studies performed *in vitro* further demonstrate that the adipose IL-6 receptor can activate the Jak/STAT pathway (134). Acute exposure of 3T3-L1 adipocytes to recombinant IL-6 results in STAT3 tyrosine phosphorylation. Several groups report the downstream actions of IL-6 in adipose tissue as well. Most importantly, IL-6 stimulates lipolysis, decreases LPL activity and causes a notable decline in the uptake of circulating triglycerides, and increases leptin production (26-30). The increased lipolysis, decreased LPL activity, and high rates of leptin production in response to IL-6 may account for a portion of the weight loss observed in IL-6 treated rodents.

2.3 Metabolic Effects of CNTF in WAT

CNTF was initially recognized for its neuroprotective effects, leading to its evaluation in patients suffering from amyotrophic lateral sclerosis (135, 136). In these clinical trials, subcutaneous administration of recombinant CNTF caused unexpected and substantial weight loss. The weight reducing effects of CNTF were further examined and confirmed in rodent models of obesity (137-139). Daily intraperitoneal administration of CNTF to *ob/ob*

mice produces a dose-dependent decrease in body weight characterized by decreased food intake and a preferential loss of fat as opposed to lean body mass (137, 138). Similarly, in *db/db* mice, treatment with CNTF causes dose- and time-dependent weight loss and suppression of food intake (137, 139). Studies performed in DIO mice show similar results (137, 138). CNTF decreases food intake in a dose-dependent manner, resulting in reduced body weight and adiposity.

The adipose reducing effects of CNTF, however, are beyond that that can be accounted for by reduced caloric intake alone. It was suggested therefore, that CNTF, like leptin, might have direct effects on adipocytes as well (139). Recent studies by Zvonic *et al*. (31) confirm this. CNTF receptor complex proteins, including the α subunit, the LIFR, and gp130, are expressed in 3T3-L1 cells. Studies performed *in vitro* and *in vivo* further demonstrate that the adipose CNTF receptor can activate the Jak/STAT pathway. Incubation of 3T3-L1 adipocytes with recombinant CNTF results in a dose- and time- dependent activation and nuclear translocation of STAT3 (31). Furthermore, intraperitoneal CNTF administration to wild-type mice causes prompt activation of adipocyte STAT3. Zvonic *et al*. also report the downstream actions of CNTF. In 3T3-L1 adipocytes, CNTF represses FAS gene expression, causes a notable reduction in sterol regulatory element binding protein-1 (SREBP-1) protein levels, and a resulting decline in fatty acid biosynthesis. Zvonic *et al*. conclude that the decreased biosynthesis of fatty acids in adipose tissue in response to CNTF may account for a portion of the weight loss observed in CNTF treated rodents.

3. Midkine

Midkine is a secreted heparin-binding growth factor encoded by a retinoic acid responsive gene (140). The mature molecule is a basic, cysteine-rich polypeptide of molecular weight 14kDa (141). Midkine's biological activities include fibrinolytic, anti-apoptotic, mitogenic, transforming, and angiogenic ones (142).

3.1 Midkine Signaling

Midkine exerts its functions through interaction with specific cell-surface receptors. Receptor-type protein tyrosine phosphatase ζ (PTPζ), low-density-lipoprotein-receptor-related protein (LRP), $\alpha_4\beta_1$- and $\alpha_6\beta_1$-integrins, and anaplastic lymphoma kinase (ALK) have been identified as receptors for midkine. PTPζ is a chondroitin sulfate proteoglycan with an intracellular tyrosine phosphatase domain. Midkine's interaction with PTPζ is important in migration and survival of embryonic neurons (143). LRP, a member of the LDL-receptor family, is involved in the anti-apoptotic activities of midkine (144), while $\alpha_4\beta_1$- and $\alpha_6\beta_1$-integrins are involved in midkine dependent cell migration and neurite outgrowth (145). Finally, ALK, a receptor-type tyrosine kinase, utilizes PI3-kinase and Erk for intracellular signaling in the promotion of cell growth (146). Midkine also utilizes the Jak/STAT pathway for midkine dependent cell proliferation (147).

3.2 Biological Effects of Midkine

The biological activities of midkine are diverse. In the nervous system, midkine regulates neurite outgrowth and neuron survival (148, 149). Accumulating evidence is defining a role for midkine in oncogenesis as well. Midkine is overexpressed in a variety of

cancers including esophageal (150), gastric (151), colon (152), pancreatic (153), lung (154), and breast (155). In addition, midkine serves as an autocrine mitogen for tumor cells (147). Midkine also possesses transforming properties: forced expression of midkine causes NIH-3T3 cells to undergo cellular transformation and causes tumor formation in nude mice (156). Finally, midkine inhibits the induction of apoptosis (157), promotes angiogenesis (158), and stimulates tyrosine phosphorylation of several cellular proteins, including Erk1, Erk2, Akt, Jak, and STAT1 (147, 157).

CHAPTER III
MECHANISM OF STAT3 ACTIVATION DURING 3T3-L1 ADIPOGENESIS

STAT3 is abundantly expressed in preadipocytes and adipocytes, and highly activated and bound to DNA in proliferating preadipocytes and adipocytes. STAT3 activation during adipogenesis is delayed, however, suggesting that STAT3 tyrosine phosphorylation occurs by an indirect mechanism. The current work aimed to identify the differentiation-induced STAT3 activating factor and determine its role in adipogenesis. Our findings are presented below in the manuscript titled "Midkine is an Autocrine Activator of STAT3 in 3T3-L1 Cells".

Manuscript #1: **Midkine is an Autocrine Activator of STAT3 in 3T3-L1 Cells**

Authors: Erin R. Cernkovich, Jianbei Deng, Kunjie Hua, Joyce B. Harp

Published in: Endocrinology. 2007 Apr;148(4):1598-604

A. ABSTRACT

Mitotic clonal expansion is believed to be necessary for 3T3-L1 adipocyte formation. Signal transducer and activator of transcription 3 (STAT3), a mitogenic signaling protein, is activated through tyrosine phosphorylation during the proliferative phases of adipogenesis. We hypothesize that this signaling protein plays a key role in mitotic clonal expansion and differentiation. Here we determined that the adipocyte differentiation cocktail containing isobutylmethylxanthine, dexamethasone, and insulin (MDI) induced STAT3 tyrosine phosphorylation indirectly through the synthesis of an autocrine/paracrine factor. We further determined that the factor has heparin binding properties, and identified the factor as midkine, a pleiotrophic growth factor previously associated with neuronal development and oncogenesis. Recombinant midkine induced STAT3 tyrosine phosphorylation in a time- and dose-dependent manner and stimulated the proliferation of post-confluent 3T3-L1 cells. Midkine neutralizing antibodies inhibited differentiation-induced STAT3 tyrosine phosphorylation as well as adipogenesis. These results show that MDI-induced synthesis and release of midkine explains the delayed activation of STAT3 during adipogenesis, and that the midkine-STAT3 signaling pathway plays a necessary role in mitotic clonal expansion and differentiation.

B. INTRODUCTION

Obesity occurs when energy intake chronically exceeds energy expenditure. Excess energy is stored in adipose tissue as triacylglycerol (159). To accommodate the increased triacylglycerol, adipose tissue expands, primarily through an increase in fat cell size. Upon reaching a critical size, enlarged adipocytes secrete factors that promote preadipocytes to proliferate and differentiate into adipocytes (160). Although much is known about the mechanisms of preadipocyte differentiation, less is known about the mechanisms of preadipocyte proliferation.

Many of the advances in our understanding of adipogenesis are based on studies in 3T3-L1 cells. 3T3-L1 preadipocytes are fibroblast-like cells committed to the adipocyte lineage. In culture, 3T3-L1 preadipocytes replicate until they form a confluent monolayer (6). At confluence, cell-cell contact triggers growth arrest. When induced with hormonal agents, often a cocktail of isobutylmethylxanthine, dexamethasone, and insulin (MDI), growth-arrested preadipocytes reenter the cell cycle and undergo 1-2 rounds of cell division known as mitotic clonal expansion (7). Following mitotic clonal expansion, preadipocytes exit the cell cycle, commit to terminal differentiation, and begin to express adipocyte specific genes (8).

The major transcriptional regulators of adipogenesis include proteins belonging to the CCAAT/enhancer binding protein (C/EBP) family and the peroxisome proliferator-activated receptor (PPAR) superfamily. Signal transducers and activators of transcription (STATs) have also been implicated in the differentiation program. A coordinated cascade involving

the above mentioned factors typifies the differentiated phenotype (9-11). Specifically, mitotic clonal expansion is characterized by a transient increase in the expression of the transcription factors C/EBPβ (38) and δ (38), as well as the tyrosine phosphorylation and activation of STAT3 (16). Furthermore, acquisition of the terminally differentiated phenotype depends on transcriptional activation of C/EBPα and PPARγ (161).

Midkine is a secreted heparin-binding growth factor encoded by a retinoic acid responsive gene (140). The mature molecule is a basic, cysteine-rich polypeptide of molecular mass 14kDa (141). Midkine's biological activities are diverse, and include regulation of neurite outgrowth and neuron survival (148, 149). Accumulating evidence is defining a role for midkine in oncogenesis as well. Midkine is overexpressed in a variety of cancers including esophageal (150), gastric (151), colon (152), pancreatic (153), lung (154), and breast (155). Additionally, midkine serves as an autocrine mitogen for tumor cells. Midkine also possesses transforming properties: forced expression of midkine causes NIH-3T3 cells to undergo cellular transformation and causes tumor formation in nude mice (156). Finally, midkine inhibits the induction of apoptosis (157), promotes angiogenesis (158), and stimulates tyrosine phosphorylation of several cellular proteins, including STAT1 (147, 157).

In this report, we identified a midkine-STAT3 signaling pathway that plays a necessary role in mitotic clonal expansion and differentiation.

C. MATERIALS AND METHODS

Materials

3T3-L1 cells were purchased from ATCC (Manassas, VA). Affinity-purified rabbit polyclonal phosphotyrosine 705-specific anti-STAT3 (STAT3-PY) and rabbit polyclonal anti-STAT3 were purchased from Cell Signaling (Beverly, MA). Affinity-purified rabbit polyclonal anti-C/EBPα, mouse monoclonal anti-PPARγ, human polyclonal anti-midkine and normal goat IgG were purchased from Santa Cruz Biotechnology, Inc. (Santa Cruz, CA). Recombinant human midkine was purchased from R&D Systems (Minneapolis, MN). The enhanced chemiluminescence detection kit and horseradish peroxidase-conjugated secondary antibodies were purchased from Pierce Biotechnology, Inc. (Rockford, IL). The HiTrap™ Heparin HP column was purchased from Amersham Pharmacia (Piscataway, NJ).

Cell culture

3T3-L1 preadipocytes were cultured in Dulbecco's Modified Eagle's Medium (DMEM) containing 10% v/v fetal bovine serum (FBS), 10 mg/ml streptomycin, 100 U/ml penicillin, and 1 mM pyruvate at 37°C in 5% CO_2 air. 3T3-L1 cells were studied as pre- and post-confluent preadipocytes and as adipocytes. To induce differentiation, 2-day post-confluent cells were treated with 0.5μM dexamethasone, 0.5 mM isobutylmethylxanthine, and 10μg/ml insulin in DMEM/10% FBS for 72 hours. On day 3, the differentiation medium was replaced with DMEM/10% FBS, which was changed every 2 days thereafter until analysis.

Immunoblot analysis

3T3-L1 cells were washed twice in PBS with 1 mM orthovanadate, then placed immediately in sample buffer (1% Nonidet P-40, 20 mM Tris-HCL (pH 8.0), 150 mM NaCl, 1 mM EDTA, 0.1% NaN_3, 10 μg/ml aprotinin, 1 μM pepstatin, 16.4 μg/ml leupeptin, 1 mM phenylmethyl-sulfonylfluoride, 0.1 mM Na_3VO_4, 2% SDS, 10% glycerol) without dithiothreitol or tracking dye. Lysates were heated and protein concentrations were determined using Bio-Rad Laboratories, Inc., DC Protein Assay kit (Richmond, CA). Bovine serum albumin (BSA) was used as a standard. Samples were heated for 2 minutes at 85°C, separated by 10% SDS-PAGE, and analyzed by immunoblotting as previously described (16). Immunoblots were developed using the enhanced chemiluminescence kit.

RNA isolation

Total RNA was isolated from 3T3-L1 cells using the RNeasy mini kit (Qiagen, Inc., Valencia, CA) at 0, 1, 3, 6, 24, 48, and 72 hours after induction of differentiation. RNA quality was confirmed by ethidium bromide staining and detection of intact 28S and 18S ribosomal RNA bands.

Reverse transcriptase PCR

Deoxyribonuclease-treated RNA, collected 0, 1, 3, 6, 24, 48, and 72 hours after induction of differentiation, was reversed transcribed using the Qiagen OneStep RT-PCR kit (Qiagen, Inc., Valencia, CA). 5'ACCGAGGCTTCTTCCTTCTCGCCCTTCTTGCCC3' and 5'CCCTGCACCTCCAAGACCAAGTCAAAGACC3' were used as forward and reverse primers respectively.

Heparin affinity column

Twenty-four hour conditioned medium (CM) was applied to a Hi Trap™ Heparin HP column. The column was washed with 0.02 M Tris-HCl (pH 7.5), and eluted with NaCl in doses ranging from 0 M to 2 M. To concentrate and desalt the eluted fractions, fractions were centrifuged three times at 5500 rpm for 45 minutes at 4ºC.

Midkine neutralization assay

Recombinant human midkine at a concentration of 10.0ng/ml was neutralized with anti-midkine antibody (M-18), in doses ranging from 0.1 μg/ml to 10.0 μg/ml, for 1 hour at 37ºC. Post-confluent preadipocytes were stimulated with recombinant human midkine, or recombinant human midkine neutralized with anti-midkine antibody. Cells were harvested after 10 minutes of treatment.

CM collected 24 hours after stimulation with MDI (A1 CM) was neutralized with 10.0 μg/ml normal goat IgG or 10.0 μg/ml anti-midkine antibody (M-18) for 1 hour at 37ºC. Post-confluent preadipocytes were stimulated with A1 CM, or A1 CM neutralized with 10.0 μg/ml normal goat IgG or 10.0 μg/ml anti-midkine antibody. Cells were harvested after 10 minutes of treatment.

Proliferation assay

Preconfluent 3T3-L1 preadipocytes were seeded in 96-well plates at a density of 2000 cells/100μl/well. Cells were seeded in DMEM containing 10% FBS. Vehicle (PBS), 10.0 ng/ml recombinant human midkine, or MDI was added to culture medium with or without

cells at 2-days post-confluence. At 0, 24, 48, and 72 hours after stimulation, a colorimetric proliferation assay (CellTiter 96 Aqueous nonradioactive cell proliferation assay; Promega, Madison, WI) was performed as directed by the manufacturer. To calculate the absorbance values at each time point, the mean absorbance of two blank wells (containing vehicle, recombinant human midkine, or MDI in culture medium without cells) was subtracted from the mean absorbance of three wells containing cells.

Oil Red O staining

Eight-twelve days after induction of differentiation, 3T3-L1 adipocytes were washed with PBS, fixed with 3.7% formaldehyde in PBS, then stained with 0.5% Oil Red-O.

D. RESULTS

An autocrine/paracrine factor induces STAT3 activation in 3T3-L1 cells.

STAT3 is activated within the first 24 hours after induction of differentiation (10). To better define the timing of MDI-induced STAT3 tyrosine phosphorylation, cell lysates were recovered 1, 3, 6, 12 and 24 h after MDI stimulation. STAT3 tyrosine phosphorylation was not observed until 3 hours after the induction of differentiation **(Figure 3.1)**. This 3 hour delay in STAT3 activation is not consistent with the immediate tyrosine phosphorylation that typically occurs minutes after ligand stimulation (162). This data suggests that induction of differentiation with MDI stimulates the tyrosine phosphorylation of STAT3 by an indirect mechanism.

To determine whether MDI induces the release of a STAT3 activating factor, post-confluent preadipocytes were induced to differentiate with MDI, and CM was collected 5 minutes and 24 hours following stimulation. Unstimulated post-confluent preadipocytes were then stimulated with either the 5 minute CM or the 24 hour CM for 5 minutes. Treatment of unstimulated preadipocytes with 24 hour CM induced STAT3 tyrosine phosphorylation, suggesting that MDI stimulated the release of a STAT3 activating factor over the 24 hour period **(Figure 3.2A)**. Treatment of unstimulated preadipocytes with 5 minute CM however, did not induce STAT3 activation, suggesting that release of the activating factor had not occurred within this short time frame.

To determine the cellular source of the STAT3 activating factor, we next collected CM daily from 3T3-L1 cells at various stages of proliferation and differentiation.

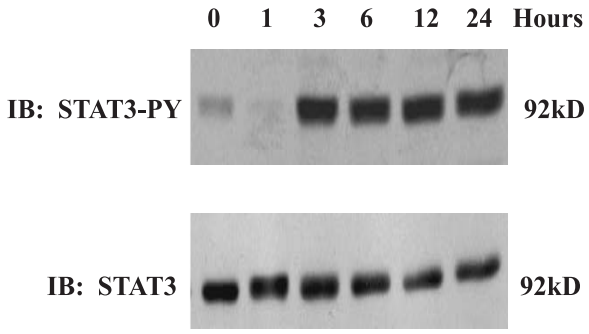


Figure 3.1 – Pattern of STAT3 activation in 3T3-L1 preadipocytes.
Whole cell lysates were prepared from 3T3-L1 cells at various times (0, 1, 3, 6, 12, and 24 hours) after induction of differentiation with MDI. Western blot analysis (IB) was performed with anti-STAT3-PY antibody. Blots were stripped and re-probed with anti-STAT3 antibody. Results are representative of 3 separate experiments.

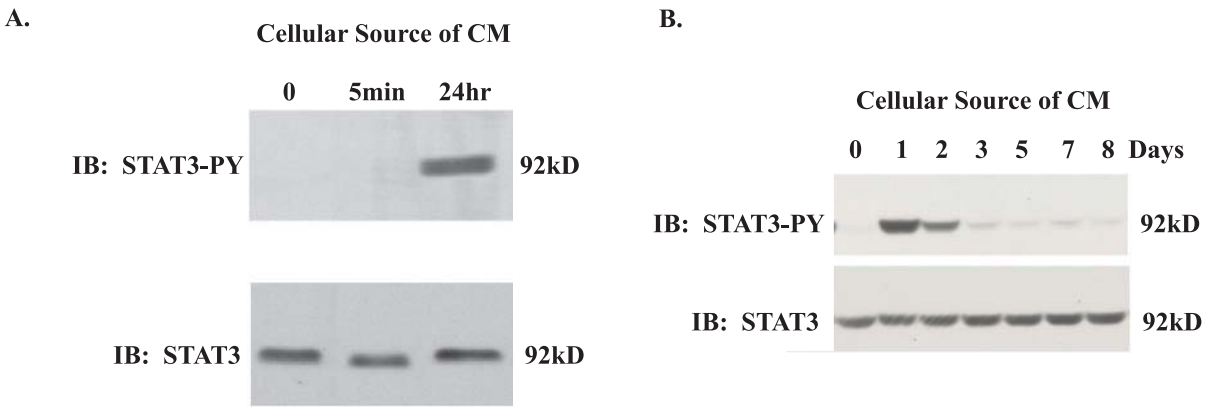


Figure 3.2 – Effect of CM stimulation on STAT3 tyrosine phosphorylation in 3T3-L1 preadipocytes and adipocytes.
(A) 3T3-L1 preadipocytes were cultured in the presence of CM generated 5 minutes after stimulation with MDI, or CM generated 24 hours after stimulation with MDI. After a 5 minute stimulation, whole cell lysates were prepared and Western blot analysis (IB) was performed with anti-STAT3-PY antibody. Blots were stripped and re-probed with anti-STAT3 antibody.
(B) 3T3-L1 preadipocytes were cultured in the presence of CM generated 1, 2, 3, 5, 7, or 8 days after stimulation with MDI. After a 5 minute stimulation, whole cell lysates were prepared and Western blot analysis was performed with anti-STAT3-PY antibody. Blots were stripped and re-probed with anti-STAT3 antibody. Results are representative of 3 separate experiments.

Unstimulated post-confluent preadipocytes were then stimulated with this CM. As shown in **Figure 3.2B**, CM from post-confluent proliferating preadipocytes (1 and 2 days after induction of differentiation) induced STAT3 tyrosine phosphorylation. STAT3 tyrosine phosphorylation was barely detectable, however, in cells stimulated with CM from growth-arrested preadipocytes (0) and adipocytes (3-8).

Transcription and translation are required for autocrine/paracrine activation of STAT3.

As 24 hour CM induced STAT3 tyrosine phosphorylation, but 5 minute CM did not, we hypothesized that the STAT3 activating factor was synthesized *de novo* in response to MDI. Post-confluent preadipocytes were pretreated with cycloheximide or actinomycin D prior to generation of 24 hour CM. A new group of post-confluent preadipocytes was then stimulated with the inhibitor pretreated CM for 5 minutes. Inhibition of protein synthesis with cycloheximide during the generation of CM significantly reduced CM-induced STAT3 tyrosine phosphorylation **(Figure 3.3A)**. Blockade of mRNA synthesis with actinomycin D completely inhibited CM-induced STAT3 tyrosine phosphorylation, indicating that RNA synthesis is required to generate the STAT3 activating factor.

Identification of a heparin binding autocrine/paracrine factor.

Efforts to identify the activating factor were first directed towards the traditional activator of STAT3, IL-6. We determined in a series of studies that IL-6 was released from post-confluent preadipocytes and that IL-6 activated STAT3 in these cells. However, removal of IL-6 from the CM had no effect on STAT3 tyrosine phosphorylation (data not

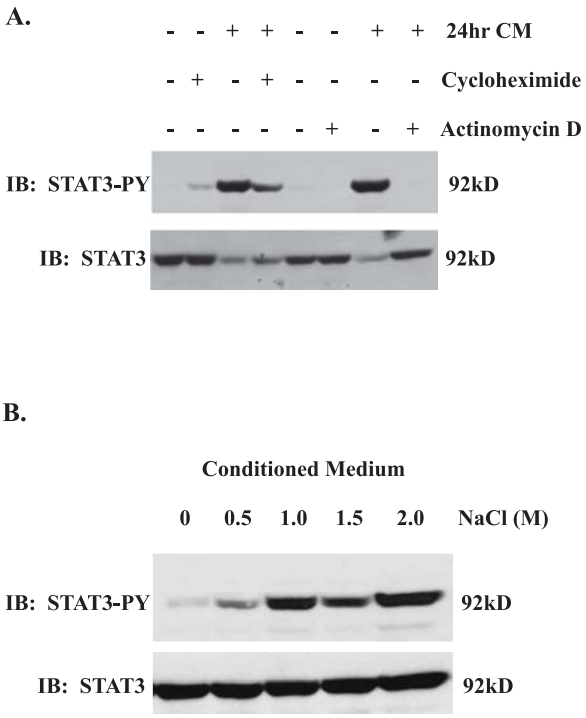


Figure 3.3 – Effects of cycloheximide, actinomycin D, and heparin affinity column pretreatment on CM-induced activation of STAT3.
(A) 3T3-L1 preadipocytes were cultured in the presence of 24 hour CM generated by preadipocytes pretreated with either 10.0µg/ml cycloheximide or 5.0µg/ml actinomycin D. After a 5 minute stimulation, whole cell lysates were prepared and Western blot analysis (IB) was performed with anti-STAT3-PY antibody. Blots were stripped and re-probed with anti-STAT3 antibody.
(B) 3T3-L1 preadipocytes were cultured in the presence of 24 hour CM eluted from a heparin affinity with increasing concentrations of NaCl (0.5M, 1.0M, 1.5M, or 2.0M). After a 5 minute stimulation, whole cell lysates were prepared and Western blot analysis was performed with anti-STAT3-PY antibody. Blots were stripped and re-probed with anti-STAT3 antibody. Results are representative of 3 separate experiments.

shown). This indicated that IL-6 was not responsible for the autocrine/paracrine activation of STAT3.

Because STAT3 has been implicated in the proliferative phases of adipogenesis, efforts to identify the activating factor were next directed towards factors known to stimulate preadipocyte proliferation. Heparin binding growth factors are released into the culture medium and act as autocrine/paracrine factors contributing to preadipocyte proliferation (160). Therefore, to narrow our search, we determined whether the STAT3 activating factor had heparin binding properties. Twenty-four hour CM was applied to a heparin affinity column and eluted with increasing concentrations of NaCl. Treatment of unstimulated post-confluent preadipocytes with 24 hour CM eluted from the heparin affinity column induced STAT3 tyrosine phosphorylation **(Figure 3.3B)**. The greatest effect was seen with CM eluted at 1-2 M NaCl. This led us to search for STAT3 activating ligands with heparin binding properties.

Midkine is the autocrine/paracrine activator of STAT3.

The heparin-binding growth factor midkine is a regulator of normal and transformed cell proliferation. Additionally, midkine stimulates tyrosine phosphorylation of STAT1 in other cell lines (147). Therefore, we tested the ability of recombinant midkine to activate STAT3 in 3T3-L1 cells. Post-confluent preadipocytes were cultured in the presence of varying doses of recombinant midkine and STAT3 tyrosine phosphorylation was measured by western blot analysis at several time points following stimulation. As shown in **Figure 3.4A**, the addition of midkine induced STAT3 tyrosine phosphorylation in a dose-dependent

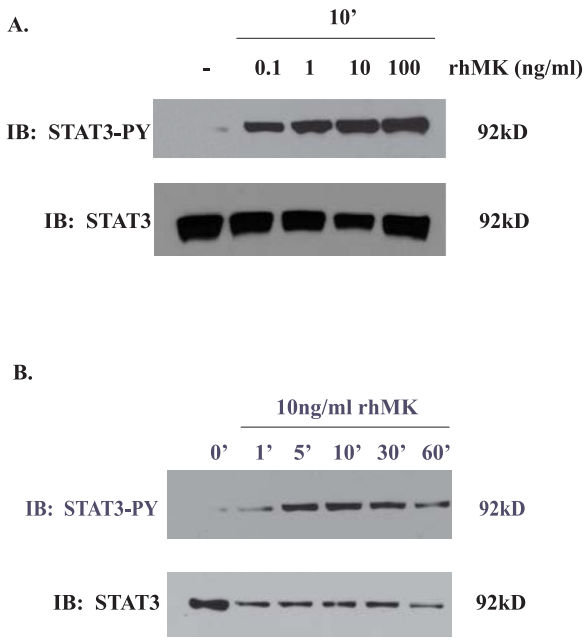


Figure 3.4 – Effect of recombinant midkine stimulation on STAT3 tyrosine phosphorylation in 3T3-L1 preadipocytes.
(A) 3T3-L1 preadipocytes were cultured in the presence of varying concentrations (0.1ng/ml, 1.0ng/ml, 10.0ng/ml, or 100.0ng/ml) of recombinant midkine (rhMK). After a 10 minute stimulation, whole cell lysates were prepared and Western blot analysis (IB) was performed with anti-STAT3-PY antibody. Blots were stripped and re-probed with anti-STAT3 antibody.
(B) 3T3-L1 preadipocytes were cultured in the presence of 10.0ng/ml rhMK. After a 1, 5, 10, 30, or 60 minute stimulation, whole cell lysates were prepared and Western blot analysis was performed with anti-STAT3-PY antibody. Blots were stripped and re-probed with anti-STAT3 antibody. Results are representative of 3 separate experiments.

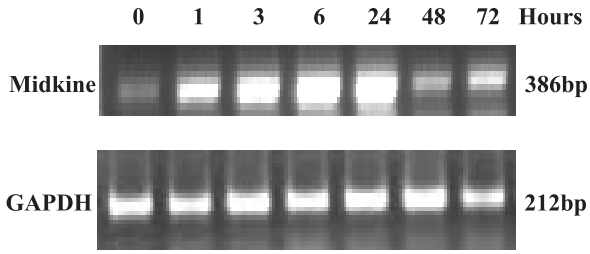


Figure 3.5 – Midkine expression in 3T3-L1 preadipocytes.
Midkine expression in 3T3-L1 cells 0, 1, 3, 6, 24, 48, and 72 hours following induction of differentiation with MDI was measured by RT-PCR.

manner. **Figure 3.4B** shows that midkine also induced STAT3 tyrosine phosphorylation in a time-dependent manner. Because STAT3 tyrosine phosphorylation peaked following a 10 minute stimulation with 10.0 ng/ml recombinant midkine, this time and dose were used for all subsequent experiments.

Earlier studies confirmed that the STAT3 activating factor was synthesized following stimulation with MDI **(Figure 3.3A)**. To determine whether midkine is expressed in 3T3-L1 cells, we measured midkine expression at several time points following stimulation with MDI using RT-PCR. Oligonucleotide primers were used to amplify a 386 bp fragment of mouse midkine. **Figure 3.5** shows that midkine is expressed in 3T3-L1 preadipocytes, and that midkine expression coincides with MDI-induced STAT3 tyrosine phosphorylation. The 386bp fragment was sequenced and confirmed to be midkine (data not shown).

As midkine is a heparin binding growth factor expressed in 3T3-L1 cells, and because recombinant midkine activates STAT3 in 3T3-L1 cells, we hypothesized that midkine was the autocrine/paracrine activator of STAT3. Consequently, we hypothesized that neutralizing midkine in CM would lead to a decrease in CM-induced STAT3 tyrosine phosphorylation. First, to confirm efficient neutralization, recombinant midkine was neutralized with varying concentrations of anti-midkine antibody. **Figure 3.6A** shows that midkine was efficiently neutralized with 10.0 μg/ml anti-midkine antibody. Although there were decreases in STAT3 tyrosine phosphorylation, STAT3 protein levels did not change.

Next, to demonstrate specificity of the neutralizing antibody, recombinant IL-6 was

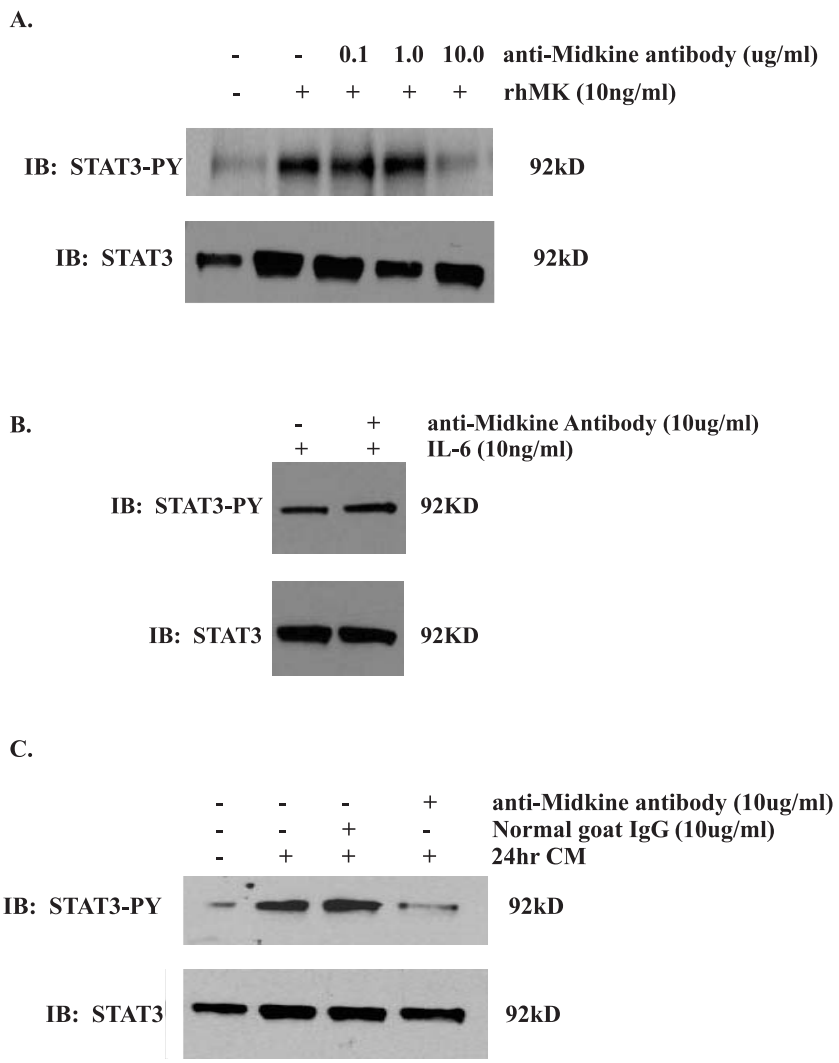


Figure 3.6 – Effect of midkine neutralization on midkine-induced STAT3 tyrosine phosphorylation in 3T3-L1 preadipocytes.
(A) 3T3-L1 preadipocytes were cultured in the presence of 10.0ng/ml recombinant midkine (rhMK) neutralized with varying concentrations of anti-midkine antibody (0.1μg/ml, 1.0μg/ml, or 10.0μg/ml). After a 5 minute stimulation, whole cell lysates were prepared and Western blot analysis (IB) was performed with anti-STAT3-PY antibody. Blots were stripped and re-probed with anti-STAT3 antibody.
(B) 3T3-L1 preadipocytes were cultured in the presence of 10.0ng/ml recombinant IL-6 neutralized with 10.0μg/ml anti-midkine antibody. After a 5 minute stimulation, whole cell lysates were prepared and Western blot analysis was performed with anti-STAT3-PY antibody. Blots were stripped and re-probed with anti-STAT3 antibody.
(C) 3T3-L1 preadipocytes were cultured in the presence of 24 hour CM neutralized with 10.0μg/ml anti-midkine antibody or 10.0μg/ml normal goat IgG. After a 5 minute stimulation, whole cell lysates were prepared and Western blot analysis was performed with anti-STAT3-PY antibody. Blots were stripped and re-probed with anti-STAT3 antibody. Results are representative of 3 separate experiments.

neutralized with 10.0 μg/ml anti-midkine antibody. **Figure 3.6B** shows that anti-midkine antibody did not block IL-6-induced STAT3 tyrosine phosphorylation. Upon confirming the efficiency and specificity of the neutralizing antibody, 24 hour CM was neutralized with 10.0 μg/ml anti-midkine antibody. Post-confluent preadipocytes were then stimulated with the neutralized CM. **Figure 3.6C** shows that 24 hour CM-induced STAT3 tyrosine phosphorylation was significantly reduced following the addition of anti-midkine antibody. Addition of control IgG, however, did not effect 24 hour CM-induced STAT3 activation. These data suggest that midkine is primarily responsible for the autocrine/paracrine activation of STAT3.

Midkine is sufficient for mitotic clonal expansion.

We previously reported that activated STAT3 plays a regulatory role during the proliferative phases of adipogenesis (16). Because midkine is the autocrine/paracrine activator of STAT3, we hypothesized that recombinant midkine would be sufficient to stimulate 3T3-L1 proliferation. To elucidate a role for midkine in mitotic clonal expansion, post-confluent preadipocytes were cultured in the presence of 10.0 ng/ml recombinant midkine, and cell proliferation was measured at several points following stimulation. Although not as potent as MDI, the addition of recombinant midkine to post-confluent preadipocytes promoted their proliferation or at a minimum maintained cell number in a time-dependent manner relative to cells in medium containing 10% FBS **(Figure 3.7)**. These results are consistent with other studies suggesting that heparin binding growth factors contribute to the development of adipocyte hyperplasia (160).

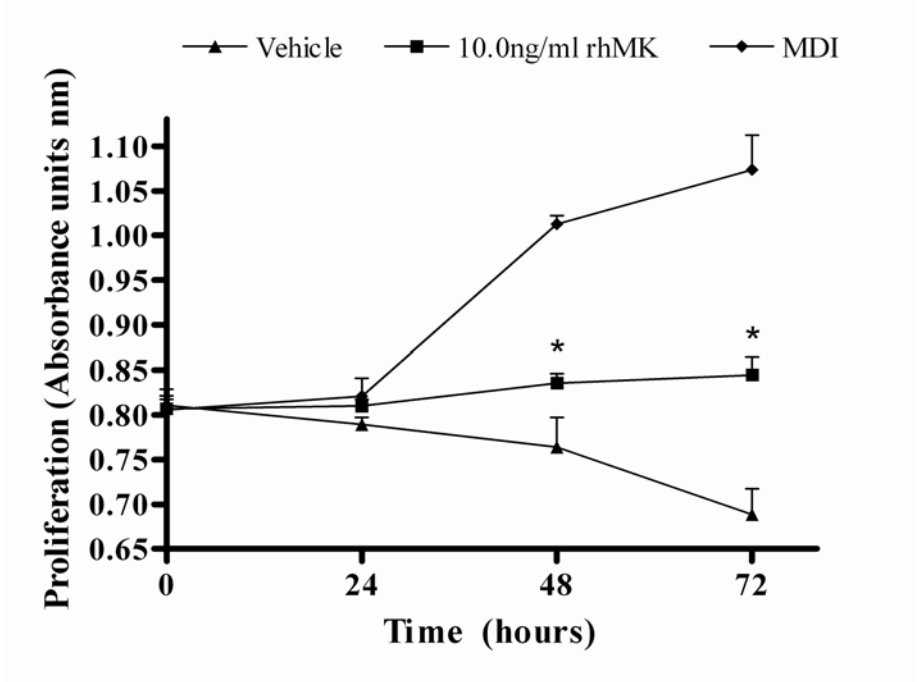


Figure 3.7 – Effect of recombinant midkine stimulation on the proliferation phases of adipogenesis.

Post-confluent preadipocytes were cultured in the presence of vehicle (PBS), 10.0ng/ml recombinant midkine (rhMK), or MDI. The degree of preadipocyte proliferation was determined *via* a colorimetric proliferation assay 0, 24, 48, and 72 hours following stimulation. Data shown reflect the means ± SE of 9 experiments. *, $P < 0.05$ when the vehicle group was compared to the midkine group for each time point by t test.

Midkine is necessary for adipogenesis.

Mitotic clonal expansion is required for progression through the differentiation program (37, 39, 40). Mitotic clonal expansion and stimulators of this process, however, may or may not be sufficient to induce differentiation in the absence of MDI. To determine the effect of exogenous midkine on differentiation, post-confluent preadipocytes were cultured in the presence of 10.0 ng/ml recombinant midkine for 72 hours. From days 3-8, cells were maintained in culture medium alone. At various times after stimulation with recombinant midkine, expression of adipogenic transcription factors and accumulation of cytoplasmic triglyceride were assessed. Cells treated with recombinant midkine neither accumulated cytoplasmic triglyceride nor expressed adipogenic transcription factors (data not shown), suggesting that midkine is not sufficient for adipogenesis.

To determine if midkine is necessary for adipogenesis, post-confluent preadipocytes were stimulated with MDI or MDI neutralized with 1.0 μg/ml anti-midkine antibody for 48 hours. From days 2-8, cells were maintained in culture medium alone. At various times after stimulation with MDI or MDI plus anti-midkine antibody, expression of adipogenic transcription factors and accumulation of cytoplasmic triglyceride were assessed. Cells treated with MDI plus anti-midkine antibody accumulated significantly less triglyceride than cells treated with MDI alone as shown by Oil Red-O staining **(Figure 3.8B)**. Consistent with these results, expression of the adipogenic transcription factors C/EBPα and PPARγ was also significantly reduced **(Figure 3.8A)**. Stimulation with MDI plus control IgG did not affect C/EBPα or PPARγ expression. These data suggest that midkine is necessary for adipogenesis.

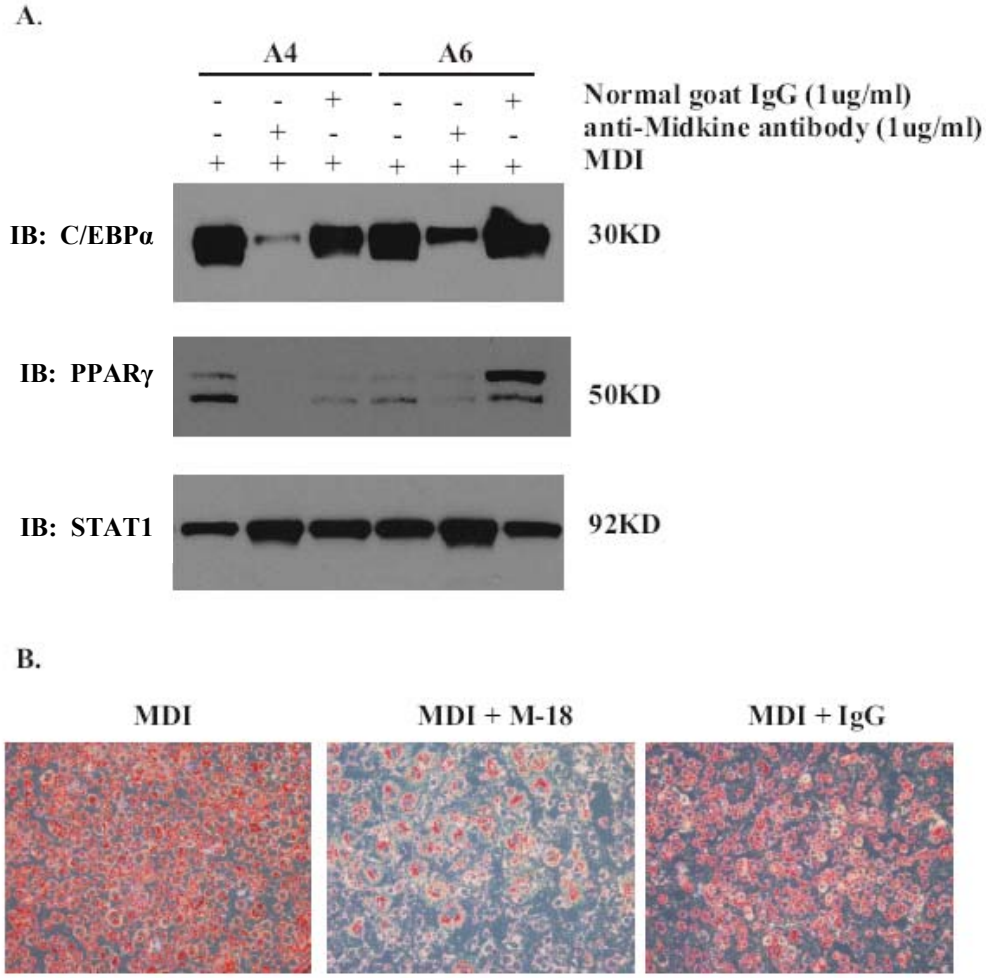


Figure 3.8 – Effect of midkine neutralization on adipogenesis.
3T3-L1 preadipocytes were cultured in the presence of MDI containing 1.0μg/ml anti-midkine antibody or 1.0μg/ml normal goat IgG for 2 days. (A) Whole cell lysates were prepared on day 4 and day 6, and expression of adipogenic transcription factors (C/EBPα and PPARγ) was assessed by Western blot analysis (IB). Blots were stripped and re-probed with anti-STAT3 antibody. (B) On day 8, cells were stained with Oil-Red O.

E. DISCUSSION

The present study reports the identification of a midkine-STAT3 signaling pathway that plays a necessary role in adipogenesis. This investigation was prompted by our initial observation that STAT3 activation during adipogenesis was delayed. These results suggested that a mechanism other than direct activation by MDI was involved. Our data showing immediate STAT3 tyrosine phosphorylation following stimulation with CM confirmed the involvement of an autocrine/paracrine factor. The fact that the autocrine/paracrine factor was identified only in CM from differentiating preadipocytes and not in CM from growth-arrested preadipocytes and adipocytes suggested that the factor was synthesized and released in a differentiation-dependent manner, and thus likely important in the regulation of adipogenesis. Our data showing inhibitory effects of cycloheximide and actinomycin D on this factor provided strong evidence for endogenous production of the factor, rather than conversion or generation of the factor from one of the components of the differentiation cocktail. Furthermore, our findings that midkine mRNA expression preceded the appearance of the STAT3 activating factor in CM, and midkine antibodies neutralized the STAT3 activating effects of CM, confirmed the identify of the autocrine activator as midkine. Because a sensitive method to detect rodent midkine protein was not available, we were not able to measure midkine levels in CM.

Leukemia inhibitory factor, oncostatin M, and IL-6, potent activators of STAT3 in 3T3-L1 cells, are capable of activating STAT3 at nanomolar or ng/ml doses (134). In the present study we report that midkine also activates STAT3 in 3T3-L1 cells at ng/ml concentrations. In the context of the above mentioned traditional activators, these data

demonstrate that midkine is a relatively potent activator of STAT3. Also in this dose range, midkine was sufficient to simulate post-confluent preadipocyte proliferation. Although the effect of midkine on proliferation was small when compared to the effect of MDI, midkine clearly enhanced cell number when compared to the effect of serum containing medium alone. Because it is well established that the individual components of MDI do little to induce differentiation when used alone, the small effect of midkine on clonal expansion was not surprising (16, 34). By contrast, the inhibitory effect of midkine neutralization on differentiation was near complete. This led us to the important conclusion that midkine is necessary but not sufficient to induce mitotic clonal expansion and subsequent differentiation.

These findings are consistent with other studies demonstrating that midkine is a regulator of normal and transformed cell proliferation. Under physiological conditions, midkine stimulates the proliferation of fibroblasts (163) and skeletal muscle myoblasts (164). The finding that midkine is overexpressed in a number of cancer cell lines and primary tumors (150-155, 165) implicates it in abnormal proliferation and carcinogenesis as well. Midkine has also been shown to serve as an autocrine mitogen for tumor cells (147), possess transforming properties (156), inhibit apoptosis (157), and promote angiogenesis (158).

Lastly, the midkine-related findings described in this report may have clinical relevance. It was previously reported that preadipocytes from massively obese persons replicate to a significantly higher degree than preadipocytes from lean persons (166), and that their exaggerated proliferative capacity is due in part, to the augmented production of

mitogenic proteins. These mitogenic factors are released into the culture medium and act as autocrine/paracrine factors contributing to adipocyte hyperplasia (166). Because heparin binding growth factors are the mitogenic factors released by preadipocytes from both lean and massively obese persons (160), it is quite possible based on the findings in this report, that midkine plays a role in the increased cellularity associated with some forms of obesity.

In summary, we provided evidence in this report that midkine is an autocrine activator of STAT3 during early phases of adipogenesis. We also demonstrated that midkine itself induces preadipocyte proliferation likely through a STAT3 signaling pathway and concluded that the midkine/STAT3 pathway is necessary for adipogenesis. These data provide insight into the complexity of the early stages of adipocyte differentiation and highlight the importance of tyrosine phosphorylation in the proliferative phases of adipogenesis. Further studies are needed to determine midkine's mechanism of STAT3 activation (i.e., receptor and associated non-receptor tyrosine kinase) as the midkine/STAT3 pathway may play a role in the development of adipocyte hyperplasia and severe obesity.

CHAPTER IV
ROLE OF STAT3 IN ADIPOGENESIS AND ADIPOCYTE METABOLISM IN MICE

Manuscript #1 (Chapter III) identified a midkine-STAT3 signaling pathway that is necessary for adipogenesis. To build on this research finding, the current work aimed to determine the physiological role of STAT3 in adipogenesis in animals. Mice with an adipocyte-specific disruption of the STAT3 gene (ASKO mice), created using aP2-Cre-*loxP* DNA recombination, and primary preadipocyte isolated from ASKO mice, were studied to achieve this aim. Our findings are presented below in the manuscript titled "Adipocyte-Specific Disruption of Signal Transducer and Activator of Transcription 3 (STAT3) Increases Body Weight and Adiposity".

Manuscript #2: **Adipocyte-Specific Disruption of Signal Transducer and Activator of Transcription 3 (STAT3) Increases Body Weight And Adiposity**

Authors: Erin R. Cernkovich, Jianbei Deng, Michael C. Bond, Terry P. Combs, Joyce B. Harp

Under review: Cell Metabolism

A. ABSTRACT

To determine the role of STAT3 in adipose tissue, we used Cre-*loxP* DNA recombination to create mice with an adipocyte-specific disruption of the STAT3 gene (ASKO mice). aP2-Cre driven disappearance of STAT3 expression occurred on day 6 of adipogenesis, a time point when preadipocytes have already undergone conversion to adipocytes. Thus, this knockout model examined the role of STAT3 in mature, but not differentiating adipocytes. Beginning at 9 weeks of age, ASKO mice weighed more than their littermate controls and had increased adipose tissue mass, associated with adipocyte hypertrophy, but not adipocyte hyperplasia, hyperphagia, or reduced energy expenditure. Leptin-induced, but not isoproterenol-induced, lipolysis was impaired in ASKO adipocytes, which may partially explain the increased cell size. Despite reduced adiponectin and increased liver triacylglycerol, ASKO mice displayed normal glucose tolerance. Overall, these findings demonstrate that adipocyte STAT3 regulates body weight homeostasis in part through direct effects of leptin on adipocytes.

B. INTRODUCTION

Obesity is a significant medical and public health concern due to its prevalence, associated co-morbidities and economic impact (1). At the cellular level obesity is characterized by an increase in adipose tissue mass; which occurs when adipocytes increase in size, through the storage of excess energy as triacylglycerol, and/or when adipocytes increase in number, through the conversion of preadipocyte to adipocytes (167).

The process of fat cell formation or adipogenesis is triggered by extracellular factors that mediate a series of coordinated intracellular events culminating in the expression and activation of several transcription factors. Members of the C/EBP and PPAR families are well known to regulate these processes (168). Recent studies have implicated members of the STAT family of transcription factors in adipogenesis as well (15, 16). STAT3, for example, is abundantly expressed in preadipocytes and adipocytes (15), and highly activated and bound to DNA in proliferating preadipocytes and adipocytes (16). In addition, inhibition of endogenous STAT3 expression with antisense morpholino oligonucleotides significantly decreases preadipocyte proliferation (16). Although, changes in expression and activation of STAT3 occur throughout adipogenesis, the precise role of this transcription factor in preadipocyte proliferation and conversion to adipocytes is not yet known.

The weight-reducing effects of the STAT3 activating ligands leptin, interleukin-6 (IL-6), and ciliary neurotrophic factor (CNTF) also implicate STAT3 in the regulation of adipocyte size. These cytokines have been shown to regulate fat cell size *via* direct peripheral effects on adipocytes. Leptin regulates fat cell size peripherally by stimulating

white adipose tissue (WAT) lipolysis, inhibiting lipogenesis, and promoting fatty acid oxidation (18-25) . IL-6 also stimulates WAT lipolysis and has been shown to cause a notable decline in the uptake of circulating TAG by decreasing lipoprotein lipase activity (26-30). Similarly, CNTF inhibits WAT fatty acid biosynthesis *via* repression of fatty acid synthase (FAS) and sterol regulatory element binding protein-1 (SREBP-1) gene expression (31, 32). It is thought that the anti-lipogenic and pro-lipolytic actions of leptin, IL-6 and CNTF, may account for a portion of the weight reducing effects of these cytokines. Because STAT3 is a downstream target of leptin, IL-6 and CNTF signaling, STAT3 likely mediates many of the effects of these cytokines in adipocytes. The contribution of STAT3 to these aspects of body weight homeostasis, however, has yet to be determined.

To determine the role of STAT3 in adipogenesis and body weight homeostasis, we generated mice with an adipocyte-specific disruption of the STAT3 gene using aP2-Cre-*loxP* DNA recombination. The late deletion of STAT3 induced by the aP2 promoter, and the resulting preservation of STAT3 expression in preadipocytes prevented us from examining the role of STAT3 in adipogenesis. Therefore, this report examines the role of STAT3 in mature adipocytes. Here, we reveal that adipocyte STAT3 is essential for body weight homeostasis and its deficiency causes higher body weight and increased adiposity. Furthermore, ASKO mice have reduced serum adiponectin levels and increased liver lipid deposits but do not develop impaired glucose tolerance or other obesity-related metabolic perturbations. Thus, ASKO mice represent a model of obesity dissociated from impaired glucose tolerance and their characterization provides insight into the physiological roles of STAT3 in adipocyte metabolism.

C. MATERIALS AND METHODS

Construction of the STAT3 targeting vector

A STAT3 targeting vector was constructed that introduced *loxP* sites upstream and downstream of exon 22. The OSfrt-*loxP* plasmid (kindly provided by the Animal Models Core at the University of North Carolina at Chapel Hill) served as the backbone for the STAT3 targeting vector. STAT3 homologous sequences were amplified and cloned into the OSfrt-*loxP* plasmid containing the neomycin resistance (*neo*) gene, the herpes simplex virus thymidine kinase gene, FRT sites flanking *neo* to facilitate removal of *neo* by FlpE recombinase, a *loxP* site to facilitate removal of the targeted exon by Cre recombinase, and five unique restriction sites. The long arm of homology, spanning exon 21 of the STAT3 gene, was amplified from 129/SvEv genomic DNA. PCR amplification introduced a SpeI restriction site and an AgeI restriction site at the 5' end and 3' end respectively. The resulting 3.3 kb PCR product was SpeI/AgeI digested and cloned into a SpeI/AgeI digested OSfrt-*loxP* plasmid. The short arm of homology, spanning exon 23 and 24 of the STAT3 gene, was amplified from 129/SvEv genomic DNA. PCR amplification introduced a BamHI restriction site and a SalI restriction site at the 5' end and 3' end respectively. The resulting 2.4 kb PCR product was BamHI/SalI digested and cloned into a BamHI/SalI digested OSfrt-*loxP* plasmid containing the long arm. The target arm, spanning exon 22 of the STAT3 gene and including a tyrosine residue necessary for STAT3 activation, was amplified from 129/SvEv genomic DNA. PCR amplification introduced a *loxP* site upstream of exon 22, and an AgeI restriction site and a XhoI restriction at the 5' end and 3' end respectively. The resulting 339 bp PCR product was AgeI/XhoI digested and cloned into an AgeI/XhoI digested OSfrt-*loxP* plasmid containing the long arm and short arm.

Generation of STAT3$^{flox/+}$ mice

2 x 10^7 129/SvEv embryonic stem cells were transfected with 20.0μg of the linearized STAT3 targeting vector by electroporation (250μF/300V). Cells were subjected to selection with G418 and gancyclovir. Surviving colonies were picked after 12-14 days of selection and screened for homologous recombination by PCR and Southern blot analysis. ES cell clones carrying the desired homologous recombination event were expanded. To remove *neo*, expanded clones were electroporated with a vector that transiently expresses FlpE recombinase (kindly provided by the Animal Models Core at the University of North Carolina at Chapel Hill). Deletion of the selection cassette was confirmed by PCR and Southern blot analysis. Targeted clones not containing *neo* were microinjected into blastocysts derived from C57BL/6 females. To generate mice chimeric from the targeted ES cells and host blastocysts (STAT3$^{flox/+}$), microinjected blastocysts were transferred to the uterus of pseudopregnant C57BL/6 recipients. Chimeric mice (as determined by coat color) were then bred with C57BL/6 mice to transmit the targeted allele through the mouse germline. The presence of the targeted allele in the agouti-colored offspring was confirmed by PCR.

Generation of adipose tissue-specific STAT3 knockout mice

Agouti mice heterozygous for the targeted STAT3 gene (STAT3$^{flox/+}$) were crossed with transgenic mice expressing Cre recombinase under the control of the adipocyte specific aP2 promoter/enhancer (B6.Cg-Tg (Fabp4-cre) 1Rev/J, Jackson Laboratories, Bar Harbor Maine). Offspring inheriting both the targeted allele and the Cre-expressing transgene (aP2-Cre STAT3$^{flox/+}$) were intercrossed to yield six derivative strains: (a) STAT3$^{+/+}$ (WT), (b)

$STAT3^{flox/+}$ (WT), (c) $STAT3^{flox/flox}$ (WT), (d) $STAT3^{+/+}$/Cre (WT), (e) $STAT3^{flox/+}$/Cre (HZ), and (f) $STAT3^{flox/flox}$/Cre (ASKO). ASKO mice and WT and HZ littermate controls maintained on a mixed background were studied for further analysis.

Animals and PCR genotyping

ASKO mice and littermate controls were housed 2-5 per cage in a temperature and humidity controlled pathogen-free facility, exposed to a 12 hour light/dark cycle, and fed a standard Purina rodent chow (LabDiet® ProLab Isopro RMH 3000, PMI Nutrition International, St. Louis, MO) and water ad libitum. All protocols for animal use and euthanasia were reviewed and approved by the University of North Carolina at Chapel Hill Institutional Animal Care and Use Committee.

Genotyping was performed by PCR amplification of genomic DNA isolated from tail tips of 3-4 week old mice. The primers for identifying a floxed allele (5' GCAAGACTGGA TGGCAAACCGCTATAACTT 3'and 5' TCGGCAGGTCAATGGTATTGCTGCAGGTCG 3') amplify a 682 bp fragment. The primers for identifying a wild-type allele (5' AGGAAT AGGGAGGACATGGGGTGAGAGTTACCGTG 3' and 5' TCGGCAGGTCAATGGTATT GCTGCAGGTCG 3') amplify a 262 bp fragment. The primers for identifying the Cre transgene (5' GCGGTCTGGCAGTAAAAACTATC 3' and 5'GTGAAACAGCATTGCTGT CACTT 3') amplify a 100 bp fragment. To detect Cre-mediated recombination, primers were designed that are located on the *loxP* site (5' GCAAGACTGGATGGCAAACCGCTA TAACTT 3') and exon 23 (5' TCGGCAGGTCAATGGTATTGCTGCAGGTCG 3'). This primer pair gives rise to a 682 bp fragment or a 336 bp PCR fragment before and after Cre-

mediated recombination respectively. In all cases, PCR was performed using the GeneAmpPCR® Fast PCR Master Mix (Applied Biosystems, Foster City, CA). PCR conditions were 94°C for 2 minutes, followed by 35 cycles of 94°C for 1 second and 64°C for 20 seconds. A final extension step of 1 minute at 72°C was performed to ensure complete synthesis of all annealed products.

Primary preadipocyte isolation and culture

WAT was aseptically removed from male mice and stromal vascular cell cultures were established as previously described (169). Briefly, WAT was excised from freshly killed ASKO mice and littermate controls. After excision, adipose tissue was minced into small pieces, washed in Dulbecco's Modified Eagle's Medium (DMEM) supplemented with 1% bovine serum albumin (BSA), and centrifuged at 1000 x g for 10 minutes to remove blood cells. Tissue was then decanted into DMEM containing 1.0 mg/ml type I collagenase and digested for 45 minutes at 37ºC with constant end-over-end inversion. Following the digestion, adipose cells and stromal vascular cells were separated by centrifugation at 500 x g for 10 minutes. The stromal vascular cell pellet was resuspended and cultured in DMEM containing 10% v/v fetal bovine serum (FBS), 10 mg/ml streptomycin, 100 U/ml penicillin, and 1 mM pyruvate at 37°C in 5% CO_2 air. To induce differentiation, 2-day post-confluent preadipocytes were treated with Zen-Bio Differentiation Medium (Zen-Bio, Raleigh, NC). On day 3, the differentiation medium was replaced with Zen-Bio Adipocyte Maintenance Medium, which was changed every 2 days thereafter until analysis on day 8.

For analysis of lipolysis, on day 8, primary cells were incubated in the presence of

vehicle, 1.0 μM isoproterenol, or recombinant leptin (R&D Systems, Minneapolis, MN), in doses ranging from 5.0 ng/ml to 100.0 ng/ml. After twenty-four hours of incubation, glycerol released into the medium was measured using the Zen-Bio Adipocyte Lipolysis Assay Kit.

Immunoblot analysis

Primary cells were washed twice in phosphate buffered saline with 1mM orthovanadate, and then placed immediately in sample buffer (1% NP40, 20 mM Tris-HCL (pH 8.0), 150 mM NaCl, 1mM EDTA, 0.1% NaN_3, 10 μg/ml aprotinin, 1 μM pepstatin, 16.4 μg/ml leupeptin, 1 mM phenylmethyl-sulfonylfluoride, 0.1 mM Na_3VO_4, 2% SDS, 10% glycerol). Tissues were homogenized in sample buffer with a PRO Scientific PRO 200 homogenizer (Oxford, CT). Primary cell lysates, and heart, liver, kidney, hypothalamus, WAT, and brown adipose tissue (BAT) homogenates were heated and protein concentrations were determined using Bio-Rad Laboratories, Inc., DC protein determination kit (Richmond, CA). BSA was used as a standard. Samples were heated for 2 minutes at 85°C, separated by 10% SDS-PAGE, and analyzed by immunoblotting. Immunoblots were developed with the Pierce enhanced chemiluminescence kit (Rockford, IL).

Dual Energy X-ray Absorptiometry (DEXA) measurement of body composition

Body composition was determined on anesthetized male mice using the Lunar PIXImus densitometer (GE Lunar Corporation, Madison, WI, USA).

Indirect calorimetry

Oxygen consumption (V_{O_2}), activity (horizontal, vertical, and ambulating), and food intake were measured using an Oxymax open-circuit indirect calorimetry system (Columbus Instruments International, Columbus, OH). Male mice were placed in calorimeter chambers for 5 days in a light (12-hour light/dark cycle) and temperature controlled environment. Mice were maintained with free access to standard Purina rodent chow and water throughout the duration of the 5-day measurement period. On day 5, lean mass was measured using the Lunar PIXImus densitometer. Oxygen consumption and activity data are reported as the mean V_{O_2} and mean counts of days 2-4 respectively. Food intake data are reported as the mean daily intake of days 1-5.

Biochemical assays

Blood was collected from cut tail tips of conscious male mice in either the fed or the fasting state. Glucose was measured by the glucose oxidase method with a commercial glucometer (FreeStyle Flash Blood Glucose Monitoring System). Blood was also obtained *via* retro-orbital sinus of anesthetized male mice in either the fed or the fasting state. Plasma was collected in EDTA coated capillary tubes, and separated *via* centrifugation at 3000 x g for 10 minutes. Plasma was used for measurement of insulin. Serum was collected in plain capillary tubes, allowed to clot at room temperature for 20 minutes, and then separated *via* centrifugation at 3000 x g for 10 minutes. Serum was used for measurement of leptin, adiponectin, TAG, and free fatty acids (FFAs). Plasma insulin and serum leptin levels were measured by ELISA (Crystal Chem, Downers Grove, IL). Serum adiponectin levels were measured by ELISA (R&D Systems, Minneapolis, MN). Serum TAG was measured by colorimetric enzyme assay (Stanbio, Boerne, TX), and FFA levels in serum were measured

using the NEFA-kit-C (Wako Chemicals GmbH, Neuss, Germany). Metabolic parameters measured in the fed state were in animals with free access to food assayed at 11:00 p.m.; for fasted-state measurements, mice were assayed at 8:00 a.m. after a 24 hour fast in a clean cage free of bedding.

Glucose tolerance test

Oral glucose-tolerance tests were performed on male mice that did not have access to food for 4 hours before administration of 2.5 mg/g body weight glucose load by oral gavage. Glucose measurements were taken prior to oral gavage and 15, 30, 45, 60, 90, 120, and 150 minutes after oral gavage. To measure corresponding insulin levels, plasma was collected from cut tail tips prior to oral gavage and 15 and 30 minutes after oral gavage.

Tissue TAG

The tissue lipid extraction procedure was adapted from methods previously described (170).

Histology

Tissues from male mice were fixed in 10% phosphate-buffered paraformaldehyde, embedded in paraffin, and sectioned (5.0 μm) for hematoxylin/eosin staining.

Quantitative real-time (TaqMan) RT-PCR

WAT was removed from male mice and total RNA was isolated using the TRIzol method (Invitrogen, Carlsbad, CA). 1.0 μg RNA was reverse transcribed with the

Superscript II First Strand Synthesis kit (Invitrogen, Carlsbad, CA) using oligo (dT) primers. CCAAT/enhancer binding protein α (C/EBPα), peroxisome proliferators activated receptor γ (PPARγ), fatty acid binding protein (FABP2/aP2), leptin, adiponectin, FAS, diacylglycerol acyltransferase (DGAT), and glyceraldehyde-3-phosphate dehydrogenase (GAPDH) mRNA were quantified by real-time PCR using the Bio-Rad iCycler PCR machine (Hercules, CA). mRNA levels were normalized to GAPDH and presented as relative mRNA expression.

Table 4.1 Primers and probes for real-time (TaqMan) RT-PCR.

Gene Name	Probe	Primer pairs
C/EBPα	5'-FAM-CAACAACATCGCGGTGCGCAAGAGCC-TAMRA-3'	5'CAGCAACGAGTACCGGGTA3' 5'TGCGTCTCCACGTTGCGTT3'
PPARγ	5'-FAM-TCCTGTCAAGATCGCCCTCGCCT-TAMRA-3'	5'CATAAAGTCCTTCCCGCTGA3' 5'TGACAAATGGTGATTTGTCCG3'
FABP2/aP2	5'-FAM-AATGGTCCAGGCCCCAGTGAGCT-TAMRA-3'	5'TTCCCTACAGTCTAGCAGAC3' 5'TCTACACGTGTGAATTTCCCA3'
Leptin	5'-FAM-CCGCCAAGCAGAGGGTCACTGG-TAMRA-3'	5'ACATTTCACACACGCAGTCG3' 5'TGAAGCCCAGGAATGAAGTC3'
Adiponectin	5'-FAM-CCGTGATGGCAGAGATGGCACTCCT-TAMRA-3'	5'ATCCTGGCCACAATGGCACA3' 5'CAAGAAGACCTGCATCTCCT3'
FAS	5'-FAM-TCCAGGTAAATGGGCCAGCCGAG-TAMRA-3'	5'AGCTGTCCCCTGATGCCA3' 5'GAGAACTCCATGCCGAGCA3'
DGAT	5'-FAM-CCACTGCGATCTCCTGCCACCTT-TAMRA-3'	5'C TGTGCTCTACTTCACCT3' 5'ACGGCCCAGTTTCGCA3'
GAPDH	5'-FAM-TGACTCCACTCACGGCAAATTCAACG-TAMRA-3'	5'GCAGTGGCAAAAGTGGAGATTG3' 5'CCATTCTCGGCCTTGCTGT3'

Statistical Analysis

All values are expressed as means ± SE. An unpaired Student's *t* test was used to assess statistical differences between ASKO mice and WT or HZ littermate controls. A *t* test with a P value < 0.05 was considered statistically significant.

D. RESULTS

Generation of STAT3$^{flox/+}$ mice.

To determine the role of STAT3 in adipogenesis and body weight homeostasis, we generated mice with an adipocyte-specific disruption of the STAT3 gene using aP2-Cre-*loxP* DNA recombination. We constructed a STAT3 targeting vector with *loxP* sites flanking exon 22 of the murine STAT3 gene **(Figure 4.1A)**. Deletion of the *loxP*-flanked exon 22 by Cre recombinase was predicted to produce a truncated nonfunctional translational product missing a tyrosine residue (Tyr 705) essential for STAT3 activation (171).

The STAT3 targeting vector was linearized and electroporated into 129/SvEv embryonic stem (ES) cells **(Figure 4.1B)**. Gancyclovir and G418 resistant clones were screened for homologous recombination by PCR and Southern blot analysis. Correctly targeted clones were transiently transfected with FlpE recombinase to delete *neo* **(Figure 4.1C)**. Deletion of the selection cassette was confirmed by PCR and Southern blot analysis. Targeted ES cell clones devoid of *neo* were microinjected into C57BL/6 blastocysts, and mice carrying the floxed STAT3 allele (STAT3$^{flox/+}$) were created as described in Materials and Methods.

Creation of ASKO mice.

ASKO mice were generated by breeding mice heterozygous for the targeted STAT3 gene (STAT3$^{flox/+}$) and transgenic mice expressing Cre recombinase under the control of the adipocyte specific aP2 promoter/enhancer as described in Materials and Methods **(Figure 4.1D)**. ASKO mice were obtained at the expected Mendelian frequency and exhibited

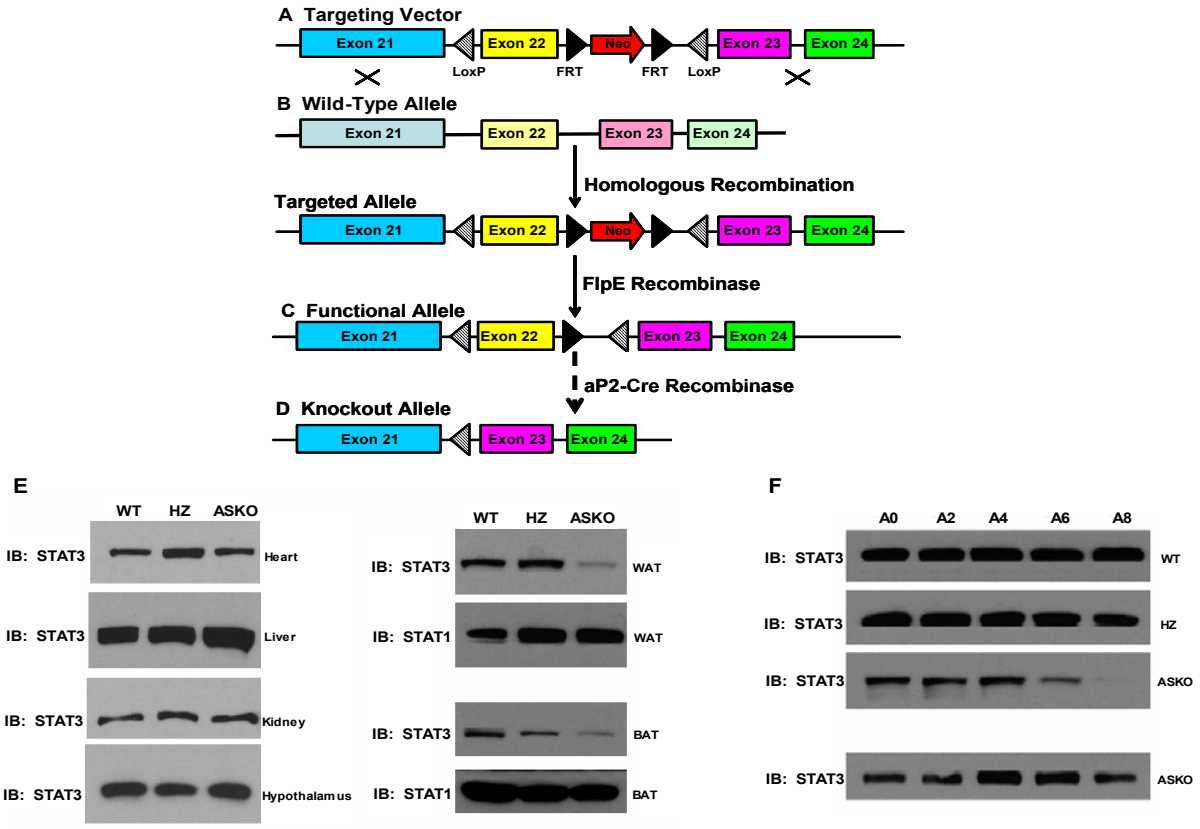


Figure 4.1 – Generation of ASKO mice.

Schematic representation of (A) the STAT3 targeting vector, (B) the endogenous STAT3 allele before (wild-type allele) and after (targeted allele) homologous recombination, (C) the targeted allele after FlpE recombination (functional allele), and (D) the functional allele after Cre-mediated deletion of exon 22 (knockout allele). (E) Western blot analysis (IB) of STAT3 protein expression in heart, liver, kidney, hypothalamus, WAT, and BAT from WT, HZ, and ASKO mice.

(F) Western blot analysis (IB) of STAT3 protein expression in subcutaneous primary preadipocytes isolated from WT, HZ, and ASKO mice 0, 2, 4, 6, and 8 days after induction of differentiation.

normal growth until the age of 9 weeks.

STAT3 expression was examined in tissue lysates from control and ASKO mice by Western blot analysis using an anti-STAT3 antibody which recognizes the C-terminal portion of the STAT3 protein. STAT3 expression was preserved in the heart, liver, kidney, and hypothalamus of ASKO mice **(Figure 4.1E)**. By contrast, STAT3 expression was significantly reduced in WAT and brown adipose tissue (BAT) from ASKO mice **(Figure 4.1E)**. The remaining STAT3 expression was likely derived from stromal vascular cells that did not express aP2. STAT3 expression was not altered, however, in either WAT or BAT obtained from wild-type (WT) or aP2-Cre $STAT3^{flox/+}$ (HZ) mice, suggesting that neither the *loxP* modification, nor expression of the aP2 transgene altered the expression of STAT3. These mice were considered controls.

The marked increase in aP2 expression during adipogenesis and the abundance of aP2 mRNA and protein in mature adipocytes established aP2 as a late marker of adipocyte differentiation (56). aP2 is also expressed in preadipocytes (172) and was recently identified as a marker for committed human preadipocytes (173). To define the timing of Cre-mediated STAT3 deletion in ASKO mice, preadipocytes isolated from WT, HZ, and ASKO were differentiated in culture and lysates were recovered 0, 2, 4, 6, and 8 days after stimulation with differentiation medium. Western blot analysis revealed disappearance of STAT3 expression beginning on day 6 of adipogenesis **(Figure 4.1F)**. STAT3 expression in preadipocytes, however, was preserved, suggesting that the Cre transgene was sufficient to direct recombination only in mature adipocytes. Therefore, ASKO mice and WT and HZ

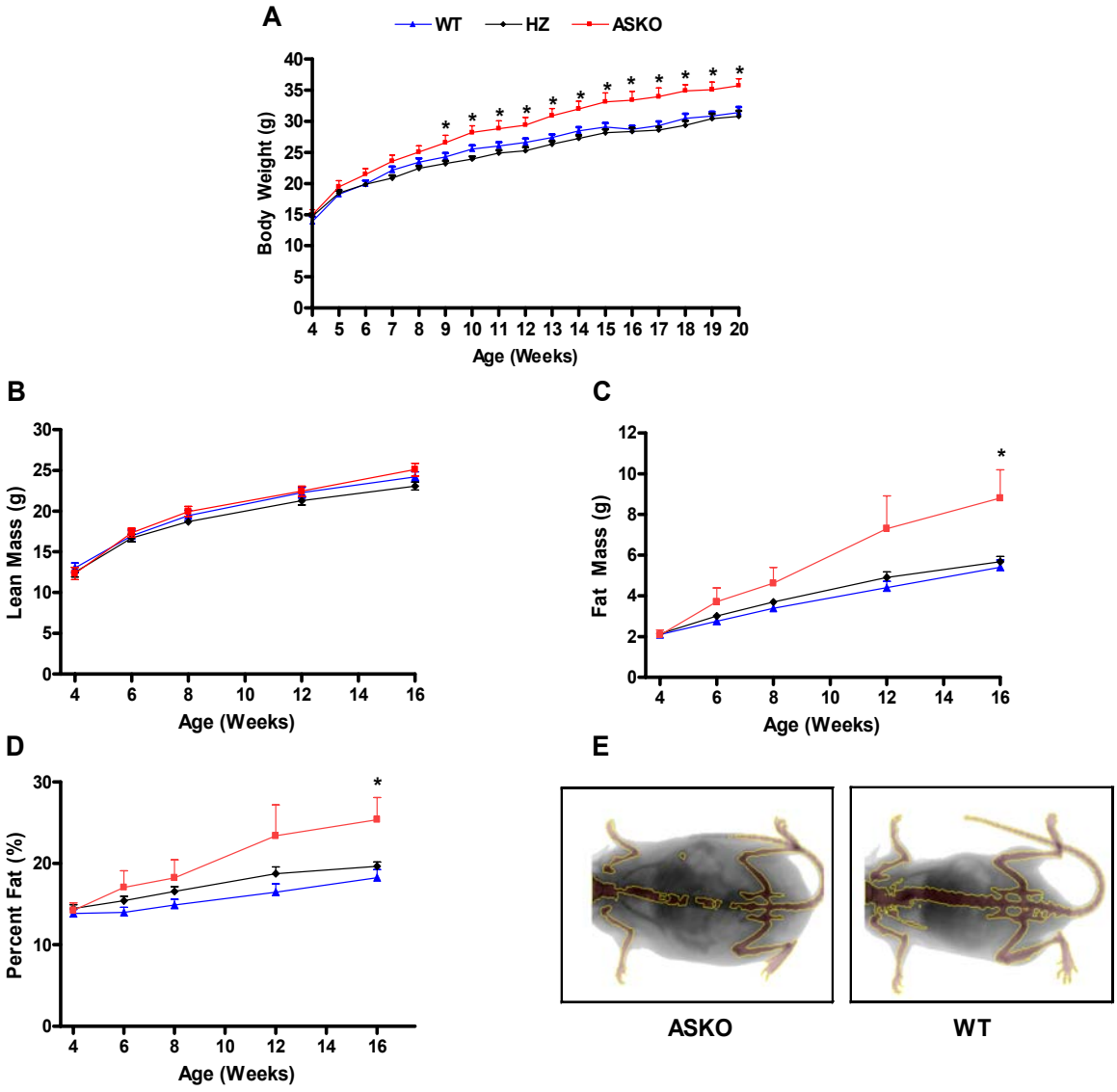


Figure 4.2 – Higher body weight and increased mass in ASKO mice.

(A) Growth curves of male ASKO mice and WT and HZ littermate controls. Data are means ± SE (n = 8-16). * Significantly different from WT and HZ littermate controls.

(B) Lean mass, (C) fat mass, and (D) percent fat of 4-, 6-, 8-, 12-, and 16-week old male ASKO mice and WT and HZ littermate controls. Data are means ± SE (n = 8-16).

* Significantly different from WT and HZ littermate controls.

(E) Representative PIXImus image of a 16-week old male ASKO mouse (left) and a 16-week WT control mouse (right).

littermate controls were studied to establish the role of STAT3 in mature adipocytes.

Higher body weight and increased adiposity in ASKO mice.

To determine the role of adipocyte STAT3 on body weight, ASKO mice and WT and HZ littermate control mice were weighed weekly. Growth curves were normal in male and female ASKO mice from birth to 4 weeks of age. Beginning at 9 weeks of age, however, male ASKO mice weighed significantly more than their littermate controls **(Figure 4.2A)**. By 20 weeks of age, male ASKO mice had gained 14% and 16% more weight than their WT and HZ littermates, respectively. Female growth curves, however, remained normal (supplemental data). To determine the basis for the higher body weight in male ASKO mice, lean mass **(Figure 2B)**, fat mass **(Figure 4.2C)**, and percent fat **(Figure 4.2D)** were measured at 4, 6, 8, 12, and 16 weeks by Dual Energy X-ray Absorptiometry (DEXA). Lean mass was similar between ASKO mice and littermate controls at all ages. Fat mass and percent fat however, were increased in ASKO mice beginning at 6 weeks of age. These differences were statistically significant by 16 weeks of age. In addition, inguinal, gonadal, retroperitoneal, and interscapular brown fat pads from ASKO mice weighed significantly more than fat pads from littermate controls. Significant differences were observed for both absolute fat pad weight **(Figure 4.3B)** and fat pad mass/g body weight **(Figure 4.3D).** Absolute liver weight was also significantly higher in male ASKO mice **(Figure 4.3A)**. Liver weight/g body weight however, was indistinguishable, as were absolute heart weight, heart weight/g body weight, and absolute kidney weight. Kidney weight/g body weight however, was significantly lower in ASKO mice. These results indicate that the higher body

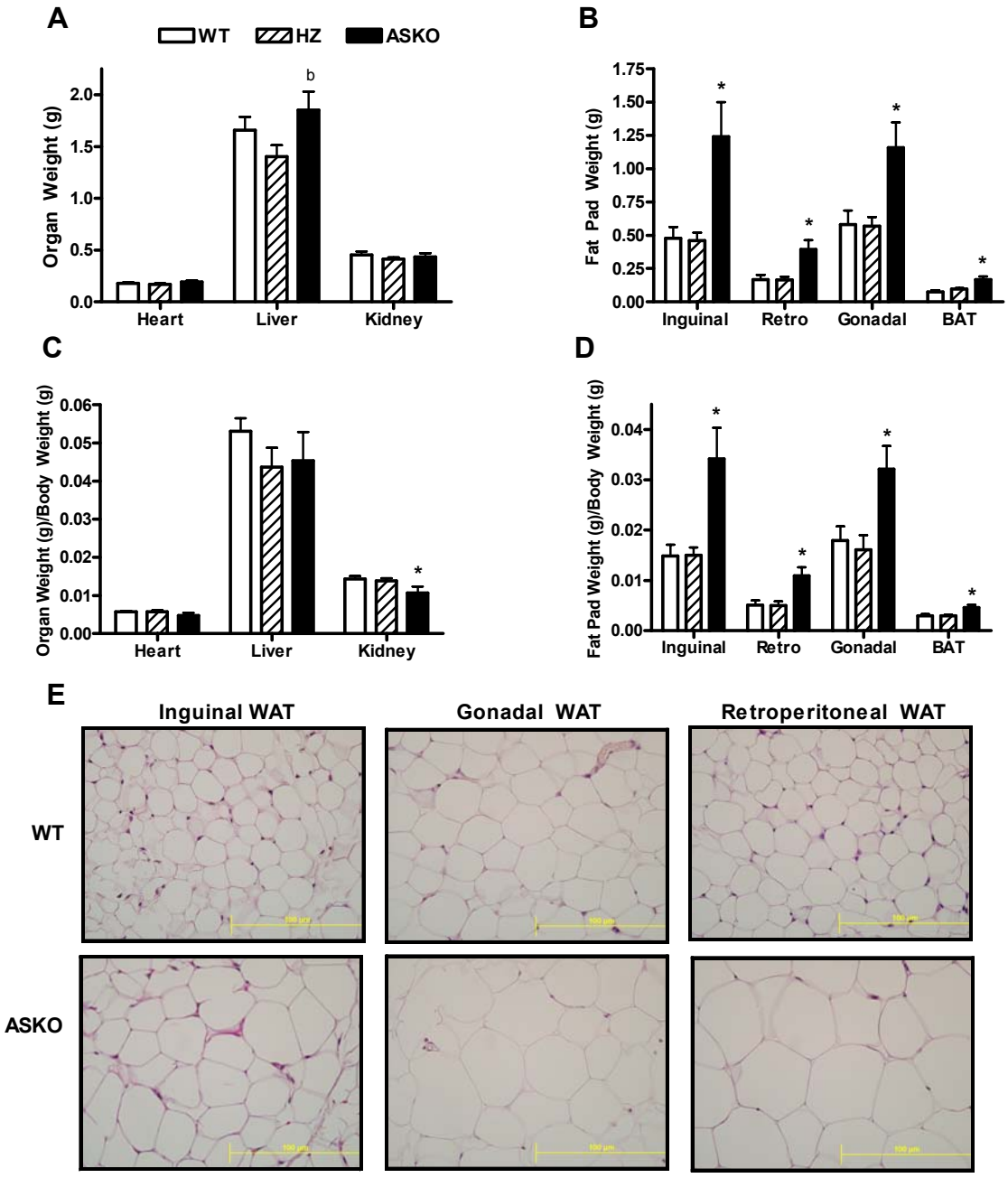


Figure 4.3 – Increased adiposity in ASKO mice.
(A) Absolute organ weight, (B) absolute fat pad weight, (C) organ weight/g body weight, and (D) fat pad weight/g body weight in 20-week old male ASKO mice and 20-week old WT and HZ littermate controls. Data are means ± SE (n = 8-12). * Significantly different from WT and HZ littermate controls. [b] Significantly different from HZ littermate controls. (E) Hematoxylin and eosin staining of inguinal WAT, gonadal WAT, and retroperitoneal WAT, from 20-week old male ASKO mice and 20-week old WT littermate controls.

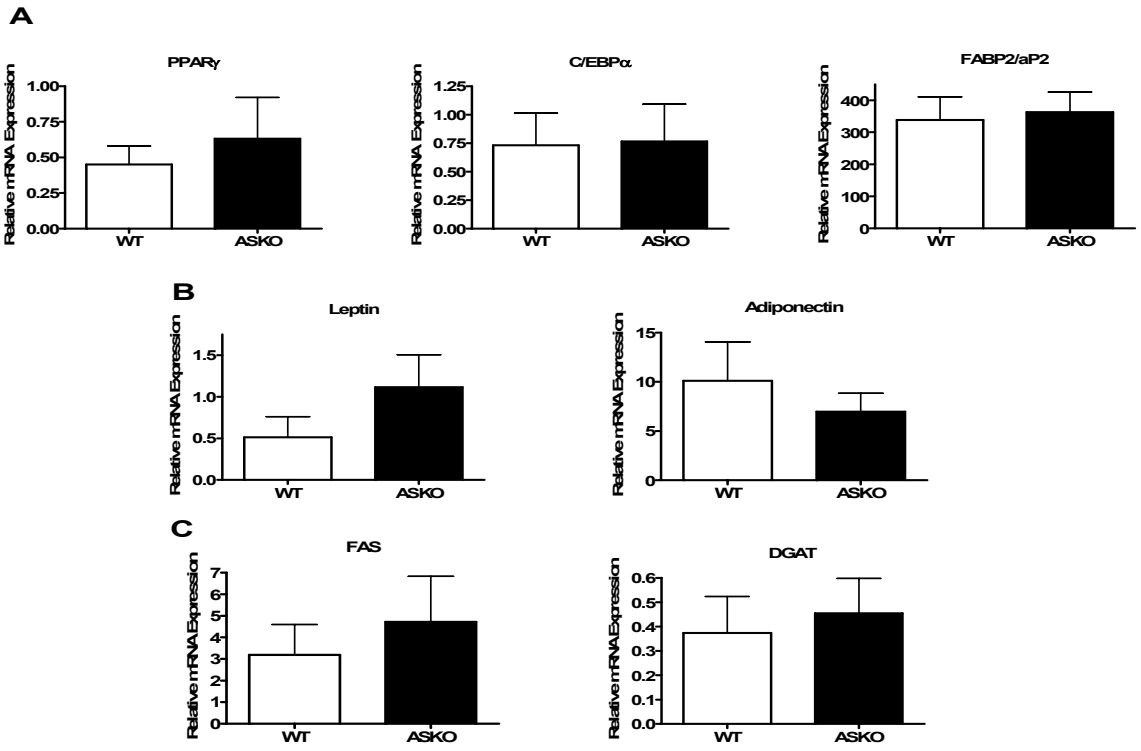


Figure 4.4 – Normal gene expression in WAT from ASKO mice.
Quantitative analysis of the expression levels of (A) PPARγ, C/EBPα, FABP2/aP2, (B) leptin, adiponectin, and (C) FAS and DGAT in WAT from 20-week old male ASKO mice and 20-week old WT littermate controls. mRNA levels are normalized to GAPDH and presented as relative mRNA expression. Data are means ± SE (n = 3-4).

weight in male ASKO mice was due to increased adiposity.

Increased adiposity can result from an increase in adipocyte cell size (hypertrophy), an increase in adipocyte cell number (hyperplasia), or both. To determine if adipocyte hypertrophy contributed to the increased adiposity in male ASKO mice, histological studies were carried out. Histological analysis of WAT sections from WT and ASKO mice revealed that ASKO mice had larger adipocytes than WT mice, indicating that the increased adiposity in male ASKO mice was due to adipocyte hypertrophy **(Figure 4.3E)**.

To determine if ASKO mice displayed changes in expression levels of adipogenic transcription factors and adipocyte-specific genes, gene expression analysis of WAT from WT and ASKO mice was conducted by real-time PCR. RT-PCR revealed no differences in the expression of C/EBPα, PPARγ, and aP2 **(Figure 4.4A)**. WAT DNA content was also similar between WT and ASKO mice indicating that the increase in adipose tissue mass observed in male ASKO mice was not due to adipocyte hyperplasia (supplemental data).

Normal food intake and energy expenditure in ASKO mice.

To determine if the increase in adiposity in male ASKO mice was due to positive energy balance, energy intake and energy expenditure were monitored in 12-week old ASKO mice and 12-week old WT littermate controls by an indirect calorimetry system as described in Materials and Methods. Analysis of food intake showed no significant differences in absolute daily food intake **(Figure 4.5A)**, or daily food intake/g body weight **(Figure 4.5B)** between ASKO mice and littermate controls. As shown in **Figure 4.5C and 4.5D**, horizontal

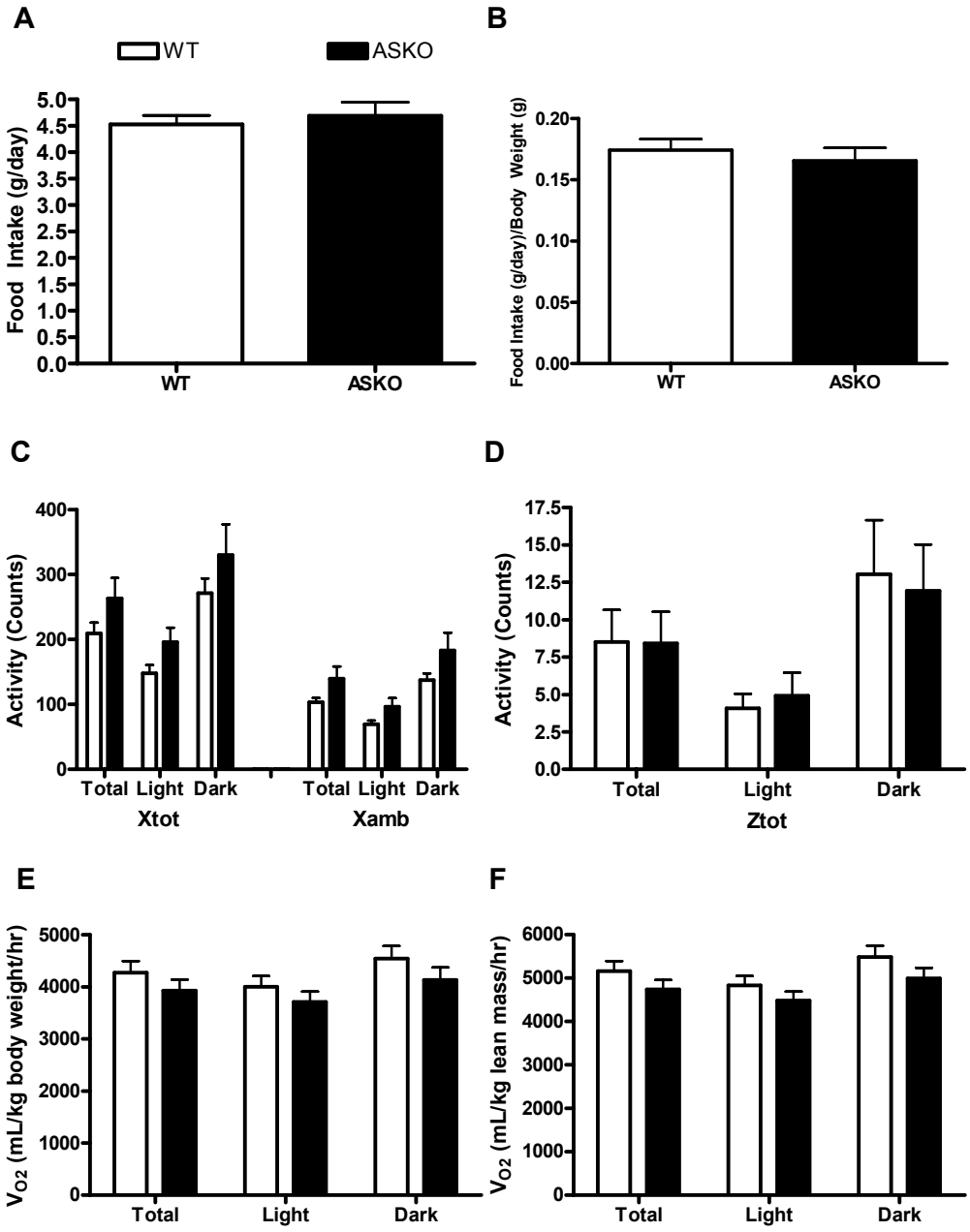


Figure 4.5 – Normal food intake and energy expenditure in ASKO mice.
(A) Absolute daily food intake and (B) daily food intake/g body weight in 12-week old male ASKO mice and 12-week old WT littermate controls. Data are means ± SE (n = 8-11). (C) Horizontal activity (Xtot), ambulation (Xamb), and (D) vertical activity (Ztot) in 12-week old ASKO mice and 12-week old WT littermate controls. Data are means ± SE (n = 8-11).
(E) O_2 consumption (ml/kg body weight/hr) and (F) O_2 consumption (ml/kg lean mass/hr) in 12-week old male ASKO mice and 12-week old WT littermate controls. Data are means ± SE (n = 8-11).

activity (Xtot), ambulation (Xamb), and vertical activity (Ztot) were also similar between ASKO mice and littermate controls. Oxygen consumption normalized to body weight **(Figure 4.5E)** and lean body mass **(Figure 4.5F)** were also similar between ASKO mice and littermate controls. These results indicate that the increased adiposity in male ASKO mice was not due to hyperphagia or reduced energy expenditure. The methodology employed, however, may not be sensitive enough to detect subtle long term disturbances in energy balance. Additionally, further studies are needed to determine if increased dietary fat absorption contributes to the higher body weight and increased adiposity.

Normal glucose tolerance in ASKO mice.

To determine the metabolic consequences of loss of adipocyte STAT3, we monitored circulating glucose, insulin, leptin, TAG, and FFAs in male ASKO mice and WT littermate controls at 12-16 weeks of age. Under both fed and fasting conditions, no differences were observed in blood glucose levels or serum TAG or FFA levels between ASKO mice and WT mice **(Table 4.2)**. Fasting plasma insulin and serum leptin levels were also similar between ASKO and WT mice. Because ASKO mice and WT mice had similar blood glucose and plasma insulin concentrations, we concluded that the increased adiposity in ASKO mice did not alter glucose homeostasis. As expected, ASKO mice and WT mice exhibited comparable blood glucose concentrations at all time points after administration of an oral glucose load **(Figure 4.6A).** Corresponding insulin levels **(Figure 4.6B)** were also similar. In addition, the pancreas from ASKO mice exhibited no gross or histological abnormalities (supplemental data).

	Fasted		Fed	
	WT	ASKO	WT	ASKO
Blood glucose (mg/dL)	70.44 ± 4.06	70.0 ± 4.00	123.7 ± 10.52	123.0 ± 9.08
Serum FFA (mEq/L)	1.06 ± 0.05	1.05 ± 0.04	0.28 ± 0.04	0.26 ± 0.03
Serum TAG (mg/dL)	141.48 ± 7.14	133.96 ± 16.77	108.48 ± 3.75	108.83 ± 8.68
Plasma Insulin (ng/mL)	0.82 ± 0.14	1.09 ± 0.27	ND	ND
Serum Leptin (ng/mL)	1.16 ± 0.26	1.30±0.46		
Serum Adiponectin (µg/mL)	**7.32 ± 0.28**	**5.48 ± 0.22 ***		

Table 4.2 – Normal biochemical parameters in ASKO mice.
Biochemical parameters in 12-16 week old male ASKO mice and WT littermate controls. Data are means ± SE (n =6-10). * Significantly different from WT and HZ littermate controls.
ND No Data

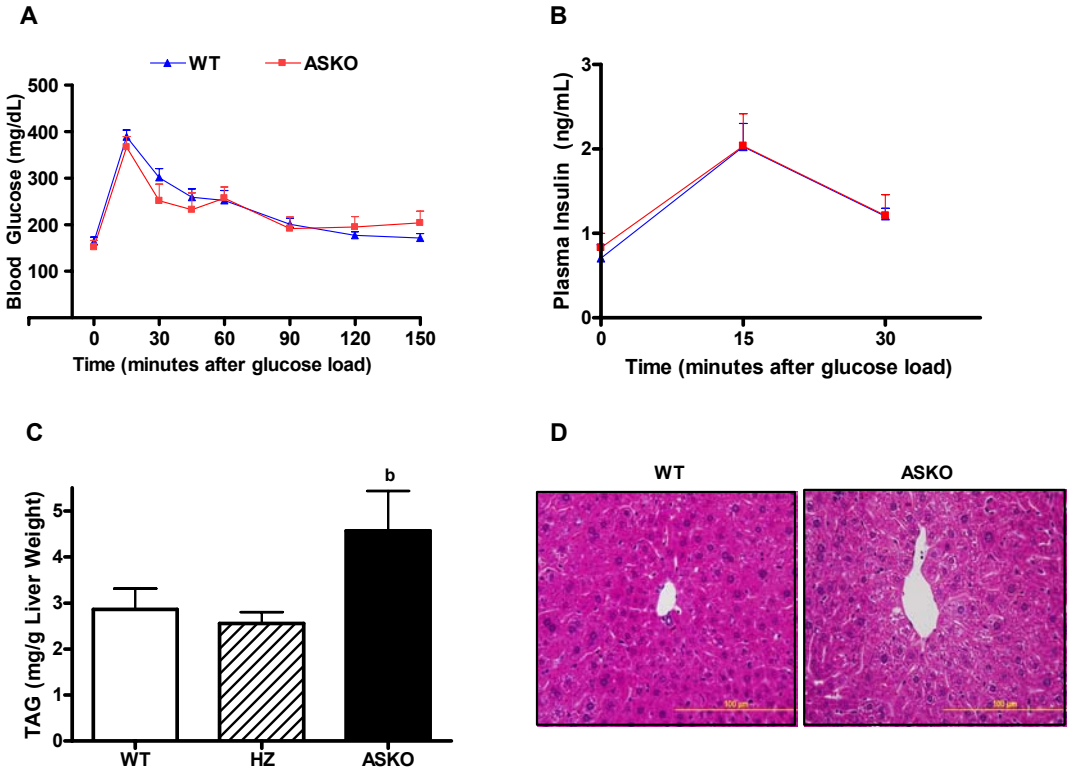


Figure 4.6 – Normal glucose tolerance and fatty liver in ASKO mice.
(A) Blood glucose concentrations during oral glucose tolerance tests in 20-week old male ASKO mice and WT littermate controls. Data are means ± SE (n = 8-11). (B) Plasma insulin concentrations during oral glucose tolerance tests in 20-week old male ASKO mice and WT and HZ littermate controls. Data are means ± SE (n = 6). (C) Liver TAG content in 20-week old male ASKO mice and WT and HZ littermate controls. Data are means ± SE (n = 4-6). [b] Significantly different from HZ mice.
(D) Hematoxylin and eosin staining of liver sections from 20-week old male ASKO mice and 20-week old WT littermate controls.

Increased liver TAG in ASKO mice.

Fatty liver is strongly associated with both hepatic and adipose tissue insulin resistance, as well as reduced whole-body insulin sensitivity (174-176). Because male ASKO mice exhibited normal glucose tolerance, as determined by oral glucose tolerance testing, we hypothesized that the increased adiposity was limited to the adipose tissue and did not affect the liver. However, liver TAG was increased in ASKO mice **(Figure 4.6C)**. Consistent with these data, histological analysis of liver sections from ASKO mice also showed a marked increase in lipid deposition **(Figure 4.6D)**. Furthermore, serum adiponectin levels, which correlate negatively with adiposity and hepatic fat (177, 178), were significantly reduced in ASKO mice **(Table 4.2)**.

Impaired leptin signaling in ASKO mice.

The STAT3-activating ligand leptin induces weight loss, in part, *via* pro-lipolytic actions on adipose tissue (18-22, 24, 25, 179). Additionally, leptinergic blockade, as demonstrated by a decrease in STAT3 tyrosine phosphorylation, protects diet-induced obese rodents from leptin's fat depleting autocrine/paracrine actions (123). To determine if loss of leptin action *via* disruption of STAT3 signaling was responsible for the increased adiposity in male ASKO mice, leptin-induced lipolysis studies were carried out in adipocytes differentiated in culture from preadipocytes isolated from WT and ASKO mice. Eight days after differentiation, WT and ASKO cells were stimulated with varying doses of recombinant leptin (rLeptin). Glycerol released into the medium was measured after 24 hours of leptin exposure. The addition of rLeptin to WT cells promoted glycerol release relative to cells treated with vehicle alone **(Figure 4.7A)**. The addition of rLeptin to ASKO cells, however,

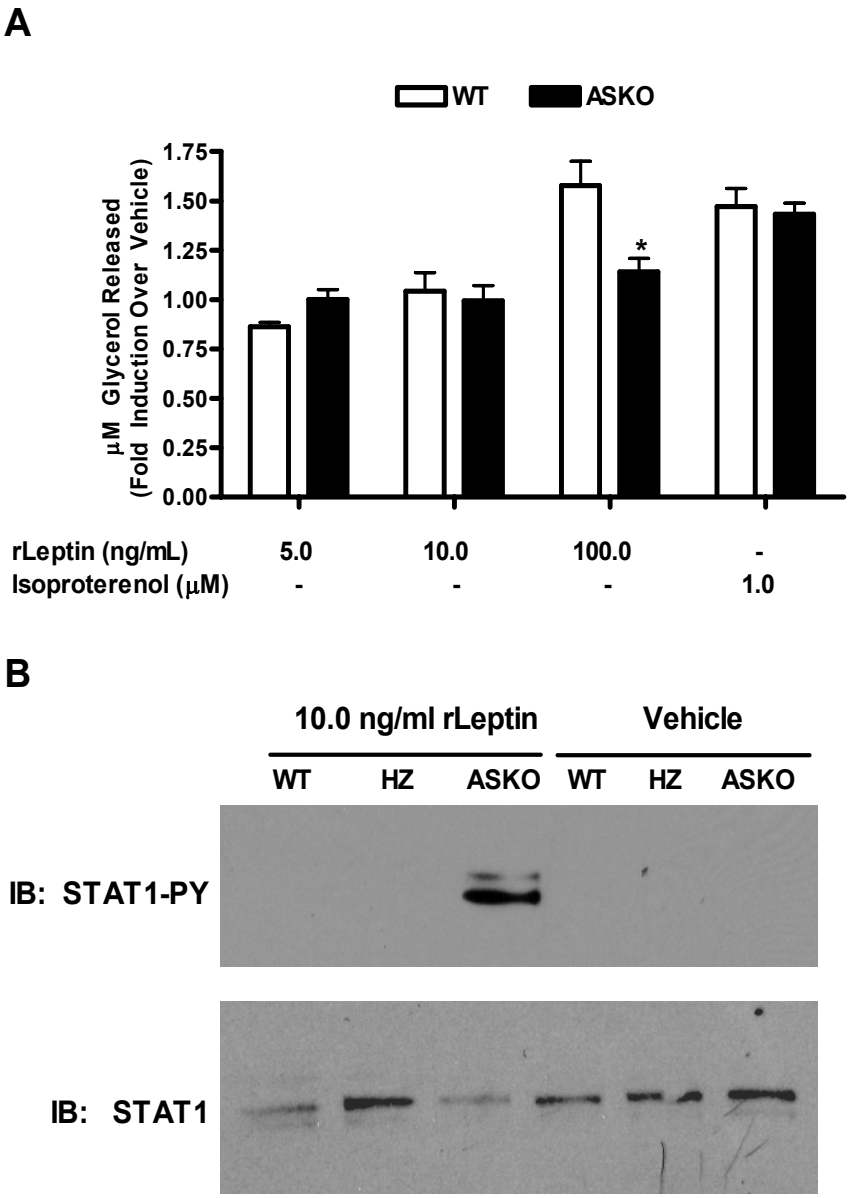


Figure 4.7 – Impaired leptin signaling in ASKO mice.
(A) Glycerol released from WT and ASKO cells stimulated with varying doses of recombinant leptin (rLeptin) or isoproterenol. Data are means ± SE from triplicate dishes repeated three times.
(B) Western blot analysis (IB) of STAT1 tyrosine phosphorylation in subcutaneous primary preadipocytes isolated from WT and ASKO mice cultured in the presence of 10.0ng/ml rLeptin for twenty-four hours.

had no effect **(Figure 4.7A)**; suggesting that adipocyte STAT3 mediates leptin-induced lipolysis. Isoproterenol-induced lipolysis, however, was unimpaired in ASKO cells **(Figure 4.7A)**. In addition, an increase in STAT1 tyrosine phosphorylation was observed only in ASKO cells exposed to rLeptin **(Figure 4.7B)**.

Leptin also induces weight loss *via* anti-lipogenic actions on adipose tissue (18-22, 24, 25, 179). To determine if loss of leptin's anti-lipogenic actions was responsible for the increased adiposity in male ASKO mice, we examined the expression of lipogenic genes. Gene expression analysis of WAT from WT and ASKO mice revealed no differences in the expression of FAS or diacylglycerol acyltransferase (DGAT) **(Figure 4.4C)**.

E. DISCUSSION

In the present studies we show that ASKO mice fed a standard chow diet weigh more than their littermate controls and demonstrate that the higher body weight is due to increased adiposity associated with adipocyte hypertrophy, but not adipocyte hyperplasia, hyperphagia, or reduced energy expenditure. The higher body weight and increased fat mass exhibited by ASKO mice in this study are in agreement with other tissue-specific STAT3 knockout models linking STAT3 and adiposity (89-91). Mice with a neural-specific disruption of the STAT3 gene are obese, hyperleptinemic, leptin resistant, diabetic, and infertile. Mice with a β cell/hypothalamic specific-disruption of the STAT3 gene are also obese, hyperphagic, hyperglycemic, and hyperinsulinemic. In contrast, ASKO mice are obese but are not hyperphagic and do not develop insulin resistance. In addition, phenotypic changes are observed in male ASKO mice only. While the mechanisms causing these sex differences are unknown, they may reflect alternative pathways compensating for the lack of STAT3 in female mice. Recent studies showing that aromatase-deficient mice have a phenotype of increased adiposity (180) suggest that estrogen signaling pathways may have a compensatory effect on STAT3 deficiency in female ASKO mice.

Because increased fat mass in ASKO mice was accompanied by adipocyte hypertrophy without changes in cell number or differentiation, we concluded that increased fat mass was the result of increased TAG accumulation in preexisting adipocytes. We hypothesized that the cause of the enhanced TAG accumulation was either increased fatty acid and TAG synthesis or decreased TAG breakdown. Because the STAT3-activating ligand leptin has been shown to have both anti-lipogenic and pro-lipolytic actions in adipose

tissue (18-22, 179), we speculated that loss of leptin action was responsible for the increased TAG accumulation in adipocytes from ASKO mice. We found that leptin-induced lipolysis was impaired in adipocytes differentiated in culture from preadipocytes isolated from ASKO mice. Isoproterenol-induced lipolysis, however, was unimpaired in ASKO cells, suggesting that leptin-induced lipolysis is dependent on STAT3, but not lipolysis induced by adrenergic stimulation. Because STAT1 was tyrosine phosphorylated in ASKO cells but not in WT cells cultured in the presence of rLeptin, STAT1 is likely not used as an alternative pathway in leptin-induced lipolysis. As for fatty acid and TAG synthesis, the expression of lipogenic genes was increased in ASKO WAT, but not to a significant degree. Because mRNA levels do not always correlate with enzyme activity, further studies examining the activity of lipogenic enzymes are needed to better understand the mechanism of TAG accumulation in adipocytes from ASKO mice.

Recent studies have shown a relationship between adipocyte size and adipokine expression and secretion. Serum adiponectin levels, for example, correlate inversely with adipocyte size (181, 182), while serum leptin levels correlate positively (183). In agreement with the significant hypertrophy of adipocytes in ASKO mice, serum adiponectin levels were significantly reduced. Serum leptin levels, however, were not increased. There are several possible explanations for this finding. The increase in WAT TAG content may not have been sufficient to trigger an increase in leptin synthesis. Furthermore, altered adipocyte differentiation is frequently associated with changes in circulating leptin levels (64, 184, 185). Response elements for adipogenic transcription factors and adipocyte-specific genes have also been identified in the leptin promoter (186). The absence of adipocyte hyperplasia

in ASKO mice, therefore, was consistent with the lack of increased serum leptin levels. Additionally, it has been shown that circulating FFAs stimulate leptin secretion (179, 187). Thus, the absence of increased serum FFAs in ASKO mice was also consistent with the observed normal circulating leptin levels.

Because ASKO mice developed a fatty liver, however, it is notable that they did not exhibit elevated FFAs. The fact that serum fatty acids were not increased in these animals suggests that an increased supply of fatty acids to the liver was not the cause of the steatosis. Rather, an imbalance in liver TAG synthesis, export, or oxidation was likely the cause. It has been shown that high adiponectin levels protect against fatty liver by reducing fatty acid synthesis through inhibition of acetyl-CoA carboxylase (ACC) and FAS expression and activity (188). The reduction of ACC activity also reduces the malonyl CoA level, which is known to inhibit carnitine palmitoyltransferase I (CPT-1) activity and fatty acid oxidation. Therefore, we speculate that the reduced serum adiponectin levels in ASKO mice likely increased fatty acid synthesis and reduced fatty acid oxidation thus causing the fatty liver. Further studies examining changes in gene expression and enzyme activity are needed to understand the exact cause of the TAG accumulation in the livers of ASKO mice.

It is also notable that while ASKO mice are obese and develop a fatty liver, they exhibit normal glucose tolerance on a standard chow diet. The ASKO mouse model is not the only mouse model in which obesity is dissociated from impaired glucose tolerance. Mice lacking AMP-activated protein kinase-α2 (AMPKα2) exhibit increased adiposity and adipocyte hypertrophy, but show no differences in glucose tolerance or insulin sensitivity

compared to WT mice (189). Mice that overexpress phosphoenolpyruvate carboxykinase (PEPCK) in WAT also have increased adipose tissue mass but do not develop insulin resistance (190). Similarly, mice that overexpress DGAT-1 in WAT have larger adipocytes and greater total fat pad weight. The increased adiposity, however, is not associated with impaired glucose disposal (191). Finally, obesity is dissociated from insulin resistance in aP2 deficient mice fed a high fat diet (192). We cannot rule out the possibility, however, that with age or following a long-term challenge with a high fat diet, ASKO mice may develop insulin resistance. Furthermore, as fat accumulation in the liver is a primary event leading to insulin resistance (193-195), it is also possible that as the severity of the fatty liver worsens, ASKO mice may develop insulin resistance as well.

In summary, here we show that loss of STAT3 in mature adipocytes causes higher body weight, increased adiposity associated with adipocyte hypertrophy, reduced serum adiponectin levels, and fatty liver, but not impaired glucose tolerance. We also show that loss of leptin action in WAT, namely loss of leptin-induced lipolysis, may play a role in the observed obese phenotype. The results of our study clearly demonstrate that STAT3 is essential for body weight homeostasis, though further studies are needed to better clarify its role in this regard, especially as it relates to the development of obesity in ASKO mice.

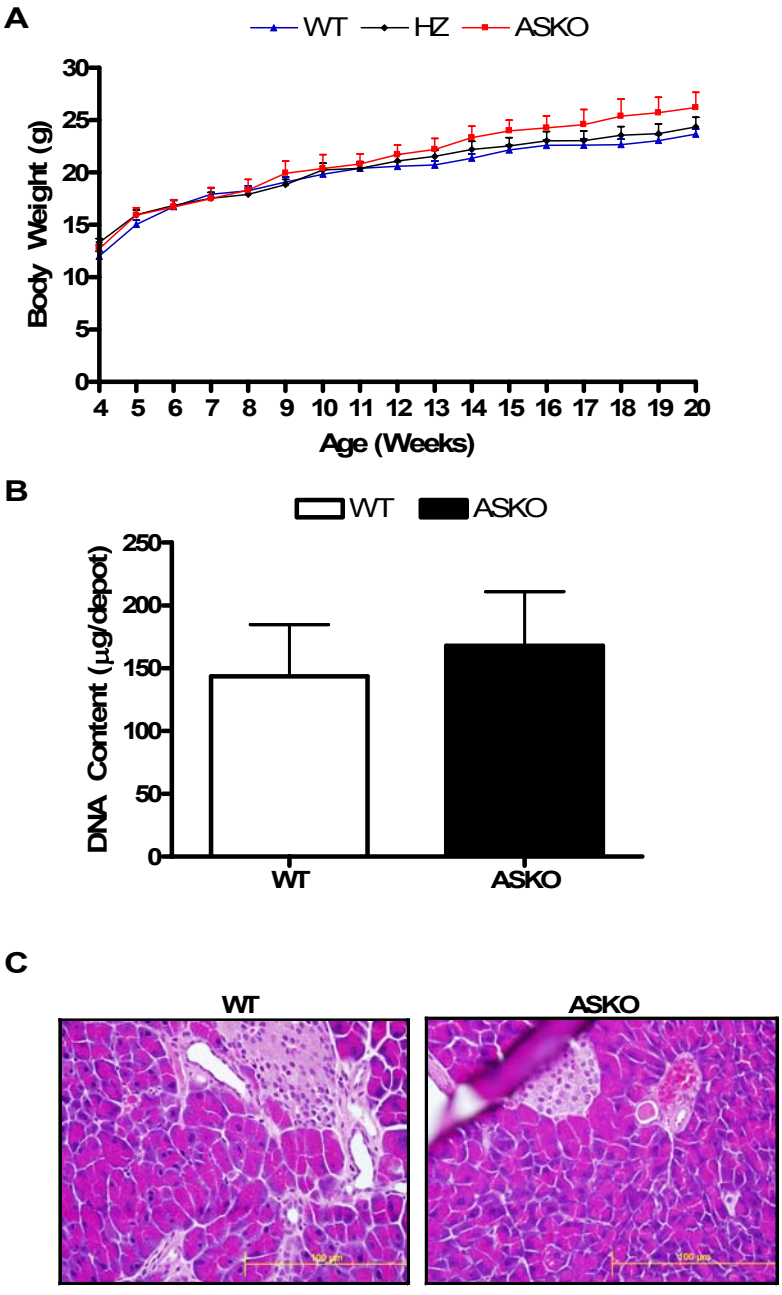


Figure 4.8 – Supplemental data

(A) Growth curves of female ASKO mice and WT and HZ littermate controls. Data are means ± SE (n = 8-16).

(B) Total DNA content in WAT from male ASKO mice and WT littermate controls. Data are means ± SE (n = 6).

(C) Hematoxylin and eosin staining of pancreas sections from 20-week old male ASKO mice and 20-week old male WT littermate controls.

CHAPTER V
SYNTHESIS

A. OVERVIEW OF RESEARCH FINDINGS

This dissertation describes two independent projects that examined the function and activation of STAT3 in adipogenesis and adipocyte metabolism. This work sought to improve our understanding of preadipocyte proliferation, differentiation, and metabolism, as well as the contribution of STAT3 and STAT3 signaling pathways to these processes. The first project identified the differentiation-induced STAT3 activating factor and determined its role in adipogenesis. The aim of the second project was to determine the role of STAT3 in adipogenesis in animals. Mice with an adipocyte-specific disruption of the STAT3 gene (ASKO mice), created using aP2-Cre-*loxP* DNA recombination, and primary preadipocytes isolated from ASKO mice, were used for this project. This section briefly summarizes this research and provides a synthesis of our findings.

1. Midkine is an Autocrine Activator of STAT3 in 3T3-L1 Cells

Our project examining the mechanism of STAT3 tyrosine phosphorylation during adipogenesis was prompted by our initial observation that STAT3 activation during adipogenesis was delayed. These results suggested that a mechanism other than direct activation by MDI was involved. In subsequent studies using conditioned medium (CM), we confirmed that an autocrine/paracrine factor, synthesized and released in response to MDI, activated STAT3. Based on a series of experiments showing that 1) midkine was expressed

in 3T3-L1 preadipocytes, 2) midkine induced STAT3 tyrosine phosphorylation in a time- and dose-dependent manner, and 3) midkine neutralizing antibodies inhibited CM-induce STAT3 tyrosine phosphorylation, we concluded that the heparin-binding growth factor midkine was the autocrine/paracrine activator of STAT3 in 3T3-L1 cells.

Next we found that midkine was sufficient to stimulate post-confluent preadipocyte proliferation, likely though a STAT3 signaling pathway. Although mitotic clonal expansion is required from progression through the differentiation program (37, 39, 40), we found that midkine was not sufficient to induce differentiation in the absence of MDI. Midkine was necessary, however, for adipogenesis. Cells treated with MDI plus anti-midkine antibody accumulated significantly less TAG than cells treated with MDI alone. The expression of adipogenic transcription factors was also significantly reduced in cells treated with MDI plus anti-midkine antibody. We concluded, therefore, that the midkine/STAT3 signaling pathway is necessary for mitotic clonal expansion and differentiation. This work supports our initial hypothesis and highlights the midkine/STAT3 signaling pathway as a potential pharmaceutical target for the treatment of obesity.

This was the first study to show that the heparin-binding growth factor midkine is sufficient for mitotic clonal expansion. This finding parallels previous studies linking adipocyte hyperplasia to an augmented production of heparin-binding growth factors (160). Similarly to midkine, these mitogens have been shown promote preadipocyte proliferation via autocrine/paracrine mechanisms (166). Although these studies suggest that midkine may contribute to the increased cellularity associated with severe obesity, continued research is

needed. Transgenic mice overexpressing midkine selectively in WAT would provide a physiological model to study the role of midkine in the development of adipocyte hyperplasia.

Another limitation of this study was the lack of a sensitive method to detect midkine protein in the CM. Continued research is also needed, therefore, to determine if midkine is released by preadipocytes, and if midkine expression and plasma concentrations are increased in models of obesity.

2. Adipocyte-Specific Disruption of Signal Transducer and Activator of Transcription 3 (STAT3) Increases Body Weight and Adiposity

Our first project identified a midkine-STAT3 signaling pathway that is necessary for adipogenesis. The aim of our second project was to build on this finding and determine the physiological role of STAT3 in adipogenesis using mice with an adipocyte-specific disruption of the STAT3 gene. Because the midkine-STAT3 signaling pathway was necessary for adipogenesis *in vitro*, we hypothesized that mice lacking adipocyte STAT3 would have dramatically reduced amounts of WAT and exhibit physiological consequences associated with lipoatrophy. In practice, however, STAT3 expression was preserved in preadipocytes limiting us from examining the physiological role of STAT3 in adipogenesis. Consequently, this mouse model was studied to determine the role of STAT3 in the mature adipocyte.

In this project, we found that male ASKO mice weighed significantly more than their

littermate controls and concluded that their higher body weight was due to increased adiposity accompanied by adipocyte hypertrophy without changes in cell number, food intake, or energy expenditure. We also found that increased adiposity was not restricted to adipose tissue. Liver TAG was increased in male ASKO mice as well. Furthermore, serum adiponectin levels, which correlate negatively with adiposity and hepatic fat (177, 196), were significantly reduced. Surprisingly, despite increased fat mass and liver TAG, male ASKO mice displayed normal glucose tolerance, and normal circulating insulin, leptin, TAG, and FFAs. We also found that leptin signaling in WAT was impaired in ASKO mice. Based on these findings, we concluded that STAT3 plays an essential role in body weight homeostasis. This work is in agreement with other studies linking STAT3 and adiposity (89-91), and highlights the importance of STAT3 in adipocyte metabolism.

One limitation of this study was the lack of a definitive mechanism to explain the ASKO phenotype. This raises several interesting questions: What is the mechanism of the fatty liver in ASKO mice? Is obesity dissociated from insulin resistance in the ASKO mouse model? Is loss of leptin, IL-6 and/or CNTF's anti-lipogenic and pro-lipolytic actions on adipocytes responsible for the obese phenotype in ASKO mice? Continued research is needed to answer these pressing questions.

B. DIRECTIONS FOR FUTURE RESEARCH

The research presented here could proceed in many natural directions that will contribute to the understanding of preadipocyte proliferation, differentiation, and metabolism, as well as the contribution of STAT3 and STAT3 signaling pathways to these

processes. In addition to studying the *in vivo* contribution of midkine to adipocyte hyperplasia and obesity, continued research is needed to better clarify the observed phenotype in ASKO mice. This work could help to direct efforts to identify potential adipose-tissue driven causes of human obesity and to discover targets for the treatment of diseases such as obesity, hepatic steatosis, and insulin resistance.

1. Adiponectin and fatty liver disease in ASKO mice

In "Adipocyte-Specific Disruption of Signal Transducer and Activator of Transcription 3 (STAT3) Increases Body Weight and Adiposity", we found that liver TAG content was significantly increased in ASKO mice, and concluded that an imbalance in liver TAG synthesis, export, and oxidation likely caused the fatty liver. Because high adiponectin levels protect against fatty liver by reducing TAG synthesis and increasing fatty acid oxidation (188), we hypothesized that reduced adiponectin levels in ASKO mice were responsible for the steatosis. Additional studies are needed, however to determine the mechanism of the fatty liver.

To characterize the impact of low adiponectin levels on fatty liver in ASKO mice, future studies will examine the expression and activity of genes involved in TAG synthesis and oxidation. Further studies will also examine the effect of chronic adiponectin administration on gene expression, enzyme activity, and liver TAG content. If decreased adiponectin levels are the cause of the liver TAG accumulation, we expect ACC and FAS expression and activity to be increased in livers from ASKO mice, and CPT-1 activity to be decreased in livers from ASKO mice. In contrast, we expect continuous administration of

adiponectin to significantly decrease ACC and FAS expression and activity, significantly increase CTP-1 activity, and as a result, dramatically reduce hepatic lipid content.

2. Evidence for a causal relationship between hepatic steatosis and insulin resistance in ASKO mice

Although hepatic steatosis and insulin resistance co-exist in many rodent models of obesity (174-176), whether insulin resistance is the cause or the effect of hepatic steatosis remains unclear. Savage *et al.* suggest that increases in liver diacylglycerol, due to increased lipogenesis and/or decreased fatty acid oxidation, activate PKC-ε, which binds to and inactivates the insulin receptor, resulting in reduced IRS-1 and IRS-2 tyrosine phosphorylation. This in turn results in reduced insulin activation of P13-kinase and AKT, resulting in lower insulin-stimulated liver glycogen synthesis and decreased suppression of hepatic gluconeogenesis (197).

As discussed in "Adipocyte-Specific Disruption of Signal Transducer and Activator of Transcription 3 (STAT3) Increases Body Weight and Adiposity", while ASKO mice are obese and develop a fatty liver, they exhibit normal glucose tolerance. As the severity of the fatty liver worsens, however, it is possible that ASKO mice will develop insulin resistance. The ASKO mouse model, therefore, provides a perfect model for determining if a causal relationship exists between hepatic steatosis and insulin resistance.

To characterize the impact of fatty liver on insulin resistance, glucose homeostasis studies will be performed on aged ASKO mice. Glucose homeostasis studies will also be

performed on ASKO mice following a long-term challenge with a high fat diet. In aged mice, we expect the severity of the fatty liver to worsen. We also expect the severity of the fatty liver to worsen in ASKO mice on a high fat diet. If a causal relationship exists between hepatic steatosis and insulin resistance, we also expect aged ASKO mice and ASKO mice on a high fat diet to develop insulin resistance.

3. Mechanism for the obese phenotype in ASKO mice

In "Adipocyte-Specific Disruption of Signal Transducer and Activator of Transcription 3 (STAT3) Increases Body Weight and Adiposity", we found that increased fat mass in ASKO mice was the result of increased TAG accumulation in preexisting adipocytes. We hypothesized that the cause of the enhanced TAG accumulation was increased fatty acid and TAG synthesis and/or decreased TAG breakdown due to loss of leptin, IL-6 and/or CNTF's anti-lipogenic and pro-lipolytic actions on adipocytes via disruption of STAT3 signaling. Although we found that leptin-induced lipolysis was impaired *ex vivo*, additional studies are needed to characterize the impact of loss of leptin, IL-6, and CNTF action on the obese phenotype in ASKO mice.

To answer these questions, WT and ASKO primary cells will be labeled with [^{14}C] oleate after stimulation with recombinant leptin, IL-6, or CNTF. Following stimulation, lipid extracts from cells and media will be separated by thin layer chromatography, and fatty acid incorporation into synthetic and oxidative pathways will be quantified. Because leptin, IL-6 and CNTF have anti-lipogenic and pro-lipolytic and oxidative actions on adipose tissue, we expect fatty acids to be channeled towards oxidative pathways and away from synthetic

pathways in WT cells. Alternatively, if STAT3 mediates the anti-lipogenic and pro-lipolytic and oxidative actions of leptin, IL-6 and CNTF, we expect fatty acids to be channeled towards synthetic pathways and away from oxidative pathways in ASKO cells.

To further clarify the impact of loss of leptin, IL-6, and CNTF action on the obese phenotype in ASKO mice, a wild-type recipient mouse will be transplanted with a fat pad resected from a wild-type donor mouse and a fat pad resected from an ASKO donor mouse. In addition, an ASKO recipient mouse will be transplanted with a fat pad resected from an ASKO donor mouse and a fat pad resected from a wild-type donor mouse. After the surgery, hyperleptinemia will be induced in the recipient mice. To determine if loss of IL-6 or CNTF action is responsible for the increased TAG accumulation in adipocytes from ASKO mice, similar experiments will be performed. If STAT3 mediates the fat depleting autocrine actions of leptin, IL-6, and CNTF, we expect that WT recipients will lose more body weight than ASKO recipients. Furthermore, we expect that fat will be depleted from native wild-type fat pads and fat pad transplants from wild-type mice, but not from native ASKO fat pads or fat pad transplants from ASKO mice. Therefore, we expect that WT recipients will also lose more fat mass than ASKO recipients.

4. A new model of STAT3 deficiency

In "Midkine is an Autocrine Activator of STAT3 in 3T3-L1 Cells" we identified a midkine-STAT3 signaling pathway that was necessary for preadipocyte mitotic clonal expansion and differentiation. In view of this finding, in "Adipocyte-Specific Disruption of Signal Transducer and Activator of Transcription 3 (STAT3) Increases Body Weight and

Adiposity", we set out to determine the role of STAT3 in adipogenesis in animals. Because aP2-Cre driven deletion of STAT3 did not occur until late in the adipogenic program, the effect of loss of STAT3 on adipogenesis could not be assessed in this knockout model. Consequently, to characterize the impact of STAT3 deficiency on adipocyte formation, a new knockout model is needed.

To create this knockout model, mice heterozygous for the targeted STAT3 gene ($STAT3^{flox/+}$) will be crossed with transgenic mice expressing Cre recombinase under the control of a preadipocyte specific promoter such as Pref-1. If STAT3 is necessary for preadipocyte proliferation and differentiation, we expect that mice lacking preadipocyte STAT3 will have dramatically reduced amounts of WAT and exhibit physiological consequences associated with lipoatrophy. Alternatively, using 3T3-L1 preadipocyte and RNAi, we will establish a STAT3 knockout cell line. If STAT3 is necessary for preadipocyte proliferation and differentiation in this model, we expect that $STAT3^{-/-}$ cells will neither undergo mitotic clonal expansion nor differentiate into adipocytes.

C. PUBLIC HEALTH SIGNIFICANE

The prevalence of obesity, the host of co-morbidities associated with the disease, as well as the economic impact of the disease, make obesity a significant public health concern. The costs associated with cancer detection and treatment, as well as the prevalence and high mortality rates of the disease also highlight cancer as a serious public health issue. Therefore, given that our findings may facilitate the development of anti-obesity drugs and cancer therapies, this work clearly has important implications for advancing public health

and generating new avenues for future research.

For example, our studies identifying a midkine-STAT3 signaling pathway in proliferating preadipocytes that is necessary for adipogenesis revealed new targets for the pharmacological treatment of obesity. Drugs designed to target this signaling pathway, particularly by inhibiting midkine or STAT3 expression, or by inhibiting STAT3 tyrosine phosphorylation, dimerization, or DNA binding, may promote weight loss by blocking adipogenesis. Furthermore, our studies establishing that adipocyte STAT3 regulates body weight homeostasis revealed an alternative means to target obesity *via* STAT3. By activating lipolytic pathways and inhibiting lipogenic pathways, pharmacological agents designed to target adipocyte STAT3 may also promote weight loss.

Additionally, because midkine is overexpressed in a variety of cancers (150-155, 165), and because constitutively active STAT3 has been observed in a variety of cancer cell lines and primary tumors (101-105), midkine and STAT3 may also serve as targets for the treatment of cancer. By promoting apoptosis and preventing proliferation, drugs designed to inhibit midkine or STAT3 expression, or block STAT3 tyrosine phosphorylation, dimerization or DNA binding, may serve to suppress tumor growth.

CHAPTER VI
DETAILED METHODS

A. ANIMAL MODELS

To determine the role of STAT3 in adipocyte formation and body weight homeostasis, using the Cre-*loxP* DNA recombination system, we generated mice with an adipocyte-specific disruption of the STAT3 gene (ASKO mice). Conditional gene inactivation involved six steps **(Figure 6.1)**:

1. Assembly of the targeting vector
2. Production and identification of targeted embryonic stem (ES) cell clones
3. Removal of the positive selection marker by FlpE recombinase
4. Production of chimeras by blastocyst injection of targeted ES cells
5. Transmission of the functional allele through the mouse germline
6. Inactivation of the functional allele by Cre recombinase

1. Assembly of the Targeting Vector

A targeting vector is designed to recombine with a specific chromosomal locus. The essential components of such a vector are a plasmid backbone and sequences which are homologous with the desired chromosomal integration site.

1.1 The OSfrt-*loxP* Plasmid

The OSfrt-*loxP* plasmid (kindly provided by Oliver Smithies and the Animal Models

Core and the University of North Carolina at Chapel Hill) served as the plasmid backbone for the STAT3 targeting vector. This OSfrt-*loxP* plasmid has several unique features including a positive selection marker and a negative selection marker, FRT sites flanking the positive selection marker to facilitate its removal by FlpE recombinase, a *loxP* site to facilitate removal of the targeted exon by Cre recombinase, and five unique restriction sites, SpeI, AgeI, XhoI, BamHI, and SalI **(Figure 6.2)**.

1.1.1 Positive-Negative Selection

Because the transfection efficiency and targeting frequency of targeting vectors are low, it is desirable to include both positive and negative selection makers. Positive selection markers are included in the targeting vector to facilitate the isolation of ES cell clones that incorporate the targeting vector by homologous recombination. The OSfrt-*loxP* plasmid relies on the neomycin phosphotransferase (*neo)* gene for positive selection. *Neo* confers resistance to G418. Therefore, because *neo* is included within the regions of homology, clones carrying the desired homologous recombination event are G418 resistant and survive. Clones in which the construct integrates randomly, however, are also resistant to G418 and survive. To facilitate the elimination of these randomly integrated ES cell clones, a negative selection marker is also included in the targeting vector. The OSfrt-*loxP* plasmid relies on the thymidine kinase (TK) gene for negative selection. TK is included outside the regions of homology. Because sequences outside the regions of homology are lost during homologous recombination, ES cell clones carrying the desired homologous recombination event do not retain the TK gene. During random integration however, all sequences in the construct are retained. Thus, random integrants retain the TK gene. In the presence of the TK gene, cells

are sensitive to gancyclovir. Therefore, homologous recombinants are gancyclovir resistant and survive, whereas the majority of clones in which the construct integrates randomly are gancyclovir sensitive and die.

1.1.2 Site-Specific Recombinase Systems: Cre-*loxP* and FlpE-FRT

Site-specific recombination systems are comprised of two elements: the recombinase enzyme and DNA sequences recognized by the recombinase enzyme. The target sites for two recombinase systems, the Cre-*loxP* system from the bacteriophage P1 and the FlpE-FRT system from the budding yeast *Saccharomyces cerevisiae*, are key components of the OSfrt-*loxP* plasmid. The *loxP* (locus of cross-over (x) in P1) site is included in the targeting vector to facilitate removal of the targeted exon by Cre recombinase. FRT sites are included to facilitate *neo* removal by FlpE recombinase.

The target sites for both Cre recombinase and FlpE recombinase are 34 base pairs. These sites consist of 13 base pair repeats flanking an 8 base pair A:T-rich asymmetric core. The 13 base pair repeats provide binding sites for the recombinase enzyme. The core sequence is the site of strand cleavage, exchange, and ligation. Furthermore, the orientation of the target sites, relative to each other, determines the type of modification catalyzed by the recombinase enzyme. Directly oriented sites, as included in the OSfrt-*loxP* plasmid, lead to excision of intervening DNA.

1.2. Homologous Sequences

Because the STAT3 gene was the desired chromosomal integration site, the murine

STAT3 gene was amplified by PCR **(Figure 6.3)** and cloned into the OSfrt-*loxP* plasmid **(Figure 6.4A)**. To increase the targeting frequency, the homologous sequences were derived from genomic DNA isogenic with the ES cells to be used in the targeting experiment (See Section 2. Production and Identification of Targeted ES Cell Clones). First, the long arm of homology was amplified from 129/SvEv genomic DNA using the LAStatF (**5'ACTAGTTCAGAGTCTCAGCACTCACTCCAC3'**) and LAStatR (**5'ACCGGTTTGCCATCCAG TCTTGCAGTTTGAAGTTCT3'**) primers. The resulting 3.3kb PCR product spanned exon 21 of the STAT3 gene. For cloning purposes, a SpeI restriction site and an AgeI restriction site were introduced at the 5'end and the 3' end of the fragment respectively. Next, the short arm of homology was amplified utilizing 129/SvEv genomic DNA and the SAStatF (**5'GGATCCTGAAGGGCTGGTAGCTGCTGGGCTTGTTTA3'**) and SAStatR (**5'GTCGACCTCAG TGTTCCAGTAAGCTGAGTGAGCGAA3'**) primers. The resulting 2.4kb PCR product spanned exons 23 and 24 of the STAT3 gene. For cloning purposes, a BamHI restriction site and a SalI restriction site were introduced at the 5'end and the 3' end of the fragment respectively. Finally, the target arm was amplified utilizing 129/SvEv genomic DNA and the E22StatF (**5'ACCGGTATAACTTCGTATAGCATACATTATACGAAGTTATGCAGCATGTGATGAGGGAGG ACAGCCCTAA3'**) and E22StatR (**5'CTCGAGCGGTAACTCTCACCCCATGTCCTCCCTATT3'**) primers. The resulting 339bp PCR product spanned exon 22 of the STAT3 gene and included a tyrosine residue necessary for STAT3 activation. A *loxP* site was introduced upstream of exon 22 (to facilitate removal by the Cre recombinase). For cloning purposes, an AgeI restriction site and a XhoI restriction site were introduced at the 5'end and the 3' end of the fragment respectively.

Next, the long arm, short arm, and target arm were cloned into the OSfrt-*loxP* plasmid at the SpeI and AgeI restriction sites, the BamHI and SalI restriction sites, and the AgeI and XhoI restriction sites of the OSfrt-*loxP* plasmid respectively. A series of diagnostic digests **(Figure 6.4B)** and sequencing experiments were performed to confirm proper assembly of the targeting vector**.**

2. Production and Identification of Targeted ES Cell Clones

Next, 20.0μg of the assembled STAT3 targeting vector was electroporated into 2 x 10^7 129/SvEv pluripotent ES cells. When a targeting vector is electroporated into ES cells, the targeting vector can either integrate into its target locus or it can integrate into a random chromosomal location. To identify ES cell clones carrying the desired homologous recombination event, ES cell were grown in the presence of gancyclovir and G418. Gancyclovir and G418 resistant clones were then screened for homologous recombination by PCR **(Figure 6.5)**. ES cell clones carrying the desired homologous recombination event (as identified by PCR) were expanded. Homologous recombination was then confirmed in these clones by Southern blot analysis **(Figure 6.6).**

3. Removal of *Neo* by FlpE Recombinase

As previously mentioned, the positive selection marker is a necessary component of the targeting vector because it facilitates the isolation of ES cell clones that stably incorporate the targeting vector. If retained however, it can interfere with the target locus and other genes linked to the target locus (198, 199). Therefore, to eliminate these undesirable effects, it is necessary to remove the positive selection marker following gene targeting.

Neo removal was accomplished with the use of the FlpE-FRT site-specific recombination system. Targeted clones were electroporated with a vector that transiently expressed FlpE recombinase (kindly provided by the Animal Models Core at the University of North Carolina at Chapel Hill). Clones were then screened for *neo* removal by PCR **(Figure 6.7)**.

4. Production of Chimeras by Blastocyst Injection of Targeted ES Cells

Next, 129/SvEv targeted ES cell clones not containing *neo* were microinjected into blastocysts derived from superovulated C57BL/6 females **(Figure 6.8)**. To generate mice chimeric from the targeted ES cells and host blastocysts, microinjected blastocysts were transferred to the uterus of pseudopregnant C57BL/6 recipients. Mice were rendered pseudopregnant through matings with vasectomized males during ovulation.

5. Transmission of the Functional Allele through the Mouse Germline

Because germ cells are derived from the same cell lineage that gives rise to the skin (primitive ectoderm), coat color was used to estimate the degree of germline contribution of the targeted ES cells. As previously mentioned, the blastocysts used to generate the chimeric mice were derived from C57BL/6 females, which have a black coat. Furthermore, the targeted ES cells that were implanted into the blastocysts were derived from the 129/SvEv substrain, which has a white coat. Consequently, male chimeric mice with a high proportion of brown fur and therefore a high probability of transmitting the targeted allele to their offspring, were mated with wild-type C57BL/6 females **(Figure 6.9)**. Agouti mice with brown coats were produced when the targeted 129/SvEv ES cell genome successfully

populated the germ cells of the chimera.

6. Inactivation of the Functional Allele by Cre Recombinase

Figure 6.9 shows the mating strategy used to create ASKO mice. First, agouti mice heterozygous for the targeted STAT3 gene ($STAT3^{flox/+}$) were mated with transgenic mice expressing Cre recombinase under the control of the adipocyte specific aP2 promoter (aP2-Cre $STAT3^{+/+}$, Jackson Laboratories, Bar Harbor, Maine). A quarter of the offspring inherited both the targeted allele and the Cre-expressing transgene (aP2-Cre $STAT3^{flox/+}$). These mice were then intercrossed to yield six derivative strains: (a) $STAT3^{+/+}$ (WT), (b) $STAT3^{flox/+}$ (WT), (c) $STAT3^{flox/flox}$ (WT), (d) $STAT3^{+/+}$/Cre (WT), (e) $STAT3^{flox/+}$/Cre (HZ), and (f) $STAT3^{flox/flox}$/Cre (ASKO). To assess the efficiency of Cre-mediated STAT3 deletion, adipose tissue excised from experimental mice was screened by PCR **(Figure 6.10).**

B. PRIMARY PREADIPOCYTES

1. Isolation and Culture of Stromal-Vascular Cells

Subcutaneous WAT was aseptically removed from 20-week old male mice and stromal vascular cell cultures were established as previously described (169). Briefly, inguinal WAT was excised from freshly killed ASKO mice and littermate controls. After excision, adipose tissue was minced into small pieces, washed in Dulbecco's Modified Eagle's Medium (DMEM) supplemented with 1% bovine serum albumin (BSA), and centrifuged at 1000 x g for 10 minutes to remove blood cells. Tissue was then decanted into DMEM containing 1.0 mg/ml type I collagenase and digested for 45 minutes at 37ºC with constant end-over-end inversion. Following the digestion, adipose cells and stromal vascular

cells were separated by centrifugation at 500 x g for 10 minutes. The stromal vascular cell pellet was then resuspended and cultured in DMEM containing 10% v/v FBS, 10 mg/ml streptomycin, 100 U/ml penicillin, and 1 mM pyruvate at 37°C in 5% CO_2 air.

To induce differentiation, 2-day postconfluent preadipocytes were treated with Zen-Bio Differentiation Medium (Zen-Bio, Raleigh, NC). On day 3, the differentiation medium was replaced with Zen-Bio Adipocyte Maintenance Medium, which was changed every 2 days thereafter until analysis on day 8. To determine whether the primary preadipocytes differentiated into mature adipocytes, eight days after induction of differentiation cells were washed with PBS, fixed with 3.7% formaldehyde in PBS, and then stained with 0.5% Oil Red-O. As shown in **Figure 6.11,** primary preadipocytes stimulated with differentiation medium efficiently differentiated into mature adipocytes**.** No differences were observed between ASKO cells and littermate control cells.

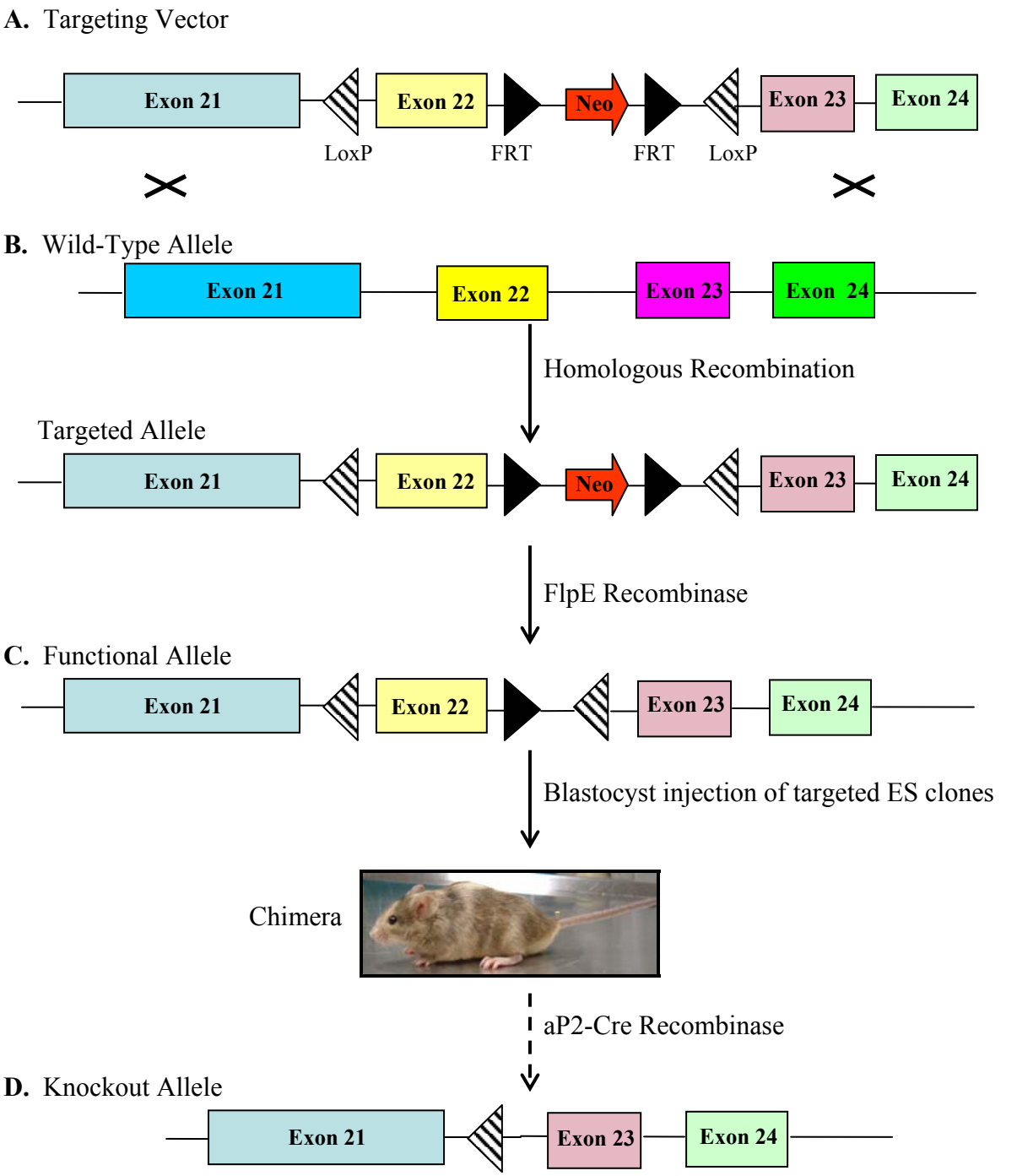


Figure 6.1 - Targeting Strategy
Schematic representation of (A) the STAT3 targeting vector, (B) the endogenous STAT3 allele before (wild-type allele) and after (targeted allele) homologous recombination, (C) the targeted allele after FlpE recombination (functional allele), and (D) the functional allele after Cre-mediated deletion of exon 22 (knockout allele).

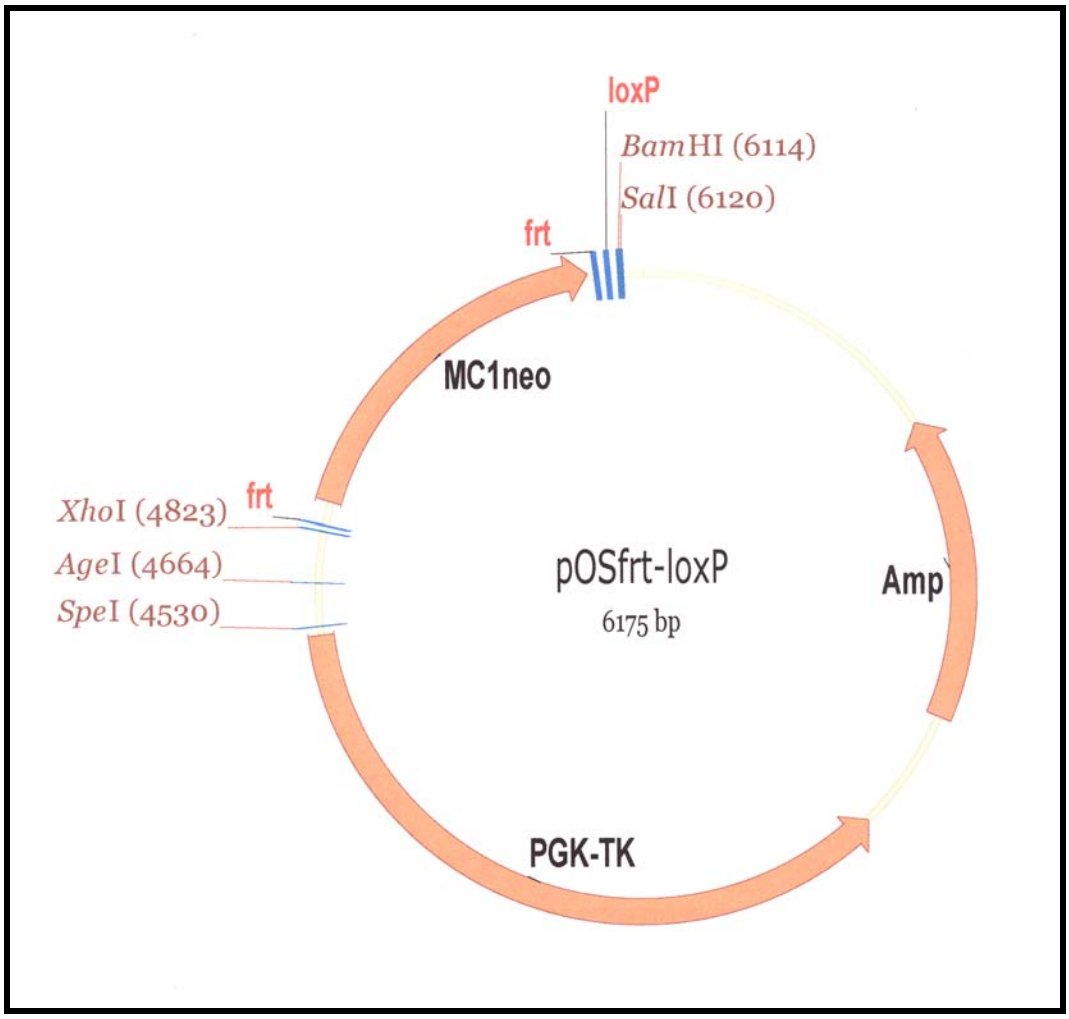


Figure 6.2 – The OSfrt-*loxP* Plasmid
Schematic representation of the OSfrt-*loxP* plasmid. This plasmid contains several unique features including a positive selection marker (*neo*), a negative selection marker (TK), FRT sites flanking *neo*, a *loxP* site, and five unique restriction sites, SpeI, AgeI, XhoI, BamHI, and SalI. The positive selection marker *neo* confer resistance to neomycin while the negative selection marker TK is sensitive to gancyclovir. FlpE recombinase and Cre recombinase catalyze the site specific recombination of DNA between FRT sites and *loxP* sites respectively.

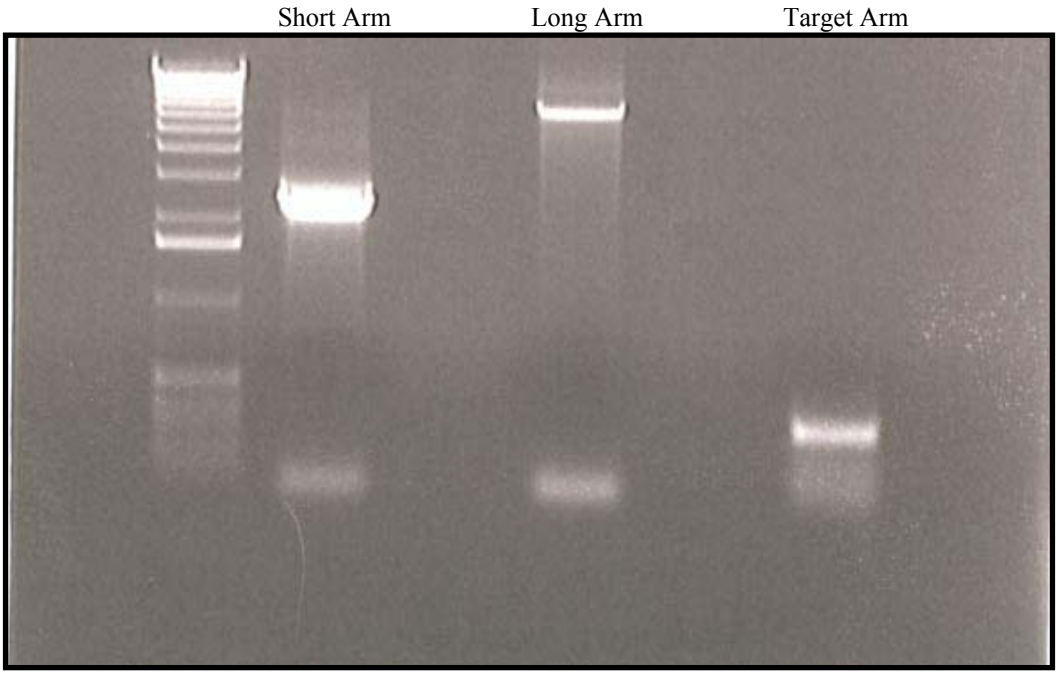
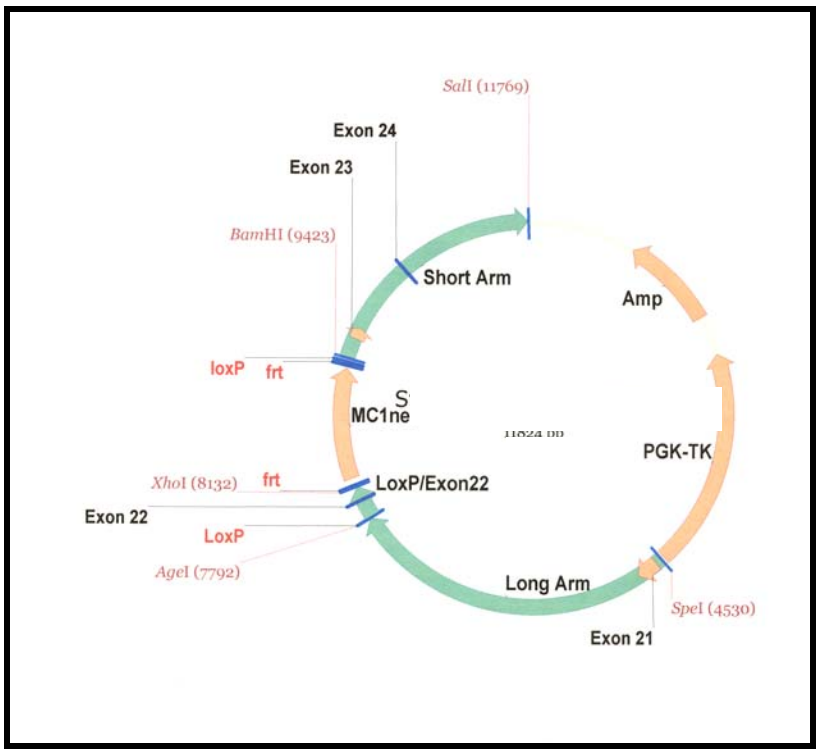


Figure 6.3 - Long Arm, Short Arm, Target Arm Amplification
PCR analysis of 129/SvEv genomic DNA amplified utilizing the SAStatF and SAStatR primers, the LAStatF and LAStatR primers, and the E22StatR and E22StatR primers.

A.



B.

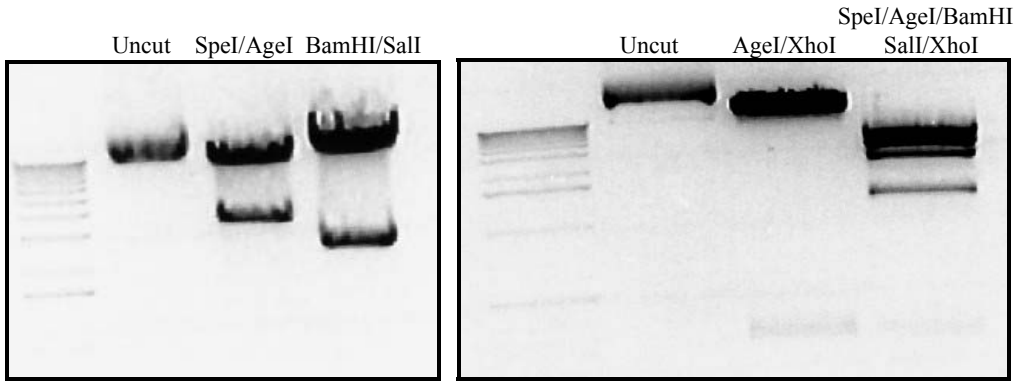


Figure 6.4 - The Assembled Targeting Vector

(A) Schematic representation of the assembled targeting vector. The long arm, spanning exon 21 of the STAT3 gene, was cloned into the OSfrt-*loxP* plasmid at the SpeI and AgeI restriction sites. The short arm, spanning exons 23 and 24 of the STAT3 gene, was cloned into the OSfrt-*loxP* plasmid at the BamHI and SalI restriction sites. The target arm, spanning exon 22 of the STAT3 gene and including a tyrosine residue necessary for STAT3 activation, was cloned into the OSfrt-*loxP* plasmid at the AgeI and XhoI restriction sites.

(B) A series of diagnostic digests were performed to confirm proper assembly of the targeting vector. A SpeI/AgeI digest produced an 8.5kb fragment and a 3.3kb fragment (long arm). A BamHI/SalI digest produced a 9.4kb fragment and a 2.4kb fragment (short arm). An AgeI/XhoI digest produced an 11.5kb fragment and a 339bp fragment (target arm). A SpeI/AgeI/BamHI/SalI/XhoI digest produced a 4.6kb fragment, a 3.3kb fragment (long arm), a 2.4kb fragment (short arm), a 1.3kb fragment, and a 339bp fragment (target arm).

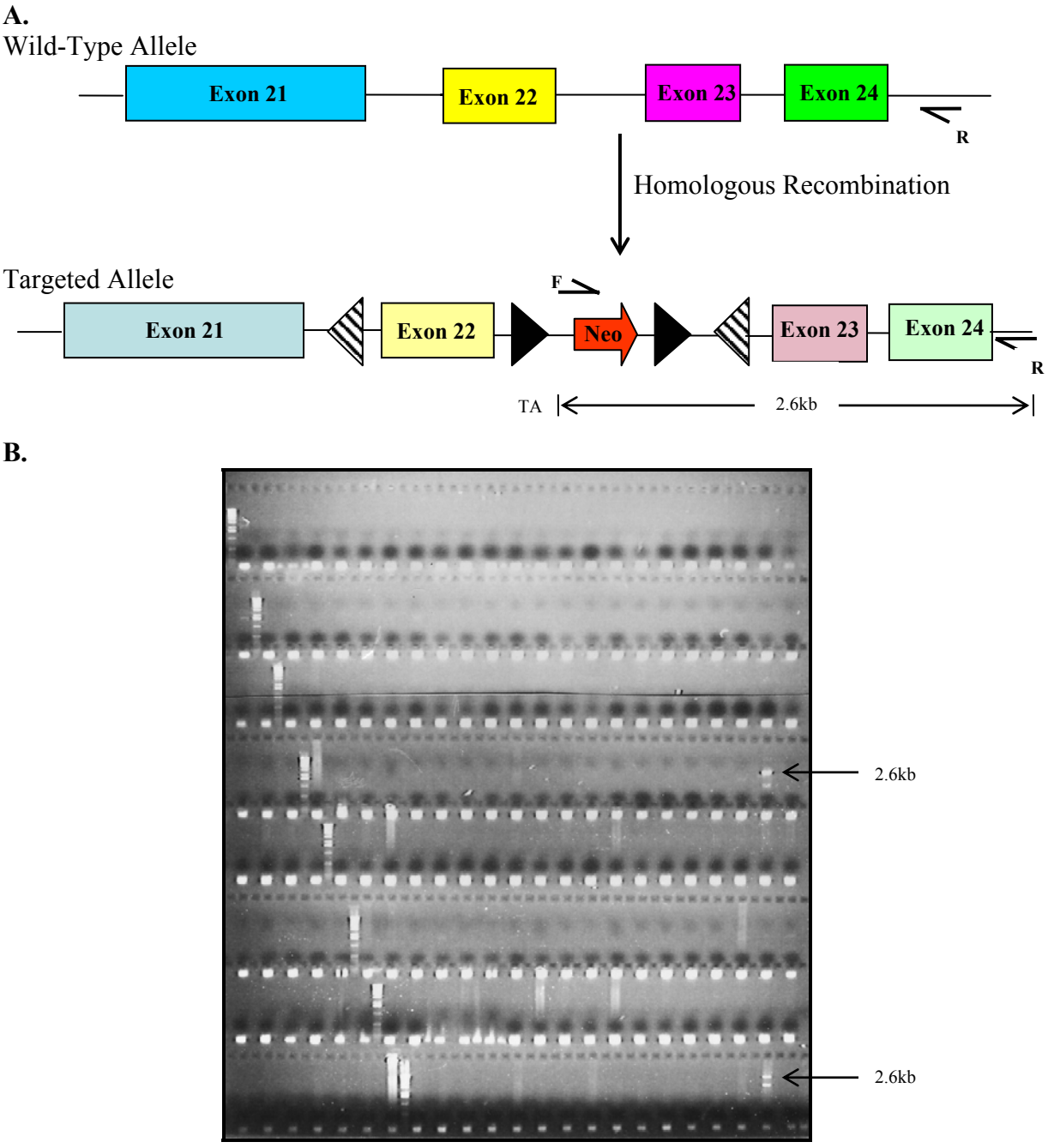
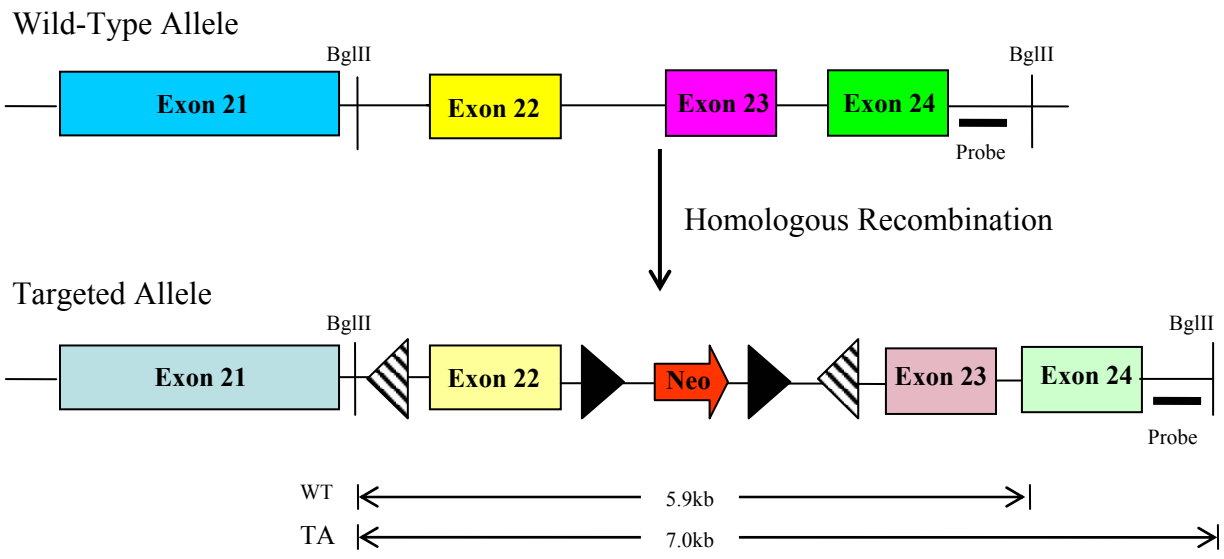


Figure 6.5 - Assessment of Homologous Recombination Using PCR
(A) Schematic representation of the STAT3 allele before (wild-type allele) and after (targeted allele) homologous recombination. The position of the forward and reverse primers used for PCR analysis are shown by the arrows labeled F and R respectively. The forward primer binds to the *neo* cassette and the reverse primer binds to a region outside of the targeting vector within the endogenous locus. A 2.6kb PCR product was expected if a recombination event occurred at the STAT3 locus. A PCR product was not expected if a recombination event did not occur.
(B) PCR analysis of DNA prepared from 129/SvEv ES cells electroporated with the assembled targeting vector.



B.

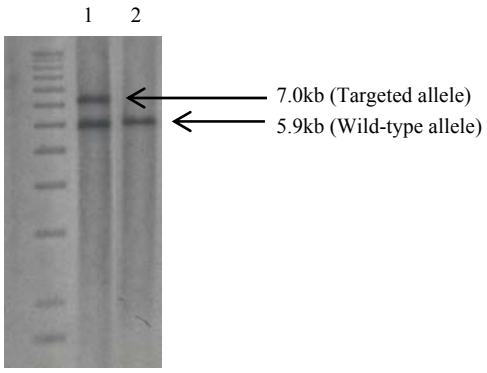
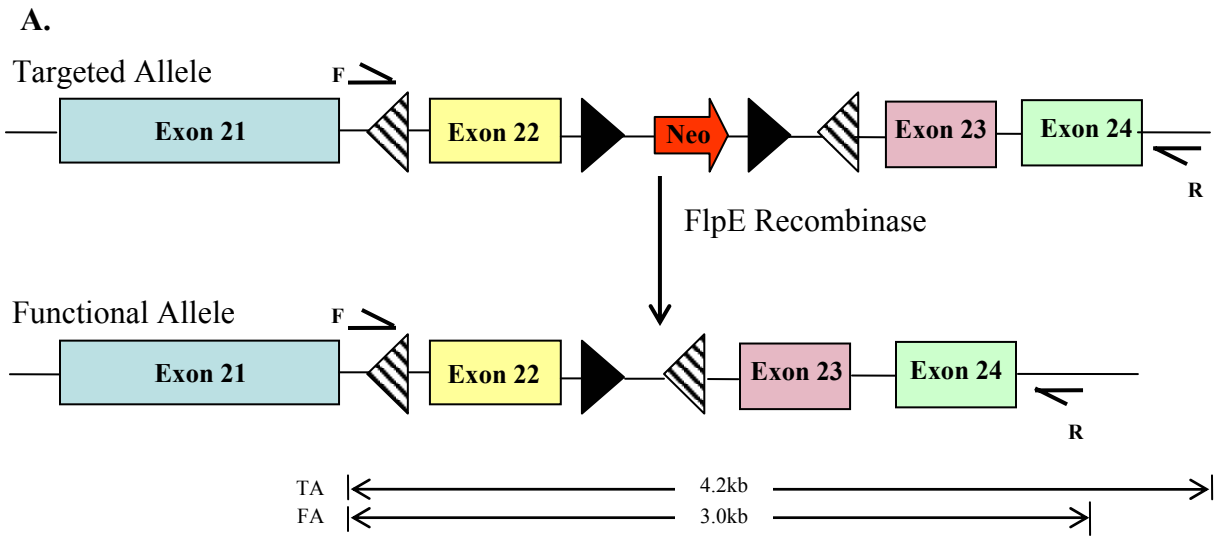


Figure 6.6 - Assessment of Homologous Recombination Using Southern Blot Analysis
(A) Schematic representation of the STAT3 allele before (wild-type allele) and after (targeted allele) homologous recombination. The position of the probe used for Southern blot analysis is shown by the line labeled Probe. Following a BglII digest, a 7.0kb band was expected if a recombination event occurred at the STAT3 locus. A 5.9kb band was expected if a recombination event did not occur.
(B) Southern blot analysis of DNA isolated from ES cell clones carrying the desired homologous recombination event as identified by PCR. DNA from clone 1 produced a 7.0kb band (targeted allele) and a 5.9kb band (wild-type allele). Only a 5.9 (wild-type allele) was detected in clone 2.



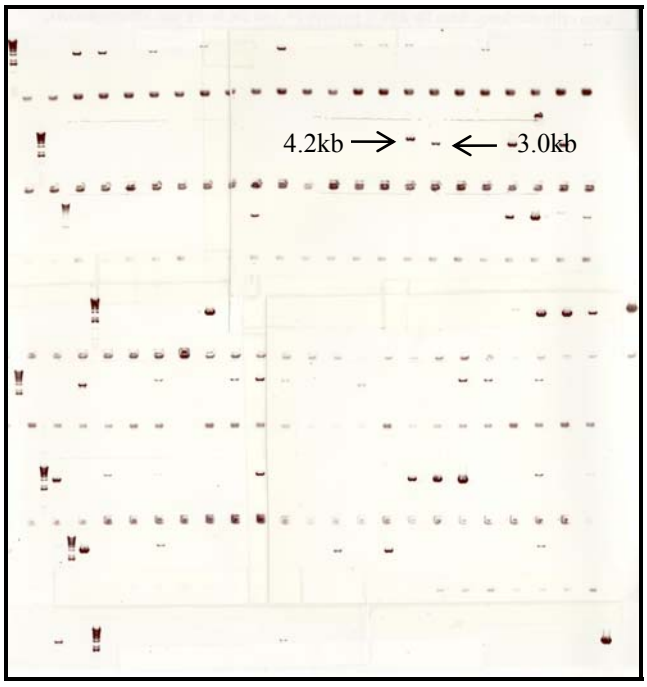


Figure 6.7 – Screening for *Neo* Removal Using PCR
(A) Schematic representation of a targeted STAT3 allele before (targeted allele) and after (functional allele) FlpE recombination. The position of the forward and reverse primers used for PCR analysis are shown by the arrows labeled F and R respectively. The forward primer binds to the *loxP* site and the reverse primer binds to a region outside of the targeting vector within the endogenous locus. A 3.0kb PCR product was expected if *neo* was removed by FlpE recombinase. A 4.2kb PCR product was expected if *neo* was not removed.
(B) PCR analysis of DNA isolated from targeted ES cell clones electroporated with FlpE recombinase.

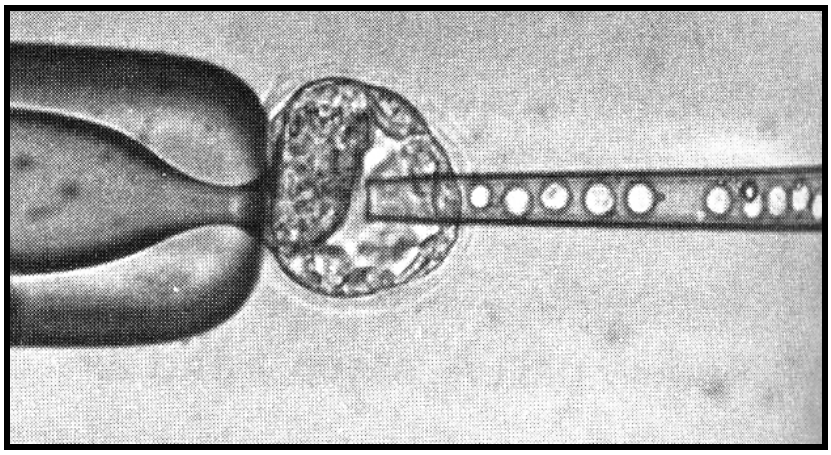
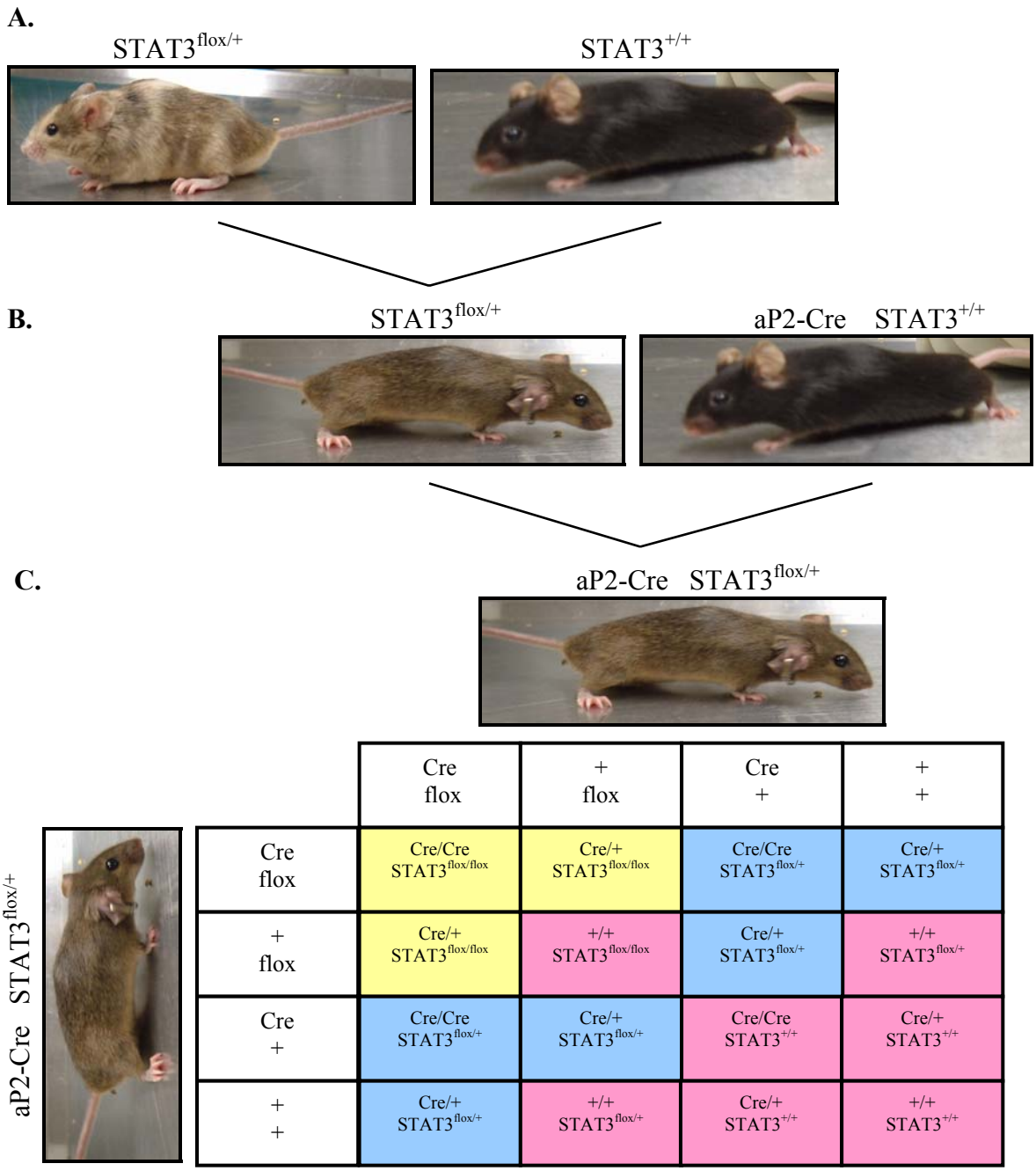


Figure 6.8 - Blastocyst Microinjection
129/SvEv targeted clones not containing neo microinjected into C57BL/6 blastocysts.



aP2-Cre STAT3flox/+ \ Cre	Cre flox	+ flox	Cre +	+ +
Cre flox	Cre/Cre STAT3flox/flox	Cre/+ STAT3flox/flox	Cre/Cre STAT3flox/+	Cre/+ STAT3flox/+
+ flox	Cre/+ STAT3flox/flox	+/+ STAT3flox/flox	Cre/+ STAT3flox/+	+/+ STAT3flox/+
Cre +	Cre/Cre STAT3flox/+	Cre/+ STAT3flox/+	Cre/Cre STAT3+/+	Cre/+ STAT3+/+
+ +	Cre/+ STAT3flox/+	+/+ STAT3flox/+	Cre/+ STAT3+/+	+/+ STAT3+/+

Figure 6.9 – Mating Strategy
Schematic representation of the mating strategy used to generate ASKO mice.
(A) Chimeric mice ($STAT3^{flox/+}$) were mated with wild-type mice ($STAT3^{+/+}$).
(B) Agouti mice heterozygous for the targeted STAT3 gene ($STAT3^{flox/+}$) were mated with transgenic mice expressing Cre recombinase under the control of the adipocyte-specific aP2 promoter (aP2-Cre).
(C) Mice inheriting both the targeted allele and the Cre-expressing transgene (aP2-Cre $STAT3^{flox/+}$) were intercrossed to yield six derivative strains. Adipocyte-specific $STAT3^{-/-}$ mice ( ) were generated at a ratio of 3:16. Adipocyte-specific $STAT3^{+/-}$ ( ) mice were generated at a ratio of 3:8. Wild-type mice ( ) were generated at a ratio of 7:16.

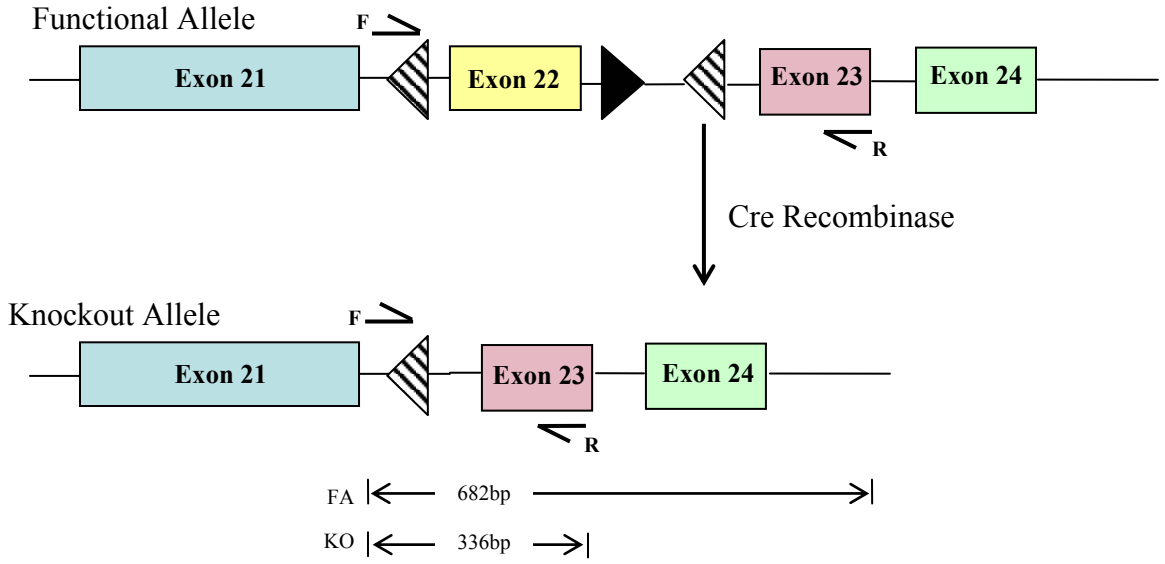


Figure 5.10 – Assessment of STAT3 Recombination in Adipose Tissue
(A) Schematic representation of the STAT3 allele before (functional allele) and after (knockout allele) recombination. The position of the forward and reverse primers used for PCR analysis are shown by the arrows labeled F and R respectively. The forward primer binds to the *loxP* site and the reverse primer binds to Exon 22. A 336bp PCR product was expected if exon 22 was removed by the Cre recombinase. A 682bp PCR product was expected if exon 22 was not removed.

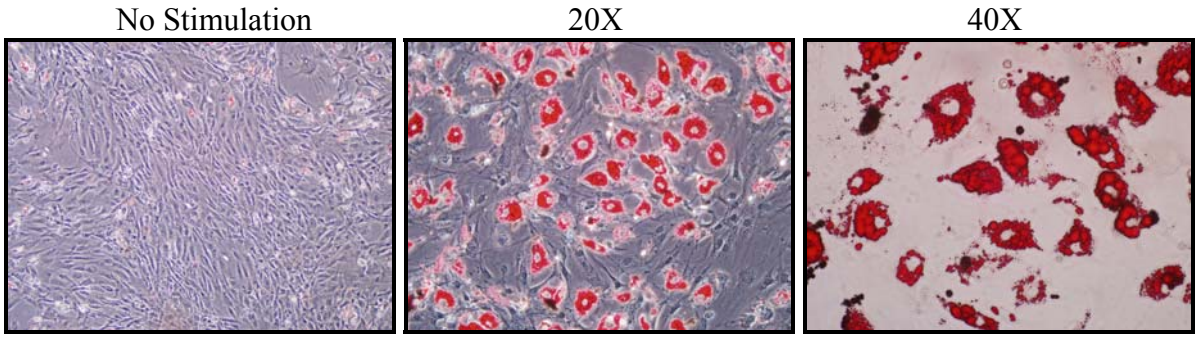


Figure 6.11 – Lipid Accumulation in Primary Preadipocytes
Eight days after induction of differentiation, ASKO cells were stained with Oil Red-O.

REFERENCES

1. **Popkin B, Doak C** 1998 The Obesity Epidemic Is A Worldwide Phenomenon. Nutr Rev. 56:106-14

2. **Spiegelman BM, Flier JS** 2001 Obesity And The Regulation Of Energy Balance. Cell 104:531-543

3. **Faust I, Johnson P, Stern J, Hirsch J** 1978 Diet-Induced Adipocyte Number Increase In Adult Rats: A New Model Of Obesity. Am J Physiol Endocrinol Metab 235:E279-286

4. **Prins J, O'Rahilly S** 1997 Regulation Of Adipose Cell Number In Man. Clin Sci (Lond) 92:3-11

5. **Hausman DB, Digirolamo M, Bartness TJ, Hausman GJ, Martin RJ** 2001 The Biology Of White Adipocyte Proliferation. Obesity Reviews 2:239-254

6. **Green H, Kehinde O** 1974 Sublines Of Mouse 3T3 Cells That Accumulate Lipid. Cell 1:113-116

7. **Tang Q-Q, Lane MD** 1999 Activation And Centromeric Localization Of CCAAT/Enhancer-Binding Proteins During The Mitotic Clonal Expansion Of Adipocyte Differentiation. Genes Dev. 13:2231-2241

8. **Cornelius P, Macdougald OA, Lane MD** 1994 Regulation Of Adipocyte Development. Annual Review Of Nutrition 14:99-129

9. **MacDougald O, Cornelius P, Lin F, Chen S, Lane M** 1994 Glucocorticoids Reciprocally Regulate Expression Of The CCAAT/Enhancer- Binding Protein Alpha And Delta Genes In 3T3-L1 Adipocytes And White Adipose Tissue. J. Biol. Chem. 269:19041-19047

10. **Macdougald O, Lane M** 1995 Adipocyte Differentiation. When Precursors Are Also Regulators. Curr Biol 5:618-21

11. **Tontonoz P, Hu E, Spiegelman B** 1995 Regulation Of Adipocyte Gene Expression And Differentiation By Peroxisome Proliferator Activated Receptor Gamma. Curr Opin Genet Dev 5:571-576

12. **Yeh W, Cao Z, Classon M, Mcknight S** 1995 Cascade Regulation Of Terminal Adipocyte Differentiation By Three Members Of The C/EBP Family Of Leucine Zipper Proteins. Genes Dev. 9:168-81

13. **Wu Z, Bucher N, Farmer S** 1996 Induction Of Peroxisome Proliferator-Activated Receptor Gamma During The Conversion Of 3T3 Fibroblasts Into Adipocytes Is

Mediated By C/Ebpbeta, C/Ebpdelta, And Glucocorticoids. Mol. Cell. Biol. 16:4128-4136

14. **Mandrup S, Lane MD** 1997 Regulating Adipogenesis. J. Biol. Chem. 272:5367-5370

15. **Stephens JM, Morrison RF, Pilch PF** 1996 The Expression And Regulation Of Stats During 3T3-L1 Adipocyte Differentiation. J. Biol. Chem. 271:10441-10444

16. **Deng J, Hua K, Lesser SS, Harp JB** 2000 Activation Of Signal Transducer And Activator Of Transcription-3 During Proliferative Phases Of 3T3-L1 Adipogenesis. Endocrinology 141:2370-2376

17. **Darnell JE, Jr.** 1997 Stats And Gene Regulation. Science 277:1630-1635

18. **Siegrist-Kaiser CA, Pauli V, Juge-Aubry CE, Boss O, PerninA, Chin WW, Cusin I, Rohner-Jeanrenaud F, Burger AG, Zapf J, Meier CA** 1997 Direct Effects Of Leptin On Brown And White Adipose Tissue. J. Clin. Invest. 100:2858-2864

19. **Chen G, Koyama K, Yuan X, Lee Y, Zhou YT, O'Doherty R, Newgard CB, Unger RH** 1996 Disappearance Of Body Fat In Normal Rats Induced By Adenovirus-Mediated Leptin Gene Therapy. Proc Natl Acad Sci U S A. 93:14795-9

20. **Shimabukuro M, Koyama K, Chen G, Wang M-Y, Trieu F, Lee Y, Newgard CB, Unger RH** 1997 Direct Antidiabetic Effect Of Leptin Through Triglyceride Depletion Of Tissues. PNAS 94:4637-4641

21. **Fruhbeck G, Aguado M, Martinez JA** 1997 In Vitro Lipolytic Effect Of Leptin On Mouse Adipocytes: Evidence For A Possible Autocrine/Paracrine Role Of Leptin. Biochemical And Biophysical Research Communications 240:590-594

22. **Fruhbeck G, Aguado M, Gomez-Ambrosi J, Martinez JA** 1998 Lipolytic Effect Of In Vivo Leptin Administration On Adipocytes Of Lean And Ob/Ob Mice, But Not Db/Db Mice. Biochemical And Biophysical Research Communications 250:99-102

23. **Wang M-Y, Lee Y, Unger RH** 1999 Novel Form Of Lipolysis Induced By Leptin. J. Biol. Chem. 274:17541-17544

24. **Bai Y, Zhang S, Kim K-S, Lee J-K, Kim K-H** 1996 Obese Gene Expression Alters The Ability Of 30A5 Preadipocytes To Respond To Lipogenic Hormones. J. Biol. Chem. 271:13939-13942

25. **Zhou Y, Wang Z, Higa M, Newgard C, Unger R** 1999 Reversing Adipocyte Differentiation: Implications For Treatment Of Obesity. Proc Natl Acad Sci U S A. 96:2391-5

26. **Path G, Bornstein SR, Gurniak M, Chrousos GP, Scherbaum WA, Hauner H** 2001 Human Breast Adipocytes Express Interleukin-6 (IL-6) And Its Receptor System: Increased IL-6 Production By {Beta}-Adrenergic Activation And Effects Of IL-6 On Adipocyte Function. J Clin Endocrinol Metab 86:2281-2288

27. **Trujillo ME, Sullivan S, Harten I, Schneider SH, Greenberg AS, Fried SK** 2004 Interleukin-6 Regulates Human Adipose Tissue Lipid Metabolism And Leptin Production In Vitro. J Clin Endocrinol Metab 89:5577-5582

28. **Greenberg A, Nordan R, Mcintosh J, Calvo J, Scow R, Jablons D** 1992 Interleukin 6 Reduces Lipoprotein Lipase Activity In Adipose Tissue Of Mice In Vivo And In 3T3-L1 Adipocytes: A Possible Role For Interleukin 6 In Cancer Cachexia. Cancer Res. 52:4113-6

29. **Van Hall G, Steensberg A, Sacchetti M, Fischer C, Keller C, Schjerling P, Hiscock N, Moller K, Saltin B, Febbraio MA, Pedersen BK** 2003 Interleukin-6 Stimulates Lipolysis And Fat Oxidation In Humans. J Clin Endocrinol Metab 88:3005-3010

30. **Lyngso D, Simonsen L, Bulow J** 2002 Metabolic Effects Of Interleukin-6 In Human Splanchnic And Adipose Tissue. J Physiol (Lond) 543:379-386

31. **Zvonic S, Cornelius P, Stewart WC, Mynatt RL, Stephens JM** 2003 The Regulation And Activation Of Ciliary Neurotrophic Factor Signaling Proteins In Adipocytes. J. Biol. Chem. 278:2228-2235

32. **Sleeman M, Anderson K, Lambert P, Yancopoulos G, Wiegand S** 2000 The Ciliary Neurotrophic Factor And Its Receptor, CNTFR Alpha. Pharm Acta Helv 74:265-72

33. **Green H, Kehinde O** 1979 Formation Of Normally Differentiated Fat Pads By An Established Preadipose Cell Line. J. Cell. Physiol. 101:169-172

34. **Rubin CS, Hirsch A, Fung C, Rosen OM** 1978 Development Of Hormone Receptors And Hormonal Responsiveness In Vitro. Insulin Receptors And Insulin Sensitivity In The Preadipocyte And Adipocyte Forms Of 3T3-L1 Cells. J. Biol. Chem. 253:7570-7578

35. **Smith P, Wise L, Berkowitz R, Wan C, Rubin C** 1988 Insulin-Like Growth Factor-I Is An Essential Regulator Of The Differentiation Of 3T3-L1 Adipocytes. J. Biol. Chem. 263:9402-9408

36. **Pairault J, Green H** 1979 A Study Of The Adipose Conversion Of Suspended 3T3 Cells By Using Glycerophosphate Dehydrogenase As Differentiation Marker. Proc Natl Acad Sci 76:5138-42

37. **Tang Q-Q, Otto TC, Lane MD** 2003 Mitotic Clonal Expansion: A Synchronous Process Required For Adipogenesis. PNAS 100:44-49

38. **Cao Z, Umek R, Mcknight S** 1991 Regulated Expression Of Three C/EBP Isoforms During Adipose Conversion Of 3T3-L1 Cells. Genes Dev. 9:1538-52

39. **Reichert M, Eick D** 1999 Analysis Of Cell Cycle Arrest In Adipocyte Differentiation. Oncogene 18:459-66

40. **Patel YM, Lane MD** 2000 Mitotic Clonal Expansion During Preadipocyte Differentiation: Calpain-Mediated Turnover Of P27. J. Biol. Chem. 275:17653-17660

41. **Qiu Z, Wei Y, Chen N, Jiang M, Wu J, Liao K** 2001 DNA Synthesis And Mitotic Clonal Expansion Is Not A Required Step For 3T3-L1 Preadipocyte Differentiation Into Adipocytes. J. Biol. Chem. 276:11988-11995

42. **Macdougald O, Lane M** 1995 Transcriptional Regulation Of Gene Expression During Adipocyte Differentiation. Annual Review Of Biochemistry 64:345-373

43. **Lekstrom-Himes J, Xanthopoulos KG** 1998 Biological Role Of The CCAAT/Enhancer-Binding Protein Family Of Transcription Factors. J. Biol. Chem. 273:28545-28548

44. **Christy R, Kaestner K, Geiman D, Lane M** 1991 CCAAT/Enhancer Binding Protein Gene Promoter: Binding Of Nuclear Factors During Differentiation Of 3T3-L1 Preadipocytes. PNAS 88:2593-2597

45. **Clarke SL, Robinson CE, Gimble JM** 1997 CAAT/Enhancer Binding Proteins Directly Modulate Transcription From The Peroxisome Proliferator- Activated Receptor [Gamma]2 Promoter. Biochemical And Biophysical Research Communications 240:99-103

46. **Tanaka T, Yoshida N, Kishimoto T, Akira S** 1997 Defective Adipocyte Differentiation In Mice Lacking The C/Ebpbeta And/Or C/Ebpdelta Gene. EMBO J 16:7432-43

47. **Tang Q-Q, Otto TC, Lane MD** 2003 CCAAT/Enhancer-Binding Protein Beta Is Required For Mitotic Clonal Expansion During Adipogenesis. PNAS 100:850-855

48. **Constance C, Morgan J, Umek R** 1996 C/Ebpalpha Regulation Of The Growth-Arrest-Associated Gene Gadd45. Mol. Cell. Biol. 16:3878-3883

49. **Christy R, Yang V, Ntambi J, Geiman DE, Landschulz WH, Friedman AD, Nakabeppu Y, Kelly TJ, Lane MD** 1989 Differentiation-Induced Gene Expression In 3T3-L1 Preadipocytes: CCAAT/Enhancer Binding Protein Interacts With And Activates The Promoters Of Two Adipocyte-Specific Genes. Genes Dev. 3:1323-35

50. **Kaestner K, Christy R, Lane M** 1990 Mouse Insulin-Responsive Glucose Transporter Gene: Characterization Of The Gene And Trans-Activation By The CCAAT/Enhancer Binding Protein. PNAS 87:251-255

51. **Park EA, Song S, Vinson C, Roesler WJ** 1999 Role Of CCAAT Enhancer-Binding Protein Beta In The Thyroid Hormone And Camp Induction Of Phosphoenolpyruvate Carboxykinase Gene Transcription. J. Biol. Chem. 274:211-217

52. **Freytag S, Paielli D, Gilbert J** 1994 Ectopic Expression Of The CCAAT/Enhancer-Binding Protein Alpha Promotes The Adipogenic Program In A Variety Of Mouse Fibroblastic Cells. Genes Dev. 8:1654-63

53. **Lin F, Lane M** 1992 Antisense CCAAT/Enhancer-Binding Protein RNA Suppresses Coordinate Gene Expression And Triglyceride Accumulation During Differentiation Of 3T3-L1 Preadipocytes. Genes Dev. 6:533-44

54. **Wu Z, Rosen E, Brun R, Hauser S, Adelmant G, Troy AE, McKeon C, Darlington GJ, Spiegelman BM** 1999 Cross-Regulation Of C/EBP Alpha And PPAR Gamma Controls The Transcriptional Pathway Of Adipogenesis And Insulin Sensitivity. Mol Cell 3:151-8

55. **Wang N, Finegold M, Bradley A, Ou CN, Abdelsayed SV, Wilde MD, Taylor LR, Wilson DR, Carlington GJ** 1995 Impaired Energy Homeostasis In C/EBP Alpha Knockout Mice. Science 269:1108-12

56. **Tontonoz P, Hu E, Graves R, Budavari A, Spiegelman B** 1994 Mppar Gamma 2: Tissue-Specific Regulator Of An Adipocyte Enhancer. Genes Dev. 8:1224-34

57. **Morrison RF, Farmer SR** 1999 Role Of Ppargamma In Regulating A Cascade Expression Of Cyclin-Dependent Kinase Inhibitors, P18(INK4c) And P21(Waf1/Cip1), During Adipogenesis. J. Biol. Chem. 274:17088-17097

58. **Tontonoz P, Hu E, Devine J, Beale E, Spiegelman B** 1995 PPAR Gamma 2 Regulates Adipose Expression Of The Phosphoenolpyruvate Carboxykinase Gene. Mol Cell Biol 15:351-7

59. **Schoonjans K, Watanabe M, Suzuki H, Mahoudi A, Krey G, Wahli W, Grimaldi P, Steals B, Yamamoto T, Auwerx J** 1995 Induction Of The Acyl-Coenzyme A Synthetase Gene By Fibrates And Fatty Acids Is Mediated By A Peroxisome Proliferator Response Element In The C Promoter. J. Biol. Chem. 270:19269-19276

60. **Rosen E, Sarraf P, Troy A, Bradwin G, Moore K, Milstone DS< Spiegelman BM, Mortensen RM** 1999 PPAR Gamma Is Required For The Differentiation Of Adipose Tissue In Vivo And In Vitro. Mol Cell 4:6111-7

61. **Tontonoz P, Hu E, Spiegelman B** 1994 Stimulation Of Adipogenesis In Fibroblasts By PPAR Gamma 2, A Lipid-Activated Transcription Factor. Cell 79:1147-56

62. **Chawla A, Lazar M** 1994 Peroxisome Proliferator And Retinoid Signaling Pathways Co-Regulate Preadipocyte Phenotype And Survival. PNAS 91:1786-1790

63. **Kubota N** 1999 PPAR Gamma Mediates High-Fat Diet-Induced Adipocyte Hypertrophy And Insulin Resistance. Mol Cell 4:597-609

64. **He W, Barak Y, Hevener A, Olson P, Liao D, Le J, Nelson M, Ong E, Olefsky JM, Evans RM** 2003 Adipose-Specific Peroxisome Proliferator-Activated Receptor {Gamma} Knockout Causes Insulin Resistance In Fat And Liver But Not In Muscle. PNAS 100:15712-15717

65. **Zhang J, Fu M, Cui T, Xiong C, Xu K, Zhong W, Xiao Y, Floyd D, Liang J, li E, Song Q, Chen YE** 2004 Selective Disruption Of PPAR{Gamma}2 Impairs The Development Of Adipose Tissue And Insulin Sensitivity. PNAS 101:10703-10708

66. **Rosen ED, Hsu C-H, Wang X, Sakai S, Freeman MW, Gonzalez FJ, Spiegelman BM** 2002 C/Ebpalpha Induces Adipogenesis Through Ppargamma : A Unified Pathway. Genes Dev. 16:22-26

67. **Shuai K** 1999 The STAT Family Of Proteins In Cytokine Signaling. Prog Biophys Mol Biol 71:405-22

68. **Leaman D, Pisharody S, Flickinger T, Commane MA, Schlessinger J, Kerr IM, Levy DE, Stark GR** 1996 Roles Of Jaks In Activation Of Stats And Stimulation Of C-Fos Gene Expression By Epidermal Growth Factor. Mol. Cell. Biol. 16:369-375

69. **Boccaccio C, Ando M, Tamagnone L, Bardelli A, Michieli P, Battistini C, Comoglio PM** 1998 Induction Of Epithelial Tubules By Growth Factor HGF Depends On The STAT Pathway. Nature 391:285-288

70. **Vignais M, Sadowski H, Watling D, Rogers N, Gilman M** 1996 Platelet-Derived Growth Factor Induces Phosphorylation Of Multiple JAK Family Kinases And STAT Proteins. Mol. Cell. Biol. 16:1759-1769

71. **Novak U, Harpur A, Paradiso L, Kanagasundaram V, Jaworowski A, Wilks AF, Hamilton JA** 1995 Colony-Stimulating Factor 1-Induced STAT1 And STAT3 Activation Is Accompanied By Phosphorylation Of Tyk2 In Macrophages And Tyk2 And JAK1 In Fibroblasts. Blood 86:2948-2956

72. **Schindler C, Strehlow I** 2000 Cytokines And STAT Signaling. Adv Pharmacol. 47:113-74

73. **Ihle J** 1996 Stats: Signal Transducers And Activators Of Transcription. Cell 84:331-334

74. **Marrero M, Schieffer B, Paxton W, Heerdt L, Berk BC, Delafontaine P, Bernstein KE** 1995 Direct Stimulation Of Jak/STAT Pathway By The Angiotensin II AT1 Receptor. Nature 373:247-50

75. **Guillet-Deniau I, Burnol A-F, Girard J** 1997 Identification And Localization Of A Skeletal Muscle Secrotonin 5-HT2A Receptor Coupled To The Jak/STAT Pathway. J. Biol. Chem. 272:14825-14829

76. **Yu C, Meyer D, Campbell G, Larner AC, Carter-SU C, Schwartz J, Jove R** 1995 Enhanced DNA-Binding Activity Of A Stat3-Related Protein In Cells Transformed By The Src Oncoprotein. Science 269:81-3

77. **Durbin J, Hackenmiller R, Simon M, Levy D** 1996 Targeted Disruption Of The Mouse Stat1 Gene Results In Compromised Innate Immunity To Viral Disease. Cell 84:443-50

78. **Meraz M, White J, Sheehan K, Bach EA, Rodig SJ, Dighe AS< Kaplan DH, Riley JK, Greenlund AC, Campbell D, Carver-Moore K, DuBois RN, Clark R, Aguet M, Schreiber RD** 1996 Targeted Disruption Of The Stat1 Gene In Mice Reveals Unexpected Physiologic Specificity In The JAK-STAT Signaling Pathway. Cell 84:431-42

79. **Park C, Li S, Cha E, Schindler C** 2000 Immune Response In Stat2 Knockout Mice. Immunity 13:795-804

80. **Thierfelder W, Van Deursen J, Yamamoto K, Tripp RA, Sarawar SR, Carson RT, Sangster MY, Vignali DA, Doherty PC, Grosveld GC, Ihle JN** 1996 Requirement For Stat4 In Interleukin-12-Mediated Responses Of Natural Killer And T Cells. Nature 382:171-4

81. **Kaplan M, Sun Y, Hoey T, Grusby M** 1996 Impaired IL-12 Responses And Enhanced Development Of Th2 Cells In Stat4-Deficient Mice. Nature 382:174-177

82. **Shimoda K, Van Deursen J, Sangster MY, Sarawar SR, Carson RT, Tripp RA, Chu C, Quelle FW, Nosaka T, Vignali DA, Doherty PC, Grosveld G, Paul WE, Ihle JN** 1996 Lack Of IL-4-Induced Th2 Response And Ige Class Switching In Mice With Disrupted Stat6 Gene. Nature 380:630-3

83. **Kaplan M, Schindler U, Smiley S, Grusby M** 1996 Stat6 Is Required For Mediating Responses To IL-4 And For Development Of Th2 Cells. Immunity 4:313-319

84. **Takeda K, Tanaka T, Shi W, Matsumoto M, Minami M, Kashiwamura S, Nakanishi K, Yoshida N, Kishimoto T, Akira S** 1996 Essential Role Of Stat6 In IL-4 Signalling. Nature 380:627-630

85. **Liu X, Robinson G, Wagner K, Garrett L, Wynshaw-Boris A, Hennighausen L** 1997 Stat5a Is Mandatory For Adult Mammary Gland Development And Lactogenesis. Genes Dev. 11:179-86

86. **Udy GB, Towers RP, Snell RG, Wilkins RJ, Park S-H, Ram PA, Waxman DJ, Davey HW** 1997 Requirement Of STAT5b For Sexual Dimorphism Of Body Growth Rates And Liver Gene Expression. PNAS 94:7239-7244

87. **Teglund S, Mckay C, Schuetz E, Van Deursen JM, Stravopodis D, Wang D, Brown M, Bodner S, Grosveld G, Ihle JN** 1998 Stat5a And Stat5b Proteins Have Essential And Nonessential, Or Redundant, Roles In Cytokine Responses. Cell 93:841-50

88. **Takeda K, Noguchi K, Shi W, Tanaka T, Matsumoto M, Yoshida N, Kishimoto T, Akira S** 1997 Targeted Disruption Of The Mouse Stat3 Gene Leads To Early Embryonic Lethality. PNAS 94:3801-3804

89. **Cui Y, Huang L, Elefteriou F, Yang G, Shelton JM, Giles JE, Oz OK, Pourbahrami T, Lu CYH, Richardson JA, Karsenty G, Li C** 2004 Essential Role Of STAT3 In Body Weight And Glucose Homeostasis. Mol. Cell. Biol. 24:258-269

90. **Gao Q, Wolfgang MJ, Neschen S, Morino K, Horvath TL, Shulman GI, Fu X-Y** 2004 Disruption Of Neural Signal Transducer And Activator Of Transcription 3 Causes Obesity, Diabetes, Infertility, And Thermal Dysregulation. PNAS 101:4661-4666

91. **Inoue H, Ogawa W, Ozaki M, Haga S, Matsumoto M, Furukawa K, Hashimoto N, Kido Y, Mori T, Sakaue H, Teshigawara K, Jin S, Iguchi H, Hiramatsu T, LeRoith D, Takeda K, Akira S, Kasuga M** 2004 Role Of STAT-3 In Regulation Of Hepatic Gluconeogenic Genes And Carbohydrate Metabolism In Vivo. 10:168-174

92. **Takeda K, Clausen B, Kaisho T, Tsujimura T, Terada N, Foster I, Akira S** 1999 Enhanced Th1 Activity And Development Of Chronic Enterocolitis In Mice Devoid Of Stat3 In Macrophages And Neutrophils. Immunity 10:39-49

93. **Chapman Rs, Lourenco P, Tonner E, Flint D, Selbert S, Takeda K, Akira S, Clarke AR, Watson CJ** 2000 The Role Of Stat3 In Apoptosis And Mammary Gland Involution. Conditional Deletion Of Stat3. Adv Exp Med Biol. 480:129-38

94. **Xu A, Ste-Marie L, Kaelin C, Barsh G** 2007 Inactivation Of Signal Transducer And Activator Of Transcription 3 In Proopiomelanocortin (Pomc) Neurons Causes

Decreased Pomc Expression, Mild Obesity, And Defects In Compensatory Refeeding. Endocrinology 146:72-80

95. **Takeda K, Kaisho T, Yoshida N, Takeda J, Kishimoto T, Akira S** 1998 Stat3 Activation Is Responsible For IL-6-Dependent T Cell Proliferation Through Preventing Apoptosis: Generation And Characterization Of T Cell-Specific Stat3-Deficient Mice. J Immunol 161:4652-4660

96. **Smithies O, Koralewski M, Song K, Kucherlapati R** 1984 Homologous Recombination With DNA Introduced Into Mammalian Cells. Cold Spring Harb Symp Quant Biol 49:161-70

97. **Fukada T, Ohtani T, Yoshida Y, Shirogane T, Nishida K, Nakjima K, Hibi M, Hirano T** 1998 STAT3 Orchestrates Contradictory Signals In Cytokine-Induced G1 To S Cell-Cycle Transition. EMBO J 17:6670-7

98. **Bromberg J, Wrzeszczynska M, Devgan G, Zhao Y, Pestell RG, Albanese C, Darnell JE** 1999 Stat3 As An Oncogene. Cell 98:295-303

99. **Catlett-Falcone R, Landowski T, Oshiro M, Turkson J, Levitzki A, Savino R, Ciliberto G, Moscinski L, Fernandez-Luna JL, Nunez G, Dalton WS, Jove R** 1999 Constitutive Activation Of Stat3 Signaling Confers Resistance To Apoptosis In Human U266 Myeloma Cells. Immunity 10:105-15

100. **Calo V, Migliavacca M, Bazan V, Macaluso M, Buscemi M, Gebbia N, Russo A** 2003 STAT Proteins: From Normal Control Of Cellular Events To Tumorigenesis. J Cell Physiol. 197

101. **Bowman T, Garcia R, Turkson J, Jove R** 2000 Stats In Oncogenesis. Oncogene 19:2474-2488

102. **Catlett-Falcone R, Dalton W, Jove R** 1999 STAT Proteins As Novel Targets For Cancer Therapy. Signal Transducer An Activator Of Transcription. Curr Opin Oncol 11

103. **Huang M, Page C, Reynolds RK, Lin J** 2000 Constitutive Activation Of Stat 3 Oncogene Product In Human Ovarian Carcinoma Cells. Gynecologic Oncology 79:67-73

104. **Bromberg J** 2002 Stat Proteins And Oncogenesis. J. Clin. Invest. 109:1139-1142

105. **Gouilleux-Gruart V, Gouilleux F, Desaint C, Claisse JF, Capoid JC, Delobel J, Weber-Nordt R, Dusanter-Fourt I, Dreyfus F, Broner B, Prin L** 1996 STAT-Related Transcription Factors Are Constitutively Activated In Peripheral Blood Cells From Acute Leukemia Patients. Blood 87:1692-1697

106. **Sinibaldi D, Wharton W, Turkson J, Bowman T, Pledger W, Jove R** 2000 Induction Of P21waf1/CIP1 And Cyclin D1 Expression By The Src Oncoprotein In Mouse Fibroblasts: Role Of Activated STAT3 Signaling. Oncogene 19:5419-5427

107. **Stephens JM, Morrison RF, Wu Z, Farmer SR** 1999 PPAR[Gamma] Ligand-Dependent Induction Of STAT1, STAT5A, And STAT5B During Adipogenesis. Biochemical And Biophysical Research Communications 262:216-222

108. **Fruhbeck J** 1998 Leptin: Physiology And Pathophysiology. Clinical Physiology 18:399-419

109. **Pelleymounter M, Cullen M, Baker M, Hecht R, Winters D, Boone T, Collins F** 1995 Effects Of The Obese Gene Product On Body Weight Regulation In Ob/Ob Mice. Science 269:540-543

110. **Lee G-H, Proenca R, Montez JM, Carroll KM, Darvishzadeh JG, Lee JI, Friedman JM** 1996 Abnormal Splicing Of The Leptin Receptor In Diabetic Mice. Nature 379:632-635

111. **Cumin F, Baum H, Levens N** 1996 Leptin Is Cleared From The Circulation Primarily By The Kidney. Int J Obes Relat Metab Disord 20:1120-1126

112. **Banks WA, Kastin AJ, Huang W, Jaspan JB, Maness LM** 1996 Leptin Enters The Brain By A Saturable System Independent Of Insulin. Peptides 17:305-311

113. **Tartaglia LA, Dembski M, Weng X, Deng N, Culpepper J, Devos R, Richards GJ, Campfield LA, Clark FT, Deeds J** 1995 Identification And Expression Cloning Of A Leptin Receptor, OB-R. Cell 83:1263-1271

114. **Bjorbak C, Uotani S, Da Silva B, Flier JS** 1997 Divergent Signaling Capacities Of The Long And Short Isoforms Of The Leptin Receptor. J. Biol. Chem. 272:32686-32695

115. **Fruhbeck J** 2006 Intracellular Signalling Pathways Activated By Leptin. Biochem J. 393:7-20

116. **Ghilardi N, Skoda RC** 1997 The Leptin Receptor Activates Janus Kinase 2 And Signals For Proliferation In A Factor-Dependent Cell Line. Mol Endocrinol 11:393-399

117. **Ghilardi N, Ziegler S, Wiestner A, Stoffel R, Heim MH, Skoda RC** 1996 Defective STAT Signaling By The Leptin Receptor In Diabetic Mice. PNAS 93:6231-6235

118. **Emilsson V, Liu Y, Cawthorne M, Morton N, Davenport M** 1997 Expression Of The Functional Leptin Receptor Mrna In Pancreatic Islets And Direct Inhibitory Action Of Leptin On Insulin Secretion. Diabetes 46:313-316

119. **Kim Y-B, Uotani S, Pierroz DD, Flier JS, Kahn BB** 2000 In Vivo Administration Of Leptin Activates Signal Transduction Directly In Insulin-Sensitive Tissues: Overlapping But Distinct Pathways From Insulin. Endocrinology 141:2328-2339

120. **Bendinelli P, Maroni P, Pecori Giraldi F, Piccoletti R** 2000 Leptin Activates Stat3, Stat1 And AP-1 In Mouse Adipose Tissue. Molecular And Cellular Endocrinology 168:11-20

121. **Flier JS, Maratos-Flier E** 1998 Obesity And The Hypothalamus: Novel Peptides For New Pathways. Cell 92:437-440

122. **Levin N, Nelson C, Gurney A, Vandlen R, De Sauvage F** 1996 Decreased Food Intake Does Not Completely Account For Adiposity Reduction After Ob Protein Infusion. Proc Natl Acad Sci U S A. 93:1726-30

123. **Wang M-Y, Orci L, Ravazzola M, Unger RH** 2005 Fat Storage In Adipocytes Requires Inactivation Of Leptin's Paracrine Activity: Implications For Treatment Of Human Obesity. PNAS 102:18011-18016

124. **Heinrich P, Behrmann I, Haan S, Hermanns H, Muller-Newen G, Schaper F** 2003 Principles Of Interleukin (IL)-6-Type Cytokine Signalling And Its Regulation. Biochem J 374:1-20

125. **Hibi M, Murakami M, Saito M, Hirano T, Taga T, Kishimoto T** 1990 Molecular Cloning And Expression Of An IL-6 Signal Transducer, Gp130. Cell 63:1149-57

126. **Gearing D, Thut C, Vandebos T, Gimpel SD, Delaney PB, King J, Price V, Cosman D, Beckmann MP** 1991 Leukemia Inhibitory Factor Receptor Is Structurally Related To The IL-6 Signal Transducer, Gp130. EMBO J 10:2839-48

127. **Snick JV** 1990 Interleukin-6: An Overview. Annual Review Of Immunology 8:253-278

128. **Mohamed-Ali V, Goodrick S, Rawesh A, Katz DR, Miles JM, Yudkin JS, Klein S, Coppack SE** 1997 Subcutaneous Adipose Tissue Releases Interleukin-6, But Not Tumor Necrosis Factor-{Alpha}, In Vivo. J Clin Endocrinol Metab 82:4196-4200

129. **Wallenius V, Wallenius K, Ahren B, Rudline M, Carlsten H, Dickson SL, Ohlsson C, Jansson J-O** 2002 Interleukin-6-Deficient Mice Develop Mature-Onset Obesity. 8:75-79

130. **Wallenius K, Wallenius V, Sunter D, Dickson S, Jansson J** 2002 Intracerebroventricular Interleukin-6 Treatment Decreases Body Fat In Rats. Biochem Biophys Res Commun 293:560-5

131. **Schobitz B, De Kloet E, Sutanto W, Holsboer F** 1993 Cellular Localization Of Interleukin 6 Mrna And Interleukin 6 Receptor Mrna In Rat Brain. Eur J Neurosci 5:1426-35

132. **Shizuya K, Komori T, Fujiwara R, Miyahara S, Ohmori M, Nomura J** 1998 The Expressions Of Mrnas For Interleukin-6 (IL-6) And The IL-6 Receptor (IL-6R) In The Rat Hypothalamus And Midbrain During Restraint Stress. Life Sciences 62:2315-2320

133. **Jansson J-O, Wallenius K, Wernstedt I, Ohlsson C, Dickson SL, Wallenius V** 2003 On The Site And Mechanism Of Action Of The Anti-Obesity Effects Of Interleukin-6. Growth Hormone & IGF Research. Proceedings Of The 34th International Symposium On Growth Hormone And Growth Factors In Endocrinology And Metabolism 13:S28-S32

134. **Stephens JM, Lumpkin SJ, Fishman JB** 1998 Activation Of Signal Transducers And Activators Of Transcription 1 And 3 By Leukemia Inhibitory Factor, Oncostatin-M, And Interferon-Gamma In Adipocytes. J. Biol. Chem. 273:31408-31416

135. 1996 A Double-Blind Placebo-Controlled Clinical Trial Of Subcutaneous Recombinant Human Ciliary Neurotrophic Factor (Rhcntf) In Amyotrophic Lateral Sclerosis. ALS CNTF Treatment Study Group. Neurology 46:1244-9

136. **Miller RG, Petajan JH Bryan WW, Armon C, Barohn RJ, Goodpasture JC, Hoagland RJ, Parry GJ, Ross MA, Stromatt SC** 1996 A Placebo-Controlled Trial Of Recombinant Human Ciliary Neurotrophic (Rhcntf) Factor In Amyotrophic Lateral Sclerosis. Rhcntf ALS Study Group. Ann Neurol. 39:256-60

137. **Gloaguen I, Costa P, Demartis A, Lazzaro D, Di Marco A, Graziani R, Paonessa G, Chen F, Rosenblum CI, Van der Ploeg, LHT, Cortese R, Ciliberto G, Laufer R** 1997 Ciliary Neurotrophic Factor Corrects Obesity And Diabetes Associated With Leptin Deficiency And Resistance. PNAS 94:6456-6461

138. **Lambert PD, Anderson KD, Sleeman MW, Wong V, Tan J, Hijarunguru A, Corcoran TL, Murray JD, Thabet KE, Yancopoulos GD, Wiegand SJ** 2001 From The Cover: Ciliary Neurotrophic Factor Activates Leptin-Like Pathways And Reduces Body Fat, Without Cachexia Or Rebound Weight Gain, Even In Leptin-Resistant Obesity. PNAS 98:4652-4657

139. **Sleeman MW, Garcia K, Liu R, Murray JD, Malinova L, Moncrieffe M, Yancopoulos GD, Wiegand SJ** 2003 Ciliary Neurotrophic Factor Improves Diabetic

Parameters And Hepatic Steatosis And Increases Basal Metabolic Rate In Db/Db Mice. PNAS 100:14297-14302

140. **Wellstein A, Fang W, Khatri A, Lu Y, Swain SS, Dickson RB, Sasse J, Riegel AT, Lippman ME** 1992 A Heparin-Binding Growth Factor Secreted From Breast Cancer Cells Homologous To A Developmentally Regulated Cytokine. J. Biol. Chem. 267:2582-2587

141. **Tomomura M, Kadomatsu K, Nakamoto M, Muramatsu H, Kondoh H, Imagawa K, Muramatsu T** 1990 A Retinoic Acid Responsive Gene, MK, Produces A Secreted Protein With Heparin Binding Activity. Biochem Biophys Res Commun 171:603-9

142. **Kadomatsu K, Muramatsu T** 2004 Midkine And Pleiotrophin In Neural Development And Cancer. Cancer Letters 204:127-43

143. **Nakanishi T, Kadomatsu K, Okamoto T, Ichihara-Tanaka K, Kojima T, Saito H, Tomoda Y, Muramatsu T** 1997 Expression Of Syndecan-1 And -3 During Embryogenesis Of The Central Nervous System In Relation To Binding With Midkine. J Biochem (Tokyo) 121:197-205

144. **Muramatsu H, Zou K, Sakaguchi N, Ikematsu S, Sakuma S, Muramatsu T** 2000 LDL Receptor-Related Protein As A Component Of The Midkine Receptor. Biochemical And Biophysical Research Communications 270:936-941

145. **Muramatsu H, Zou P, Suzuki H, Oda Y, Chen G-Y, Sakaguchi N, Sakuma S< Maeda N, Noda M, Takada Y, Muramatsu T** 2004 {Alpha}4{Beta}1- And {Alpha}6{Beta}1-Integrins Are Functional Receptors For Midkine, A Heparin-Binding Growth Factor. J Cell Sci 117:5405-5415

146. **Stoica GE, Kuo A, Aigner A, Sunitha I, Souttou B, Malerczyk C, Caughey DJ, Wen D, Karavanov A, Riegel AT, Wellstein A** 2001 Identification Of Anaplastic Lymphoma Kinase As A Receptor For The Growth Factor Pleiotrophin. J. Biol. Chem. 276:16772-16779

147. **Ratovitski EA, Kotzbauer PT, Milbrandt J, Lowenstein CJ, Burrow CR** 1998 Midkine Induces Tumor Cell Proliferation And Binds To A High Affinity Signaling Receptor Associated With JAK Tyrosine Kinases. J. Biol. Chem. 273:3654-3660

148. **Muramatsu T** 1993 Midkine (MK), The Product Of A Retinoic Acid Responsive Gene, And Pleiotrophin Constitute A New Protein Family Regulating Growth And Differentiation. Int J Dev Biol 37:183-8

149. **Horiba M, Kadomatsu K, Nakamura E, Muramatsu H, Ikematsu S, Sakuma S, Hayashi K, Yazawa Y, Matsuo S, Kuzuya M, Kaname T, Hirai M, Saito H,**

Muramatsu T 2000 Neointima Formation In A Restenosis Model Is Suppressed In Midkine-Deficient Mice. J. Clin. Invest. 105:489-495

150. **Miyauchi M, Shimada H, Kadomatsu K, Muramatsu T, Matsubara S, Ikematsu S, Takenaga K, Asano T, Ochiai T, Sakiyama S, Tagawa M** 1999 Frequent Expression Of Midkine Gene In Esophageal Cancer Suggests A Potential Usage Of Its Promoter For Suicide Gene Therapy. Jpn J Cancer Res 90:469-75

151. **Aridome K, Tsutsui J, Takao S, Kadomatsu K, Ozawa M, Aikou T, Muramatsu T** 1995 Increased Midkine Gene Expression In Human Gastrointestinal Cancers. Jpn J Cancer Res 86:655-61

152. **Ye C, Qi M, Fan Q, Ito K, Akiyama S, Kasai Y, Matsuyama M, Muramatsu T, Kadomatsu K** 1999 Expression Of Midkine In The Early Stage Of Carcinogenesis In Human Colorectal Cancer. Br J Cancer 79:179-84

153. **Kaname T, Kadomatsu K, Aridome K, Yamashita S, Sakamoto K, Ogawa M, Muramatsu T, Tamamura K** 1996 The Expression Of Truncated MK In Human Tumors. Biochemical And Biophysical Research Communications 219:256-260

154. **Garver RJ, Chan C, Milner P** 1993 Reciprocal Expression Of Pleiotrophin And Midkine In Normal Versus Malignant Lung Tissues. Am J Respir Cell Mol Biol 9:463-6

155. **Garver RJ, Radford D, Donis-Keller H, Wick M, Milner P** 1994 Midkine And Pleiotrophin Expression In Normal And Malignant Breast Tissue. Cancer 74:1584-90

156. **Kadomatsu K, Hagihara M, Akhter S, Fan Q, Muramatsu H, Muramatsu T** 1997 Midkine Induces The Transformation Of NIH3T3 Cells. Br J Cancer 75:354-9

157. **Owada K, Sanjo N, Kobayashi T, Mizusawa H, Muramatsu H, Muramatsu T, Michikawa M** 1999 Midkine Inhibits Caspase-Dependent Apoptosis Via The Activation Of Mitogen-Activated Protein Kinase And Phosphatidylinositol 3-Kinase In Cultured Neurons. J Neurochem 73:2084-2092

158. **Choudhuri R, Zhang H, Donnini S, Ziche M, Bicknell R** 1997 An Angiogenic Role For The Neurokines Midkine And Pleiotrophin In Tumorigenesis. Cancer Res. 57:1814-9

159. **Wasserman F** The Development Of Adipose Tissue. In: Renold AE, Cahill Jr GF (Eds) Handbook Of Physiology, Sect 5. American Physiological Society, Washington, DC

160. **Teichert-Kuliszewska K, Hamilton B, Deitel M, Roncari D** 1992 Augmented Production Of Heparin-Binding Mitogenic Proteins By Preadipocytes From Massively Obese Persons. J Clin Invest. 90:1226–1231

161. **Rosen ED, Spiegelman BM** 2000 Molecular Regulators Of Adipogenesis. Annual Review Of Cell And Developmental Biology 16:145-171

162. **Marrero MB, Schieffer B, Li B, Sun J, Harp JB, Ling BN** 1997 Role Of Janus Kinase/Signal Transducer And Activator Of Transcription And Mitogen-Activated Protein Kinase Cascades In Angiotensin II- And Platelet-Derived Growth Factor-Induced Vascular Smooth Muscle Cell Proliferation. J. Biol. Chem. 272:24684-24690

163. **Muramatsu H, Muramatsu T** 1991 Purification Of Recombinant Midkine And Examination Of Its Biological Activities: Functional Comparison Of New Heparin Binding Factors. Biochem Biophys Res Commun. 177:652-8

164. **Hu J, Higuchi I, Yoshida Y, Shiraishi T, Osame M** 2002 Expression Of Midkine In Regenerating Skeletal Muscle Fibers And Cultured Myoblasts Of Human Skeletal Muscle. Eur Neurol. 47:20-5

165. **Miyashiro I, Kaname T, Shin E, Wakasugi E, Monden T, Takatsuka Y, Kikkawa N, Muramatsu T, Monden M, Akiyama T** 1997 Midkine Expression In Human Breast Cancers: Expression Of Truncated Form. Breast Cancer Research And Treatment 43:1-6

166. **Lau D, Roncari D, Hollenberg C** 1987 Release Of Mitogenic Factors By Cultured Preadipocytes From Massively Obese Human Subjects. J Clin Invest. 79:632-636

167. **Hausman D, Digirolamo M, Bartness T, Hausman G, Martin R** 2001 The Biology Of White Adipocyte Proliferation. Obes Rev. 2:239-54

168. **Rosen E, Macdougald O** 2006 Adipocyte Differentiation From The Inside Out. Nat Rev Mol Cell Biol 7:885-96

169. **Rodbell M** 1964 Metabolism Of Isolated Fat Cells. I. Effects Of Hormones On Glucose Metabolism And Lipolysis. J. Biol. Chem. 239:375-380

170. **Folch J, Lees M, Stanley GHS** 1957 A Simple Method For Then Isolation And Purification Of Total Lipids From Animal Tissues. J. Biol. Chem. 226:497-509

171. **Zhong Z, Wen Z, Darnell JJ** 1994 Stat3: A STAT Family Member Activated By Tyrosine Phosphorylation In Response To Epidermal Growth Factor And Interleukin-6. Science 264:95-8

172. **Soukas A, Socci ND, Saatkamp BD, Novelli S, Friedman JM** 2001 Distinct Transcriptional Profiles Of Adipogenesis In Vivo And In Vitro. J. Biol. Chem. 276:34167-34174

173. **Tchoukalova YD, Sarr MG, Jensen MD** 2004 Measuring Committed Preadipocytes In Human Adipose Tissue From Severely Obese Patients By Using Adipocyte Fatty Acid Binding Protein. Am J Physiol Regul Integr Comp Physiol 287:R1132-1140

174. **Marchesini G, Brizi M, Bianchi G, Tomassetti S, Bugianesi E, Lenzi M, McCullough AJ, Natale S, Forlani G, Melchionda N** 2001 Nonalcoholic Fatty Liver Disease: A Feature Of The Metabolic Syndrome. Diabetes 50:1844-1850

175. **Bugianesi E, Gastaldelli A, Vanni E, Gambino R, Cassader M, Baldi S, Ponti V, Pagano G, Ferrannini E, Rizzetto M** 2005 Insulin Resistance In Non-Diabetic Patients With Non-Alcoholic Fatty Liver Disease: Sites And Mechanisms. Diabetologia 48:634-42

176. **Seppala-Lindroos A, Vehkavaara S, Hakkinen A-M, Goto T, Westerbacka J, Sovijarvi A, Halavaara J, Yki-Jarvinen H** 2002 Fat Accumulation In The Liver Is Associated With Defects In Insulin Suppression Of Glucose Production And Serum Free Fatty Acids Independent Of Obesity In Normal Men. J Clin Endocrinol Metab 87:3023-3028

177. **Bugianesi E, Pagotto U, Manini R, Vanni E, Gastaldelli A, de Lasio R, Gentilcore E, Natale S, Cassader M, Rizzetto M, Pasquali R, Marchesini G** 2005 Plasma Adiponectin In Nonalcoholic Fatty Liver Is Related To Hepatic Insulin Resistance And Hepatic Fat Content, Not To Liver Disease Severity. J Clin Endocrinol Metab 90:3498-3504

178. **Hui J, Hodge A, Farrell G, Kench J, Kriketos A, George J** 2004 Beyond Insulin Resistance In NASH: TNF-Alpha Or Adiponectin? Hepatology 40:46-54

179. **Wang J, Liu R, Hawkins M, Barzilai N, Rossetti L** 1998 A Nutrient-Sensing Pathway Regulates Leptin Gene Expression In Muscle And Fat. 393:684-688

180. **Jones M, Thorburn A, Britt K, Hewitt KN, Wreford NG, Proietto J, Oz OK, Leury BJ, Robertson KM, Yao S, Simpson ER** 2000 Aromatase-Deficient (Arko) Mice Have A Phenotype Of Increased Adiposity. Proc Natl Acad Sci 97:2735-40.

181. **Arita Y, Kihara S, Ouchi N, Takahashi M, Maeda K, Miyagawa J, Hotta K, Shimomura I, Nakamura T, Miyaoka K, Kuriyama H, Nishida M, Yamashita S, Okubo K, Matsubara K, Muraguchi M, Ohmoto Y, Funahashi T, Matsuzawa Y** 1999 Paradoxical Decrease Of An Adipose-Specific Protein, Adiponectin, In Obesity. Biochem Biophys Res Commun. 257:79-83

182. **Hu E, Liang P, Spiegelman BM** 1996 Adipoq Is A Novel Adipose-Specific Gene Dysregulated In Obesity. J. Biol. Chem. 271:10697-10703

183. **Friedman JM, Halaas JL** 1998 Leptin And The Regulation Of Body Weight In Mammals. Nature 395:763-770

184. **Lin J, Arnold HB, Della-Fera MA, Azain MJ, Hartzell DL, Baile CA** 2002 Myostatin Knockout In Mice Increases Myogenesis And Decreases Adipogenesis. Biochemical And Biophysical Research Communications 291:701-706

185. **Lee K, Villena J, Moon Y, Kim K-H, Lee S, Kang C, Sul HS** 2003 Inhibition Of Adipogenesis And Development Of Glucose Intolerance By Soluble Preadipocyte Factor-1 (Pref-1). J Clin Invest. 111

186. **Gong D-W, Bi S, Pratley RE, Weintraub BD** 1996 Genomic Structure And Promoter Analysis Of The Human Obese Gene. J. Biol. Chem. 271:3971-3974

187. **Fabris R, Nisoli E, Lombardi AM, Tonello C, Serra R, Grazotto M, Cusin I, Rohner-Jeanrenaud F, Rederspil G, Carruba MO, Vettor R** 2001 Preferential Channeling Of Energy Fuels Toward Fat Rather Than Muscle During High Free Fatty Acid Availability In Rats. Diabetes 50:601-608

188. **Xu A, Wang Y, Keshaw H, Xu L, Lam K, Cooper G** 2003 The Fat-Derived Hormone Adiponectin Alleviates Alcoholic And Nonalcoholic Fatty Liver Diseases In Mice. J. Clin. Invest. 112:91-100

189. **Villena JA, Viollet B, Andreelli F, Kahn A, Vaulont S, Sul HS** 2004 Induced Adiposity And Adipocyte Hypertrophy In Mice Lacking The AMP-Activated Protein Kinase-{Alpha}2 Subunit. Diabetes 53:2242-2249

190. **Franckhauser S, Munoz S, Pujol A, Casellas A, Riu E, Otaegui P, Su B, Bosch F** 2002 Increased Fatty Acid Re-Esterification By PEPCK Overexpression In Adipose Tissue Leads To Obesity Without Insulin Resistance Diabetes 51:624-630

191. **Chen HC, Stone SJ, Zhou P, Buhman KK, Farese RV, Jr** 2002 Dissociation Of Obesity And Impaired Glucose Disposal In Mice Overexpressing Acyl Coenzyme A:Diacylglycerol Acyltransferase 1 In White Adipose Tissue Diabetes 51:3189-3195

192. **Hotamisligil G, Johnson R, Distel R, Ellis R, Papaioannou V, Spiegelman B** 1996 Uncoupling Of Obesity From Insulin Resistance Through A Targeted Mutation In Ap2, The Adipocyte Fatty Acid Binding Protein. Science 274:1377-9

193. **Dresner A, Laurent D, Marcucci M, Griffin ME, Dufour S, Cline GW, Slezak LA, Andersen DK, Hundal RS, Rothman DL, Petersen KF, Shulman GI** 1999 Effects Of Free Fatty Acids On Glucose Transport And IRS-1-Associated Phosphatidylinositol 3-Kinase Activity. J Clin Invest. 103:253-9

194. **Griffin M, Marcucci M, Cline G, Bell K, Barucci N, Lee D, Goodyear LJ, Kraegen EW, White MF, Shulman GI** 1999 Free Fatty Acid-Induced Insulin Resistance Is Associated With Activation Of Protein Kinase C Theta And Alterations In The Insulin Signaling Cascade. Diabetes 48:1270-1274

195. **Randle P, Garland P, Hales C, Newsholme E** 1963 The Glucose Fatty-Acid Cycle. Its Role In Insulin Sensitivity And The Metabolic Disturbances Of Diabetes Mellitus. Lancet 1:785-9

196. **Hui J, Hodge A, Farrell G, Kench J, Kriketos A, George J** 204 Beyond Insulin Resistance In NASH: TNF-Alpha Or Adiponectin? Hepatology 40:46-54

197. **Savage D, Petersen K, Shulman G** 2007 Disordered Lipid Metabolism And The Pathogenesis Of Insulin Resistance. Physiological Reviews 87:507-520

198. **Rabinowitz JE, Rutishauser U, Magnuson T** 1996 Targeted Mutation Of Ncam To Produce A Secreted Molecule Results In A Dominant Embryonic Lethality. PNAS 93:6421-6424

199. **Hakem R, de La Pompa JL, Sirard C, Mo R, Woo M, Hakem A, Wakeham A, Potter J, Reitmair A, Billia F, Firpo E, Hui CC, Roberts J, Rossant J, Mak TW** 1996 The Tumor Suppressor Gene Brca1 Is Required For Embryonic Cellular Proliferation In The Mouse. Cell 85:1009-1023